European Journal of Medicinal Chemistry 259 (2023) 115716

Contents lists available at ScienceDirect

European Journal of Medicinal Chemistry

journal homepage: www.elsevier.com/locate/ejmech

Research paper

Tetrazole and oxadiazole derivatives as bioisosteres of tariquidar and elacridar: New potent P-gp modulators acting as MDR reversers

Laura Braconi [a], Silvia Dei [a,*], Marialessandra Contino [b], Chiara Riganti [c], Gianluca Bartolucci [a], Dina Manetti [a], Maria Novella Romanelli [a], Maria Grazia Perrone [b], Nicola Antonio Colabufo [b], Stefano Guglielmo [d], Elisabetta Teodori [a]

[a] Department of Neuroscience, Psychology, Drug Research and Child Health - Section of Pharmaceutical and Nutraceutical Sciences, University of Florence, Via Ugo Schiff 6, 50019, Sesto Fiorentino, Italy
[b] Department of Pharmacy - Drug Sciences, University of Bari "A. Moro", via Orabona 4, 70125, Bari, Italy
[c] Department of Oncology, University of Turin, Via Santena 5/bis, 10126, Torino, Italy
[d] Department of Drug Science and Technology, University of Turin, Via P. Giuria 9, 10125, Torino, Italy

ARTICLE INFO

Keywords:
Multidrug resistance
MDR reversers
ABC transporter modulators
P-glycoprotein
Tetrazole
Oxadiazole

ABSTRACT

New 2,5- and 1,5-disubstituted tetrazoles, and 2,5-disubstituted-1,3,4-oxadiazoles were synthesized as tariquidar and elacridar derivatives and studied as multidrug resistance (MDR) reversers. Their behaviour on the three ABC transporters P-gp, MRP1 and BCRP was investigated. All compounds inhibited the P-gp transport activity in MDCK-MDR1 cells overexpressing P-gp, showing EC_{50} values even in the low nanomolar range (compounds **15**, **22**). Oxadiazole derivatives were able to increase the antiproliferative effect of doxorubicin in MDCK-MDR1 and in HT29/DX cells confirming their nature of P-gp modulators, with derivative **15** being the most potent in these assays. Compound **15** also displayed a dual inhibitory effect showing good activities towards both P-gp and BCRP. A computational study suggested a common interaction pattern on P-gp for most of the potent compounds. The bioisosteric substitution of the amide group of lead compounds allowed identifying a new set of potent oxadiazole derivatives that modulate MDR through inhibition of the P-gp efflux activity. If compared to previous amide derivatives, the introduction of the heterocycle rings greatly enhances the activity on P-gp, introduces in two compounds a moderate inhibitory activity on MRP1 and maintains in some cases the effect on BCRP, leading to the unveiling of dual inhibitor **15**.

1. Introduction

The therapeutic treatment of tumors is often compromised by the emergence of multidrug resistance (MDR), an acquired cross-resistance that tumor cells develop during clinical treatments after the exposure to structurally and mechanistically unrelated anticancer agents. The onset of MDR is linked to complex and multifactorial mechanisms; one of the major contributors to the progression of resistance in cancer cells is the overexpression of efflux pumps that are transmembrane transporter proteins [1]. In humans, the most important efflux pumps involved in MDR belong to the ATP-binding cassette (ABC) protein family [2]. The human genome encodes 49 ABC transmembrane proteins, divided into seven subfamilies (ABCA to ABCG) [3]. Among these, three are mainly responsible for the onset of MDR: P-glycoprotein (P-gp, ABCB1), multidrug resistance-associated protein 1 (MRP1, ABCC1), and breast cancer resistance protein (BCRP, ABCG2) [4]. These proteins are overexpressed in many resistant tumors, and it is now established that this overexpression is related to poor prognosis in many patients [5]. More recently, it has been reported that these three ABC transporters can also be co-expressed in resistant tumor cells [6]. In particular, P-gp and BCRP are co-overexpressed in both solid tumors and cancer stem cells, making long-lasting chemotherapeutic treatments ineffective [7–9]. Since MDR may be due to ABC transporters overexpression, a possible strategy to address this phenomenon is the co-administration of anticancer drugs, which are substrates of the efflux pumps, with compounds that act as inhibitors/substrates of these transporter proteins, to improve both the patient's therapeutic response and prognosis. Therefore, in recent years, research has been directed towards the discovery of modulators of these three efflux pumps [10–12]. These compounds are also defined chemosensitizers or MDR reversers.

* Corresponding author.
E-mail address: silvia.dei@unifi.it (S. Dei).

https://doi.org/10.1016/j.ejmech.2023.115716
Received 11 May 2023; Received in revised form 22 June 2023; Accepted 7 August 2023
Available online 9 August 2023

Many efflux pump modulators have been identified so far, in particular against P-gp, which was the first membrane protein to be identified and still the most studied today [13]. A great number of compounds showing P-gp modulating activity has been reported, and were classified as first, second- or third-generation [14,15] but none of these compounds has overcome the clinical trials, because no substantial benefits have been established although some of the latest MDR reversing compounds show a better profile. The negative aspects are related to problems of pharmacokinetic interactions, adverse effects and toxicity, due to which the clinical efficacy is not significant [16–18].

So, to overcome these drawbacks, the search for novel ABC transporter-dependent MDR modulators is still being pursued, looking for more potent or safer efflux pump inhibitors [19–21] or multitarget ligands [22,23]. Moreover, recently MDR modulation has been also studied in brain disorders, since these transporters are highly expressed in the blood brain barrier, reducing the activity of some drugs active at this level [24].

Among the third generation P-gp chemosensitizers, two of the most interesting ones are elacridar (GF120918 or GW120918) [25] and tariquidar (XR9576) [26]. These compounds have shown good pharmacodynamic and pharmacokinetic characteristics [27], even if subsequent clinical studies [28] failed to show a significant effect on the efficacy of anticancer agents [17,18]. Both elacridar and tariquidar bear the 6,7-dimethoxy-2-phenethyl-1,2,3,4-tetrahydroisoquinoline residue and an aryl-substituted amide function (Chart 1). Both compounds have been reported to be non-specific for P-gp because they are also capable of binding the BCRP transporter [15]. Structure-activity relationship (SAR) studies suggested that the 6,7-dimethoxy-2-phenethyl-1,2,3,4-tetrahydroisoquinoline core is essential for the inhibition of the two proteins, P-gp and BCRP, while the changes in the aryl part of the substituted amide may modify the selectivity [29]. In the case of tariquidar, recent evidence has indicated that this molecule is also capable of interacting with other members of the ABC subfamily [30,31]. So, a large number of analogues of these two compounds have been synthesized maintaining the tetrahydroisoquinoline moiety, to optimize the MDR reversal activity and gain insight into the structure-activity relationships [32].

To expand the information on the structural characteristics that increase potency and/or selectivity in this series of derivatives, in previous studies [33,34] we described the synthesis and the biological activity of a series of amides and isosteric esters carrying the 6,7-dimethoxy-2-phenethyl-1,2,3,4-tetrahydroisoquinoline scaffold linked to several aryl moieties. These compounds were evaluated for their P-gp interaction profile and selectivity towards the two other efflux pumps MRP1 and BCRP. All derivatives were active, at a different extent, and in most cases showed selectivity towards P-gp. As an example, compound **I** [34] (Chart 1) was tested in co-administration with doxorubicin in cancer cell lines and showed a potent sensitizing effect towards the antineoplastic drug. As regard SARs, the presence of an amide function was not essential for modulating the transporter proteins, and its isosteric substitution with an ester group led to compounds that maintained a good activity on P-gp.

In fact, the replacement of the amide group with an ester moiety or with bioisosteric rings, such as triazole or tetrazole (reviewed in Ref. [32]), gave compounds endowed with good MDR modulating properties, exemplified by HM30181 (encequidar), a tetrazole analogue of tariquidar (Chart 1), which is a selective P-gp inhibitor used in preclinical and clinical studies [35]. Moreover, oxadiazole analogues have been described, which are active also on BCRP protein [36].

On these bases, we designed and synthesized a new series of derivatives, where the amide function of the lead compounds was substituted with two bioisosteric heterocycles, tetrazole and oxadiazole, connected to a methoxy-substituted aryl moiety (Chart 2). Notably, we designed both the 2,5- (**1**–**8**) and the 1,5-disubstituted (**9-14**) tetrazoles, and the 2,5-disubstituted-1,3,4-oxadiazoles (**15**–**22**) (Chart 2). The selected methoxy-substituted aryl groups had conferred good inhibitory effects on P-gp to the previously synthesized amide and ester derivatives [33,34]. In particular, the hydrogen bond acceptor methoxy group is considered important for the MDR-reversing activity and it is present in many well-known P-gp modulators [15,37].

The synthesized compounds **1**–**22** were evaluated for their P-gp interaction profile and activity on the two other ABC transporters, MRP1 and BCRP. The P-gp interacting-mechanism was investigated combining three assays: (*i*) apparent permeability (P_{app}) determination (BA/AB) in Caco-2 cell monolayer; (*ii*) ATP cell depletion in cells overexpressing the transporter (MDCK-MDR1); (*iii*) the inhibition of Calcein-AM transport in MDCK-MDR1 cells. The activity on MRP1 and BCRP was evaluated on cancer cell lines overexpressing each transporter (MDCK-MRP1 and MDCK-BCRP cells), by measuring the inhibition of the efflux of the profluorescent probe Calcein-AM in MDCK-MRP1 cells or the fluorescent probe Hoechst 33342 in MDCK-BCRP cells.

Therefore, selected compounds were also tested in the same MDCK cell lines, in co-administration with doxorubicin, to measure how they affected the antiproliferative activity of the antineoplastic drug, also evaluating the effect on the release of lactate dehydrogenase (LDH). Moreover, the ability of the most promising oxadiazole derivatives to increase the accumulation of doxorubicin in MDCK-MDR1 cells was evaluated. These tests were also performed in the human adenocarcinoma colon cell line (HT29) and in its doxorubicin-resistant counterpart (HT29/DX) that overexpress P-gp.

Finally, molecular modeling studies were performed to identify the binding mode of these compounds within the P-gp binding pocket.

2. Results and discussion

2.1. Chemistry

The reaction pathways used to synthesize the 2,5-disubstituted-2*H*-tetrazoles **1**–**8** are reported in Schemes 1 and 2. The key intermediates were the suitable methoxy-substituted aryl benzenesulfonohydrazides **31**–**38**, that were prepared starting from the corresponding aldehydes. 2,3,4-Trimethoxy-1-benzaldehyde, 2-methoxy-1-benzaldehyde, 2-methoxy-1-naphthaldehyde and 2,3-dimethoxy-1-naphthaldehyde are commercially available, while (*E*)-3-(3,4,5-trimethoxyphenyl)acrylaldehyde **23** was synthesized as reported in Ref. [33] and 3,4,5-trimethoxy-1-benzaldehyde **24** was obtained by oxidation of the commercially-available alcohol with pyridinium chlorochromate (PCC) in dry CH_2Cl_2 (Scheme 1). To synthesize the aldehydes **29** and **30**, 2,3-dimethoxybenzoic acid and 2,6-dimethoxybenzoic acid were first transformed in the corresponding methyl esters **25** and **26**, then reduced with $LiAlH_4$ to alcohols **27** and **28**, that were oxidized with PCC to afford the desired compounds (Scheme 1).

Thus, all the aldehydes were treated with benzenesulfonyl hydrazide in ethanol, yielding the corresponding benzenesulfonohydrazides **31**–**38** (Scheme 2). Finally, the aniline **39** (obtained as reported in Ref. [33]) was reacted with $NaNO_2$ in an acid mixture of ethanol/water, affording

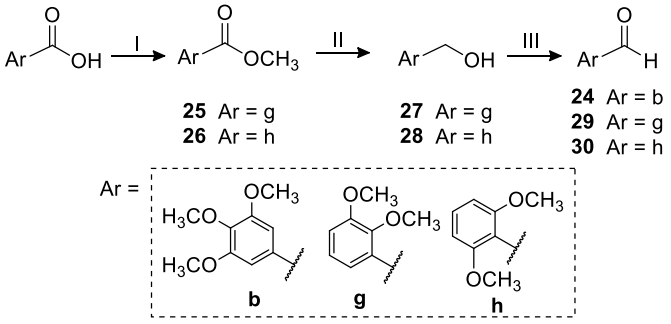

Scheme 1. Reagents and conditions: I) $SOCl_2$, dry CH_3OH, reflux; II) $LiAlH_4$, dry THF, rt; III) PCC, Celite, dry CH_2Cl_2, rt.

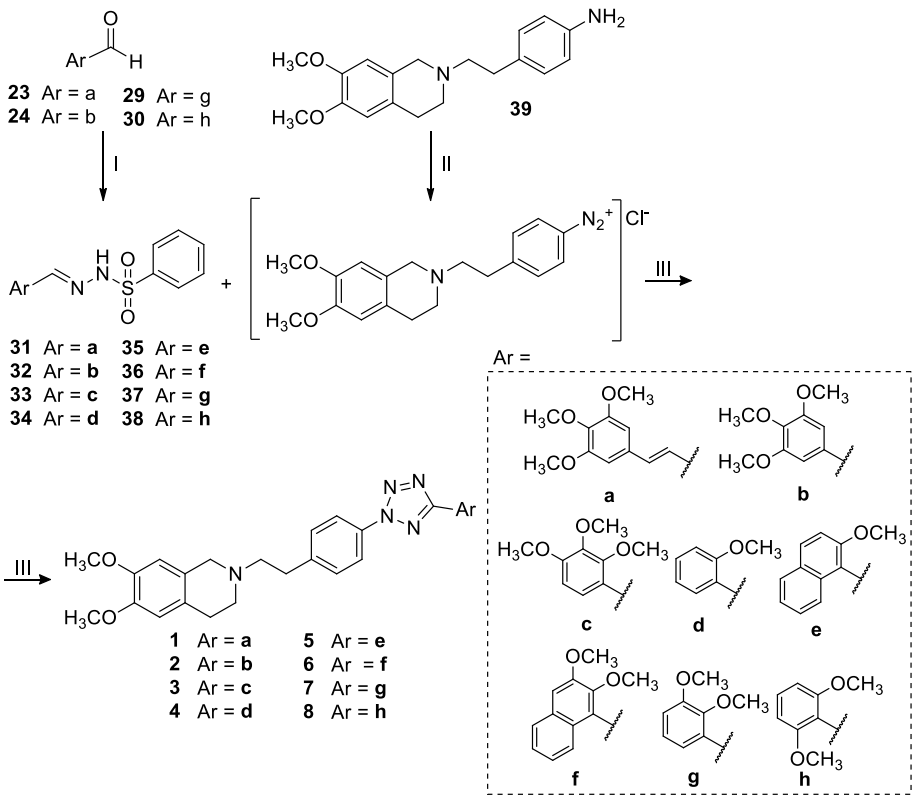

Scheme 2. Reagents and conditions: I) benzenesulfonyl hydrazide, EtOH, rt; II) $NaNO_2$, HCl conc., EtOH/H_2O, 0 °C; III) pyridine, T = −10 to −15 °C.

the corresponding diazonium salt, which was not isolated but treated with the proper benzenesulfonohydrazide in pyridine between −10 °C and −15 °C, following the procedure described by Köhler et al. [38]: in this way, the 2,5-dibustituted-2*H*-tetrazoles **1**–**8** were obtained with good yields (Scheme 2).

The 1,5-disubstituted-1*H*-tetrazoles **9**–**14** were synthesized starting from the commercially available 2-(4-aminophenyl)acetic acid, which was transformed in the corresponding methyl ester **40**, then treated with the acyl chloride, obtained by treatment of the proper methoxy-substituted aryl carboxylic acid with $SOCl_2$, or coupled with the suitable carboxylic acid using EDC hydrochloride and DMAP, to afford the corresponding amides **41**–**46** (Scheme 3, for details see the Materials and Methods Section). Most of the methoxy-substituted aryl acids are commercially available, while 2-methoxy-1-naphthoic acid **47** and 2,3-dimethoxy-1-naphthoic acid **48** were synthetized as previously reported [34].

Treatment with PCl_5 or oxalyl chloride transformed the amides **41**–**46** in the corresponding imidoyl chlorides, which were not isolated, but reacted with NaN_3, affording tetrazoles **49**–**54** (Scheme 3). Then, the esters **50**–**54** were reduced using $LiAlH_4$ to give alcohols **56**–**60**; this procedure was not effective for tetrazole **49**, thus it was treated with DIBAL-H in dry CH_2Cl_2, yielding the desired intermediate **55**. The reaction of alcohols **55**–**60** with *p*-toluenesulfonyl chloride gave the corresponding tosyl derivatives **61**–**66**, which were condensed with 6,7-dimethoxy-1,2,3,4-tetrahydroisoquinoline, obtaining compounds **9**–**14** (Scheme 3).

The synthesis of the 2,5-disubstituted-1,3,4-oxadiazoles **15**–**22** is reported in Scheme 4. Friedel-Crafts acylation of the commercially available (2-bromoethyl)benzene with acetyl chloride in presence of $AlCl_3$ gave the acyl intermediate **67** [39], which was oxidized to the corresponding carboxylic acid **68** with Br_2 under basic conditions. Esterification of **68** and subsequent treatment of the methyl ester **69** with 6,7-dimethoxy-1,2,3,4-tetrahydroisoquinoline afforded **70**, which reacted with hydrazine hydrate in ethanol, yielding the hydrazide **71**. Finally, following the procedure described by Stabile et al. [40], the proper methoxy-substituted aryl acids were first activated, using HATU as the coupling agent in presence of DIPEA, then reacted with the hydrazide **71**: the resulting diacylhydrazine intermediates were not isolated, but cyclized in presence of *p*-toluenesulfonyl chloride as dehydrating agent, affording the desired oxadiazoles **15**–**22**.

2.2. Characterization of P-gp interacting profile and ABC transporters selectivity

The interaction potency between the obtained compounds and P-gp was evaluated by measuring the transport inhibition of the profluorescent probe Calcein-AM, that is a P-gp substrate, in a cell line overexpressing P-gp (MDCK-MDR1) [41]. The P-gp interacting profile was further investigated with other two assays: the Apparent Permeability (P_{app}) determination (BA/AB) in Caco-2 cell monolayer [42,43], and the ATP cell depletion in the MDCK-MDR1 cell line [44]. Taking into account the results of the combined tests, an interacting compound can be classified as substrate or inhibitor. P_{app} determination measures the ratio between two fluxes: from the basolateral to apical compartments (BA, representative of passive diffusion) and from the apical to basolateral compartments (AB, representative of active transport). A (BA/AB) value < 2 suggests that the compound can be considered an inhibitor. In the same manner, if (BA/AB) > 2, the compound should probably be classified as a substrate [45]. The other assay detects the consumption of ATP elicited by the transport mediated by the pump; in general, a substrate induces ATP cell depletion being transported by the pump (unambiguous substrate, category I), while a P-gp inhibitor does not induce ATP consumption. There is also a third substrate category (known as category IIB3) displaying a P_{app} value > 2 but not inducing an ATP cell depletion [41]. The selectivity of ligands **1**–**22** was then evaluated by detecting their activity towards the other ABC transporters MRP1 and BCRP, by measuring the inhibition of the efflux of Calcein-AM (that is also a MRP1 substrate) in cells overexpressing MRP1

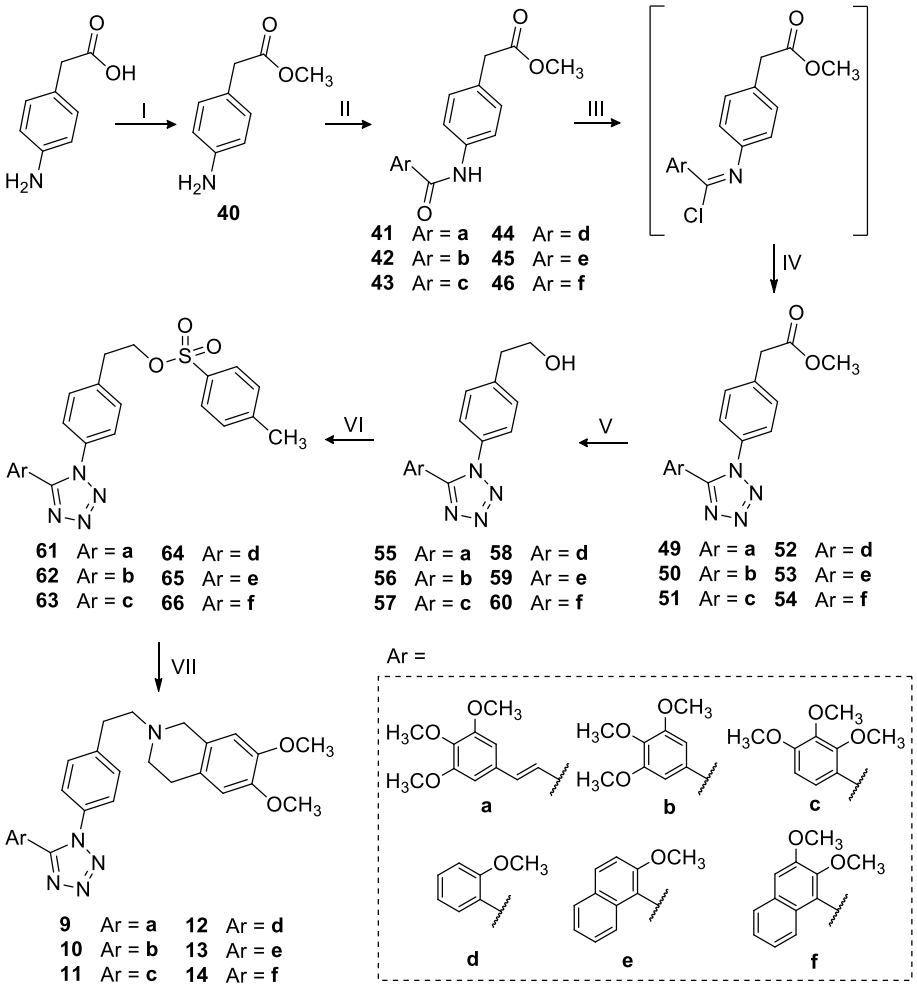

Scheme 3. Reagents and conditions: I) $SOCl_2$, dry CH_3OH, reflux; II) ArCOCl, $CHCl_3$ (free of ethanol), rt (for **41**–**45**) or ArCOOH, EDC hydrochloride, DMAP, dry CH_2Cl_2, rt (for **46**); III) PCl_5, dry pyridine, dry CH_2Cl_2, reflux (for **49**), or oxalyl chloride, dry pyridine, dry CH_2Cl_2, rt (for **50**–**54**); IV) NaN_3, dry DMF, rt (for **49**), or NaN_3, dry DMF, 60 °C (for **50**–**54**); V) DIBAL-H, dry CH_2Cl_2, -30 °C and −15 °C (for **55**), or $LiAlH_4$, dry THF, rt (for **56**–**60**); VI) *p*-toluenesulfonyl chloride, Et_3N, dry CH_2Cl_2, rt; VII) 6,7-dimethoxy-1,2,3,4-tetrahydroisoquinoline hydrochloride, Et_3N, dry CH_3CN, reflux. For details, see the Materials and Methods Section.

(MDCK-MRP1 cells), and the inhibition of the efflux of the fluorescent probe Hoechst 33342 (that is a BCRP substrate) in cells overexpressing BCRP (MDCK-BCRP cells), respectively.

Expression levels of P-gp, MRP1 and BCRP were periodically measured by immunoblotting analysis in MDCK-MDR1, MDCK-MRP1 and MDCK-BCRP cells, respectively [34].

The results of the three inhibition assays on compounds **1**–**22** are reported in Table 1 together with those on tariquidar and elacridar, used as reference compounds.

As shown in Table 1, all the compounds were active on P-gp, showing activity values ranging from low nanomolar to micromolar range. Indeed, only two of them (**9** and **14**) exhibited a weak P-gp inhibitory activity, with EC_{50} values higher than 1 μM. Compounds **2**, **3**, **6**, **7**, **10**–**13**, **17** and **21** exhibited EC_{50} values in the low micromolar range. The other derivatives showed a high P-gp inhibitory potency, reaching the medium nanomolar range, as in the case of compounds **1**, **4**, **5**, **8**, **16**, **18**, **19** and **20** (EC_{50} = 12.0 nM, 82.0 nM, 90.0 nM, 41.0 nM, 71.0 nM, 19.0 nM, 24.0 nM and 46.0 nM, respectively), or even the low nanomolar range, as in the case of compounds **15** and **22** (EC_{50} = 1.6 nM and 3.3 nM, respectively). Notably, derivatives **1**, **15** and **22** displayed higher activity than lead tariquidar and elacridar.

As general trend, the 2,5-disubstituted tetrazoles **1**–**8** (series I in Table 1) and the 2,5-disubstituted-1,3,4-oxadiazoles **15**–**22** (series III) displayed excellent activities. Concerning the aryl residues inserted on these two scaffolds, derivatives **1** and **15**, bearing the *(E)*-3-(3,4,5-trimethoxyphenyl)vinyl moiety (**a**), and compound **22**, decorated with the 2,6-dimethoxyphenyl moiety (**h**), showed an outstanding potency. Also the 2-methoxyphenyl (**d**) and the 2-methoxynaphthalene (**e**) residues conferred a high P-gp inhibitory effect to both series of 2,5-disubstituted heterocycle derivatives. As regard aryl moieties **b**, **c**, **f** and **g**, their presence exerted different inhibitory activity on P-gp in the two series. Indeed, tetrazoles **2**, **3**, **6** and **7** showed EC_{50} values in the low micromolar range (EC_{50} values between 0.14 and 0.55 μM). Otherwise, in the case of the corresponding oxadiazoles, derivatives **17** (Ar = **c**) and **21** (Ar = **g**) had a low effect (EC_{50} = 0.44 μM and 0.40 μM, respectively), while **16** (Ar = **b**) and **20** (Ar = **f**) were more active, displaying EC_{50} values in the medium nanomolar range, as already outlined. Instead, the 1,5-disubstituted tetrazoles **9**–**14** (series II) turned out to be definitely less potent overall, regardless the aryl group to which the tetrazole is linked.

Therefore, as a general remark, a thorough evaluation of the P-gp inhibition values indicated that the activity of these compounds seems to be mainly influenced by the chosen heterocycle; within the various series it is then possible to highlight that the introduction of some substituents (mainly **a** and **h**) has a further influence on the inhibitory activity of the compounds.

As regard the P-gp interacting mechanism, all the compounds behaved as P-gp substrates since they had a BA/AB ratio >2 and inhibited Calcein-AM transport. Moreover, according to Polli classification, they should be considered not transported substrates (category IIB3) since in the ATP depletion assay in MDCK-MDR1 cells they are not able to induce ATP consumption, at 10-fold over and under their EC_{50} values [41].

As far as the other transporters are concerned, compounds **2**, **3** and **15**, and to a lesser extent **1** and **12**, were active also on BCRP and, among them, **2** displayed the highest potency (EC_{50} = 0.15 μM). Based on these

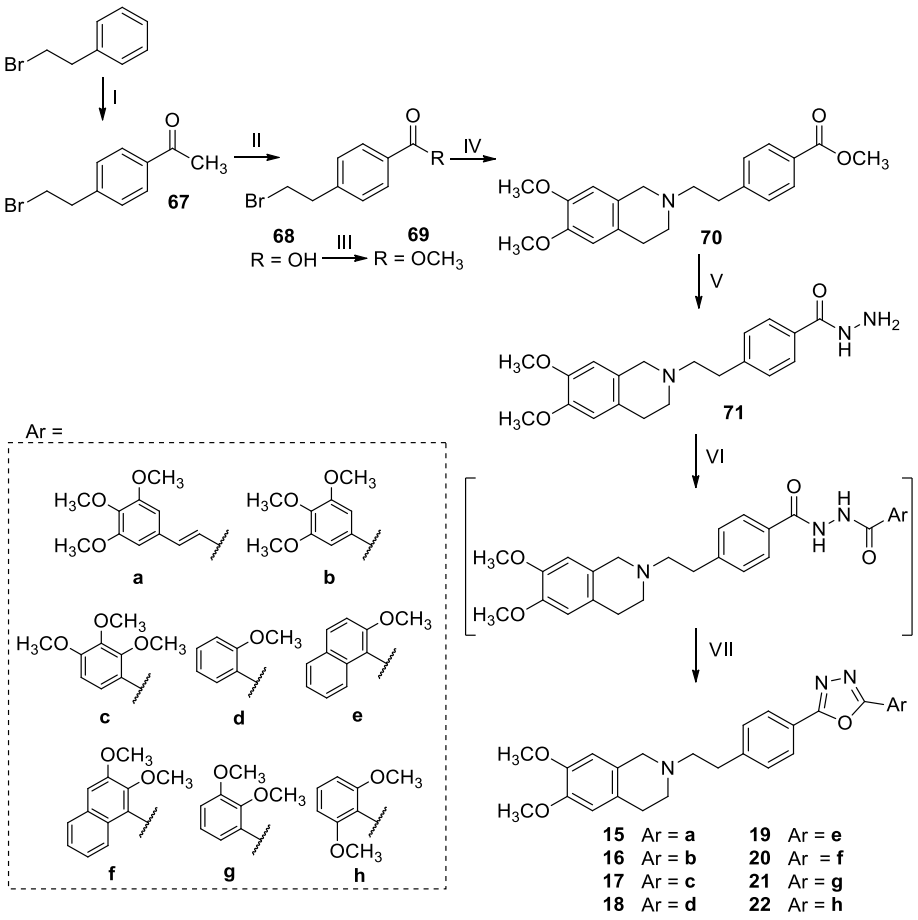

Scheme 4. Reagents and conditions: I) $AlCl_3$, CH_3COCl, CH_2Cl_2, rt; II) Br_2, NaOH in H_2O/dioxane, rt; III) $SOCl_2$, dry CH_3OH, reflux; IV) 6,7-dimethoxy-1,2,3,4-tetrahydroisoquinoline, K_2CO_3, dry CH_3CN, reflux; V) $NH_2NH_2.H_2O$, EtOH, reflux; VI) ArCOOH, HATU, DIPEA, dry CH_3CN, rt; VII) DIPEA, *p*-toluenesulfonyl chloride, dry CH_3CN, rt.

data, it is not possible to outline structure-activity relationships; however, it is interesting to note compound **15**, which is the most active on P-gp and is a potent BCRP inhibitor. Compound **15** is thus a novel P-gp/BCRP dual inhibitor. Its discovery is noteworthy, as interest in MDR modulators capable of interacting on different transporters has recently emerged [4]. Regarding MRP1 inhibition, most compounds could be considered inactive, but the two 1,5-disubstituted tetrazoles **10** and **11** displayed an EC_{50} in the micromolar range (4.33 and 7.49 μM).

So, if compared to the corresponding amide and ester derivatives previously studied [33,34], the introduction of the bioisosteric heterocycles greatly enhances the activity on P-gp, introduces in two compounds a moderate inhibitory activity on MRP1 and maintains in some cases the effect on BCRP, leading to the unveiling of the dual P-gp/BCRP inhibitor **15**.

2.3. Enhancement of doxorubicin cytotoxicity and doxorubicin accumulation assays

Compounds **1**–**8** (series I) and **15**–**22** (series III), endowing with the best P-gp activity profile in MDCK-MDR1, were selected to further characterize their P-gp inhibitory activity. They were tested in co-administration with the antineoplastic drug doxorubicin, that, being a P-gp substrate, is usually inactive in tumors overexpressing the pump. We first measured the effects of the derivatives in MDCK cell lines selectively overexpressing P-gp, MRP1 or BCRP. The compounds at both concentrations of 1 and 10 μM did not reduce the cell viability induced by doxorubicin in parental MDCK cells, devoid of ABC transporters (Fig. S23, Supplementary data). By contrast, they enhanced anti-tumor doxorubicin's effects in MDCK-MDR1 cells in a dose-dependent way, confirming their nature of P-gp modulators (Fig. 1). Elacridar, used at its EC_{50} concentration (10 nM), was reported as positive control. Particularly, compounds **1**, **8**, **15** and **22** were the most potent enhancer of doxorubicin effects, with a potency comparable to elacridar co-incubated with doxorubicin. Noteworthy, these derivatives also showed a good activity in the Calcein-AM assay (see Table 1). Instead, compounds **1**–**8** and **15**–**22** had no effects in MDCK-MRP1 and MDCK-BCRP cells (Fig. S23, Supplementary data).

The reduction of cell viability was caused by an increased cytotoxicity induced by doxorubicin, as demonstrated by the increased release of lactate dehydrogenase (LDH), an index of cell necrosis induced by doxorubicin [46], in MDCK-MDR1 cells (Fig. S24, Supplementary data). In line with the reduction of viability, **1**, **8**, **15** and **22**, at 10 μM, induced the highest increase in doxorubicin cytotoxicity. As expected, in parental MDCK cells, no modification of the LDH release was observed in presence of the tested compounds (Fig. S24, Supplementary data).

These results confirm the trend already emerged in the previous MDCK-MDR1 cell assays; since compounds **15** and **22** showed the best results in the Calcein-AM assay and an outstanding activity in the co-administration test, we focused on the oxadiazole series **15**–**22** as the most promising reverser agents. Therefore, to learn more about their mechanism of action, compounds **15**–**22** were further tested at 1 μM and 10 μM concentrations in MDCK-MDR1 cells to evaluate their ability to increase the intracellular accumulation of 5 μM doxorubicin. Results are reported in Fig. 2. All the oxadiazoles showed a relevant ability to increase intracellular doxorubicin when used at 10 μM concentration. The most potent molecules were, also in this case, **15** and **22**, along with the

Table 1
Biological results of compounds **1**–**22**: activity towards P-gp, MRP1 and BCRP, in MDCK transfected cells overexpressing each transporter, and Apparent Permeability (P_{app}) values.

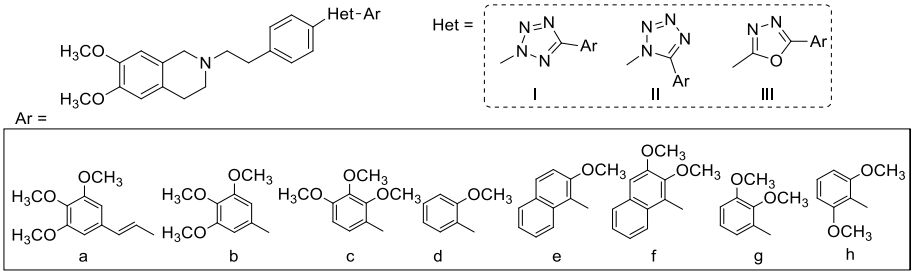

Cmpd	Het	Ar	(EC_{50}) μM [a]			P_{app} [b]
			P-gp	MRP1	BCRP	
1	I	a	0.012 ± 0.004	NA	53.60 ± 7.87	5.4
2	I	b	0.26 ± 0.043	NA	0.15 ± 0.018	8.9
3	I	c	0.55 ± 0.035	NA	0.99 ± 0.19	8.3
4	I	d	0.082 ± 0.0024	NA	NA	6.5
5	I	e	0.090 ± 0.004	NA	NA	4.5
6	I	f	0.26 ± 0.03	NA	NA	6.8
7	I	g	0.14 ± 0.02	NA	NA	5.3
8	I	h	0.041 ± 0.011	NA	NA	6.0
9	II	a	5.27 ± 0.69	NA	NA	7.0
10	II	b	0.63 ± 0.08	4.33 ± 0.88	NA	4.3
11	II	c	0.75 ± 0.12	7.49 ± 0.80	NA	5.5
12	II	d	0.95 ± 0.08	NA	28.9 ± 2.79	5.2
13	II	e	0.75 ± 0.15	NA	NA	9.7
14	II	f	1.06 ± 0.097	NA	NA	3.3
15	III	a	0.0016 ± 0.0003	NA	0.60 ± 0.046	11.8
16	III	b	0.071 ± 0.0016	NA	NA	3.1
17	III	c	0.44 ± 0.06	NA	NA	6.5
18	III	d	0.019 ± 0.0016	NA	NA	6.3
19	III	e	0.024 ± 0.001	NA	NA	4.2
20	III	f	0.046 ± 0.007	NA	NA	9.7
21	III	g	0.40 ± 0.078	NA	NA	6.8
22	III	h	0.0033 ± 0.0014	NA	NA	6.8
Tariq.			0.044 ± 0.001	ND	0.010 ± 0.005	22.0
Elacr.			0.014 ± 0.003	NA	10.0 ± 2.0	32.7

[a] Values are the mean ± SEM of three independent experiments, with samples in duplicate.
[b] BA/AB ratio obtained from the P_{app}BA and P_{app}AB values from three independent experiments, with samples in duplicate. NA = EC_{50} > 100 μM; ND = not determined.

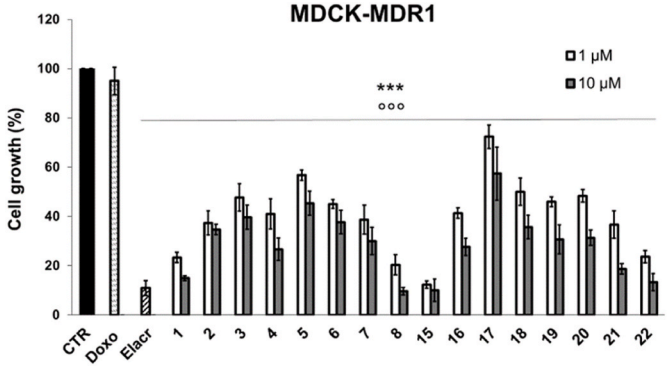

Fig. 1. Antiproliferative activity in MDCK-MDR1 cells of doxorubicin (Doxo) at 5 μM, alone and in co-administration with compounds **1**–**8** and **15**–**22** at 1 μM and 10 μM, or elacridar (Elacr) at 10 nM, measured after 48 h. Each bar represents the mean ± SD of three independent experiments, with technical duplicates. CTR represents the untreated cells. One-way analysis of variance (ANOVA) analysis: ***$p < 0.001$ *vs* control; °$p < 0.001$ *vs* doxorubicin alone.

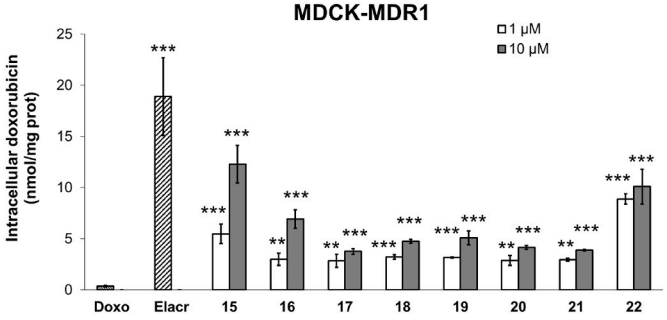

Fig. 2. Intracellular accumulation of doxorubicin in MDCK-MDR1, incubated 24 h with doxorubicin (Doxo) at 5 μM, alone and in co-administration with oxadiazole derivatives **15**–**22** at 1 μM and 10 μM or elacridar (Elacr) at 10 nM. Each bar represents the mean ± SD of three independent experiments, with technical duplicates. One-way analysis of variance (ANOVA) analysis: ***$p < 0.001$; **$p < 0.01$ *vs* doxorubicin alone.

well-known P-gp inhibitor elacridar (Fig. 2).

To move toward a setting closer to real cancers, that have a mix of different ABC transporters, compounds **1**–**8** and **15**–**22** were tested in the human adenocarcinoma colon cell line (HT29), displaying low amount of P-gp, and in its resistant counterpart (HT29/DX), in which P-gp is overexpressed [47]. Before studying the co-administration of our molecules with the chemotherapeutic drug, we preliminary studied the cytotoxicity of the ligands alone, which showed a very negligible

cytotoxic effect (around 10%) at 48 h of incubation on HT29 and HT29/DX at 1 μM e 10 μM (Figs. S25 and S26, Supplementary data).

The derivatives were then assayed at these concentrations in co-administration with 5 μM doxorubicin, a concentration known to discriminate well between sensitive and resistant cells [47]. In HT29 cells, which express low levels of P-gp [47], the tested compounds did not significantly increase the cytotoxicity of doxorubicin, measured as percentage of cell growth, as reported in Fig. S27 (Supplementary data), for the potent derivatives **1**, **8**, **15**, **16**, **18**–**20** and **22.**

By contrast, in the resistant counterpart HT29/DX, which have high levels of the transporter [47], compounds **1**–**8** and **15**–**22**, used at 1 or 10 μM, markedly increased the reduction of cell viability induced by doxorubicin alone (Fig. 3) in a dose dependent way. In particular, as regard tetrazole derivatives, at 10 μM, the most active compounds are **7** and **8**, which reduced cell viability by 58.0% in doxorubicin-treated HT29/DX cells. In the case of oxadiazoles, the co-administration of **16**, **18**, **19** and **21** at 10 μM led to a high increase of doxorubicin toxicity, reaching a 64.3% reduction of the cell viability for compound **18**.

Notably, however, the cytotoxicity assays measured as LDH release from HT29/DX cells indicated that the most potent compounds were **1**, **8**, **15** and **22** (Fig. S28, Supplementary data), as in the MDCK-MDR1 cells. In HT29 cell line, the tested derivatives did not enhance the LDH release (Fig. S28, Supplementary data).

Instead, in terms of doxorubicin accumulation, the most potent molecules were **15, 18** and **20**, that allowed a 3.3-, 3.8- and 3.7- fold greater accumulation of the drug, respectively (Fig. 4).

Cancer cells have multiple mechanism of drug resistance, not only relying of drug efflux via ABC transporters but also caused by reduced drug uptake, increased metabolic inactivation or lysosomal sequestration, alteration of the target of the drugs, changes in apoptotic and pro-survival pathways. We cannot exclude that different uptake, metabolism and sequestrations of the compounds occur in these cancer cells. These events may justify the discrepancy obtained by our derivatives between the MDCK model, purely based on the activity of ABC transporters, and

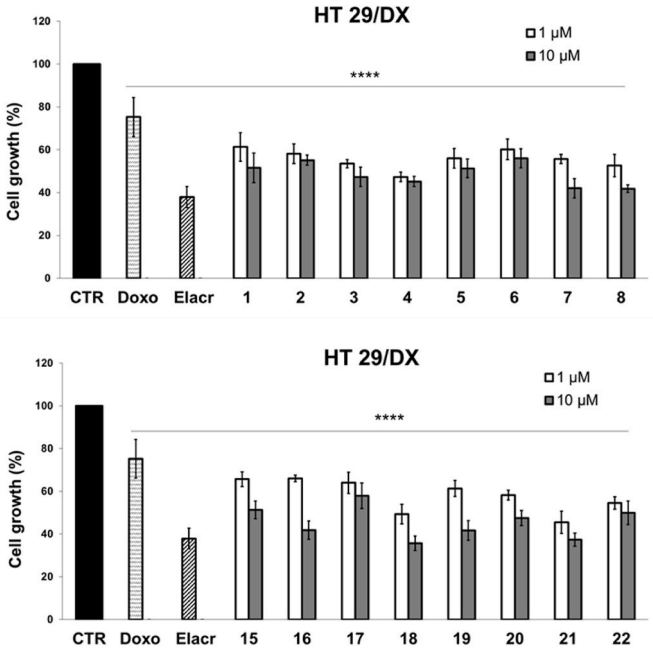

Fig. 3. Antiproliferative activity in HT29/DX cells of doxorubicin (Doxo) at 5 μM, alone and in co-administration with tetrazole derivatives **1**–**8** (top) and oxadiazole derivatives **15**–**22** (bottom) at 1 μM and 10 μM, or elacridar (Elacr) at 10 nM, measured after 48 h. Each bar represents the mean ± SD of three independent experiments, with technical duplicates. CTR represents the untreated cells. One-way analysis of variance (ANOVA) analysis: ****$p < 0.0001$ *vs* control.

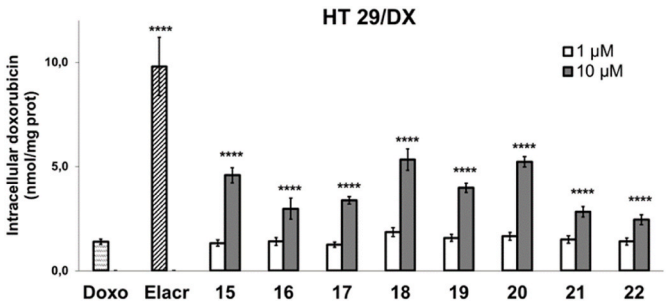

Fig. 4. Intracellular accumulation of doxorubicin in HT29/DX cells, incubated 24 h with doxorubicin (Doxo) at 5 μM, alone and in co-administration with oxadiazole derivatives **15**–**22** at 1 μM and 10 μM or elacridar (Elacr) at 10 nM. Each bar represents the mean ± SD of three independent experiments, with technical duplicates. One-way analysis of variance (ANOVA) analysis: ****$p < 0.0001$ *vs* doxorubicin alone.

the spurious colon cancer models (HT29/DX cells).

Indeed, the different potency showed by elacridar, that is a dual inhibitor, in the two cell lines (MDCK-MDR1 and HT29/DX cells) may be due to its effects on BCRP that is expressed together with P-gp in HT29/DX cells.

Altogether, the results in MDCK-MDR1 and HT29/DX models confirm the starting hypothesis. The bioisosteric substitution of the amide group of elacridar and tariquidar allowed identifying a new set of potent oxadiazole derivatives that modulate MDR through inhibition of the P-gp efflux activity.

2.4. *Molecular modeling studies*

In the attempt to explain the activity of target compounds on MDR1 transporter, a multi-approach molecular modelling study was undertaken. As first "access point" to atomistic detail scenario, a molecular docking study was carried out, to get a reasonable binding conformation for the compounds. Briefly structures were drawn with Marvin (Marvin 22.22, Chemaxon, https://www.chemaxon.com). 3D structures were obtained and optimized using Flare™ [48–51]. Receptor structure (PDB ID: 4XWK [52]) was prepared using Flare™. Input files for molecular docking were then generated using Cambridge Crystallographic Data Centre Hermes 2022.2 and docking was fulfilled with Cambridge Crystallographic Data Centre Gold 2022.2 using default settings.

The best ranked pose of each ligand was selected for further analysis. As emerged in a previous study of ours [53], neither in this case was possible to establish a correlation between docking score and activity ranking. In order to rationalize this result, common features possibly characterizing the binding modes of most active compounds were searched. With this aim and in the attempt to keep the approach as quantitative as possible, cluster analysis was used; all the residues involved in the interactions with all the ligands were collected and grouped in 7 clusters according to the geometric center of their backbone, using k-means clustering as implemented in Scikit-learn [54] (for details, see Table S2 in Supplementary data). For each compound an interaction fingerprint was then generated, accounting for the presence or absence of interaction with the residue clusters (Table S3, Supplementary data). These fingerprints were used to populate clusters of compounds sharing partially common interaction patterns that may help to explain activity data as related to binding poses. From these analysis, four clusters of compounds (binding poses) were generated, reported in Fig. 5 (for distribution of compounds in clusters, see Table S3, Supplementary data).

The compounds of each group show indeed fairly overlapping binding poses. Among these groups, cluster 3 is the most populated by compounds endowed with high activity in the nanomolar or submicromolar range (**1**, **4**, **5**, **8**, **18**, **19**, **20**). The other ligands with

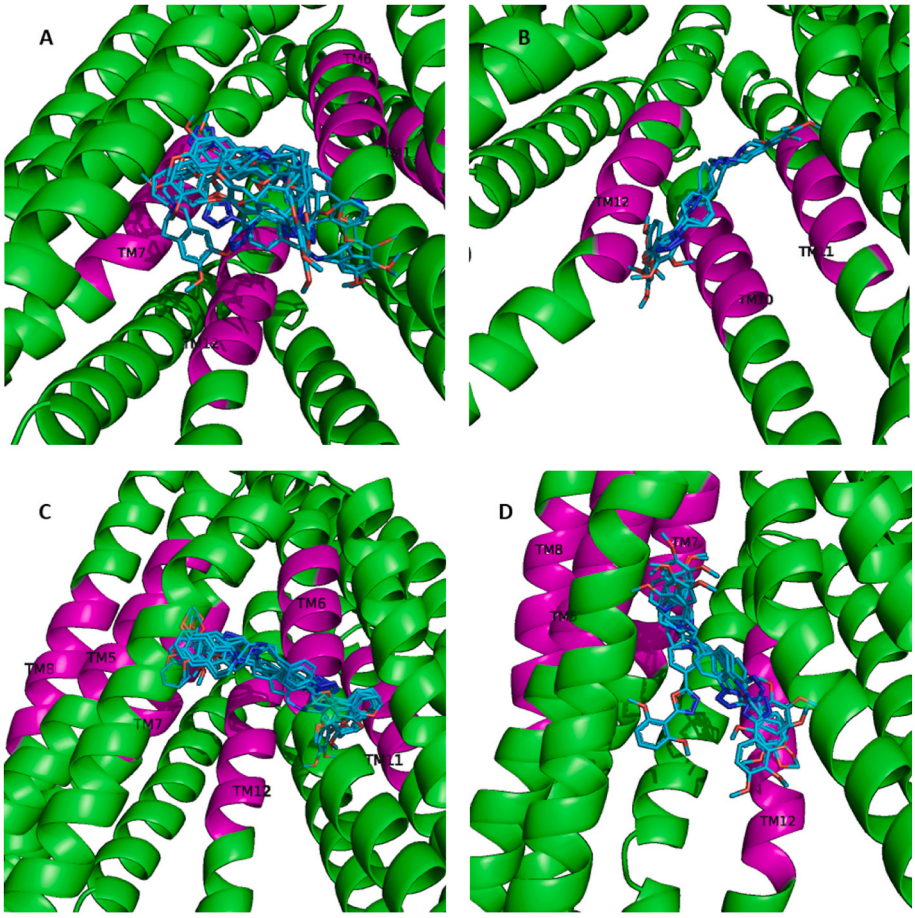

Fig. 5. Representation of the four clusters (**A-D** for cluster 1–4, respectively) in which ligands were grouped. The figure reports the four clusters accounting for common interaction features. Ligands are represented in cyan, protein is represented in green cartoon; transmembrane regions (TM) involved in the interaction with ligands are colored in magenta: TM's 1, 6, 7 and 12 for cluster 1, TM's 10, 11 and 12 for cluster 2, TM's 5, 6, 7, 11 and 12 for cluster 3, TM's 5, 7, 8 and 12 for cluster 4.

nanomolar activity are in cluster 1 (**15**) and in cluster 4 (**16** and **22**). The analysis of the patterns of cluster 3 may give indications about the interactions possibly responsible for high activity on the transporter. In particular, this pattern is characterized by extensive interactions with residues belonging to transmembrane domains (TM) 5, 6, 7, 8, 11 and 12. The interactions involved are essentially hydrophobic or aromatic.

Considering the number of highly active compounds comprised in the cluster, a deeper characterization of the binding poses of some of these compounds have been carried out through molecular dynamics simulation (MD): **1**, **5**, **8**, **19** and **20** were chosen as they display a generally high activity, spanning from low nanomolar to submicromolar range. Briefly, starting from the binding pose obtained through molecular docking, using CHARMM-GUI web server [55,56], hexagonal simulation boxes were generated, comprising the complex of the whole MDR1 structure with the ligand soaked in membrane bilayer and solvation box. The systems thus obtained were carefully equilibrated through several steps and then run for 50 ns in NPT ensemble at 1 atm and 303 K using Gromacs 2022.3 engine [57] (see Supplementary data for details). From the last 40 ns of the trajectories, a representative structure was extracted for each complex, being the medoid of the cluster accounting for more than 50% of the frames. These structures are reported in Fig. 6A–E, in which they are overlapped to the structures obtained from docking simulations.

In the case of **1**, **8** and, to a good extent, **5** (Fig. 6A–C, respectively), the comparison essentially indicates a good accordance between docking and MD: in all cases, changes in ligand pose led to gaining a π-π interaction (with Tyr806 for **1** and with Phe755 for **8**), or an edge-face interaction with Tyr946 in case of **5**. As for **19** (Fig. 6D), a slight rotation of the molecule can be seen, which leads the 2-methoxynaphtalene moiety to lose π-π interaction with Tyr303 and establish another one with Phe754, and the tetrahydroisoquinoline ring to gain a hydrogen bond with Gln343.

In case of **20** (Fig. 6E), a more substantial rearrangement is observed during MD, leading to a less extended pose. This change seems to be driven by the formation of a π-π interaction between benzene ring of tetrahydroisoquinoline moiety and Phe332 and by a more efficient packing of the bulky 2,3-dimethoxynaphtalene moiety inside a highly hydrophobic cleft formed by several aliphatic side chains: Val861, Ile864, Val978, Ala981 and Met982.

The other highly populated cluster (cluster 1, Fig. 5A) shows a larger variability in the binding poses of the ligands. Only one highly active compound is found, **15**, which is stretched toward the cytoplasmatic compartment in a peculiar way. In view of its unique very high activity inside the cluster, also in this case a MD study has been undertaken. Fig. 7 shows the representative structure of the 50 ns MD simulation (yellow sticks) overlapped on the binding pose coming from docking (cyan sticks). In this case a significant change has involved the conformation of the ligand, in which the (3,4-dimethoxyphenyl)ethenyl moiety loses contacts with TM6 and establishes contacts with TM2 and TM5.

In consideration of the very high activity and of the ample conformational change observed in the MD simulation, the system was simulated for a longer time, up to 200 ns to explore further possible conformational changes. The conformation corresponding to the most representative cluster of the trajectory is reported in Fig. 7 in light grey sticks: it shows significant differences both from the structure resulting from 50 ns MD or the one obtained from molecular docking. Noteworthy the ligand establishes a double interaction with Tyr306: a charge enforced hydrogen bond between phenol oxygen atom and the protonated nitrogen of the ligand, and a π-π stacking between phenol ring and benzene ring of the ligand; this quite favorable interaction may be

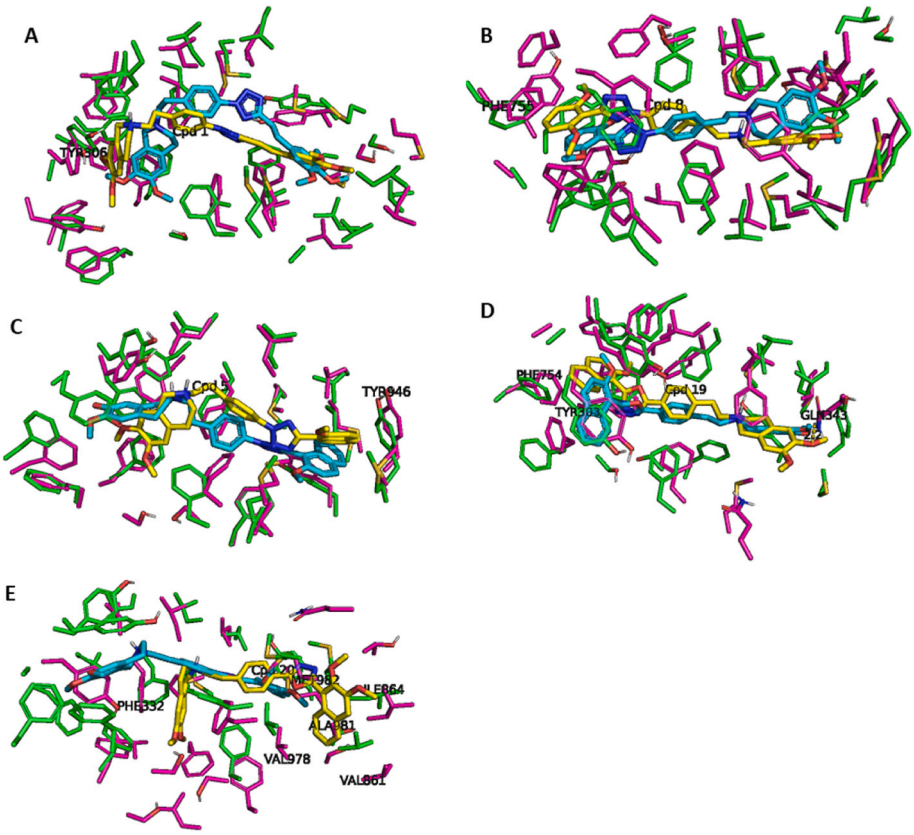

Fig. 6. Overlapped conformations of ligands belonging to cluster 3 studied through MD. (**A**) **1**; (**B**) **8**; (**C**) **5**; (**D**) **19**; (**E**) **20**. The figure reports the comparison between conformations obtained with molecular docking (cyan) and conformations obtained with MD (yellow). Interacting residues are reported in green for docking conformations and magenta for MD conformations.

responsible for an "optimized" conformation, better packed in the cavity.

Regarding cluster 4 (Fig. 5D), all ligands, with the exception of **22**, show a good overlap in binding pose, characterized by a projection towards the exit of the internal cavity. This cluster includes the last compound endowed with high activity in nanomolar range, **16**. Also for this compound, a MD study has been carried out; as it was not possible to gather meaningful information from 50 ns MD, being the conformation overlapping to the one obtained from docking and comparable to the ones of the other compounds of the cluster (data not shown), also in this case MD was extended to 200 ns. The representative structure extracted from the 200 ns trajectory is reported in Fig. 8: it indeed displays a significant conformational change in comparison with the one produced by docking; in particular, it assumes a transverse conformation in the internal cavity, gaining a π-π interaction with Phe299 and a more extensive cross-linking with several transmembrane domains (TM's 5, 6, 10 and 12).

Few words may be spent for cluster 2 (Fig. 5B), in which the three compounds share a fairly overlapping binding mode, with the tetrahydroisoquinoline ring engaged in contacts with TM11 and the distal trimethoxyphenyl moiety projected toward the membrane bilayer by means of interactions with TM10.

In order to get deeper insights into the interaction of some non-active compounds as well, 200 ns MD study was carried out on compound **12** and compound **9** belonging to cluster 1 and 2, respectively, both characterized by the presence of azole substructure II. In case of compound **12**, the representative structure of MD trajectory displays a more folded conformation, with a subsequent loss of several contacts and in particular of the hydrogen bond with Ser725 which was present in the conformation obtained through docking (Fig. S29A, Supplementary data).

On the other hand, in case of compound **9**, also the conformation resulting from MD simulation resembles the one generated through molecular docking, in a marginal position close to the membrane bilayer and with limited interaction with the transporter (Fig. S29B, Supplementary data).

To further rationalize the activity profile of the compounds, we tried to make a comparison between interactions with P-gp and BCRP. For this purpose, we selected compound **22**, which shows a remarkable difference in the two activities. The compound was docked inside the cavity of BCRP (PDB ID: 8BHT [58]). The most favored docked conformation is reported in Fig. S30 (Supplementary data), in which it is overlapped with the conformation of tariquidar from crystal structure. Starting from the docked conformation, a molecular dynamics simulation was run, extending trajectory until about 300 ns. For comparison, a molecular dynamics run for **22** bound to P-gp was carried out as well, and the trajectory was extended for about 200 ns. The two trajectories were analyzed using principal component analysis. The first component vector is reported in Fig. S31 (Supplementary data) for the two structures, while Fig. S32 (Supplementary data) reports the comparison between first and last frames of the two simulations: as for P-gp, even after a shorter molecular dynamics run, a conformational change is seen, involving mainly the nucleotide binding region, which get in closer proximity during the simulation. This movement is considered essential for triggering the hydrolysis of ATP and thus the efflux of transported ligands [59].

Also in case of BCRP, a conformational change is necessary for efflux activity [58], but during the simulation with compound **22**, more subtle movements were observed, suggesting a less productive interaction of the ligand.

Overall, even though it was not possible to draw a general view of the structure activity relationships for the target compounds, clustering

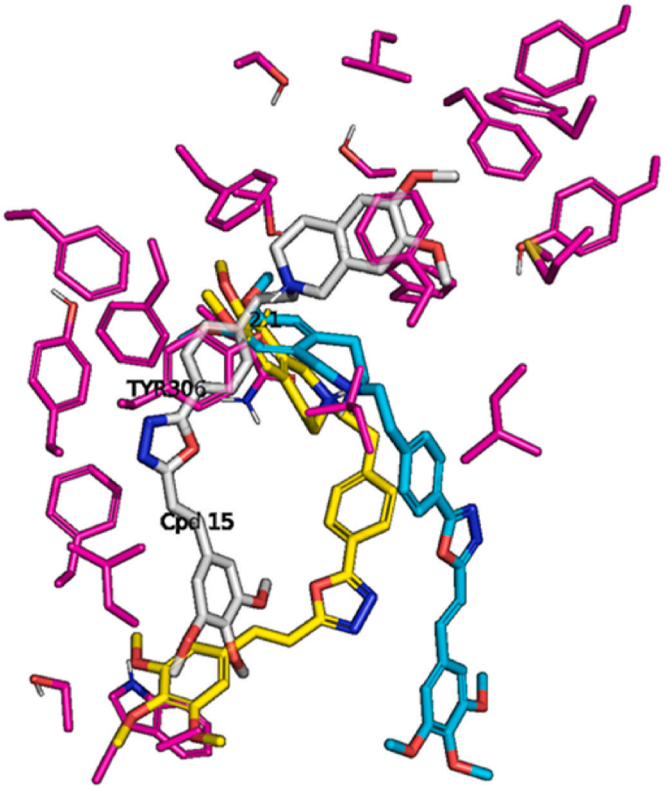

Fig. 7. Comparison of binding poses obtained through docking (cyan sticks), 50 ns MD (yellow sticks) and 200 ns MD (light grey sticks) for **15**. Interacting residues for the long MD conformation are reported in magenta sticks.

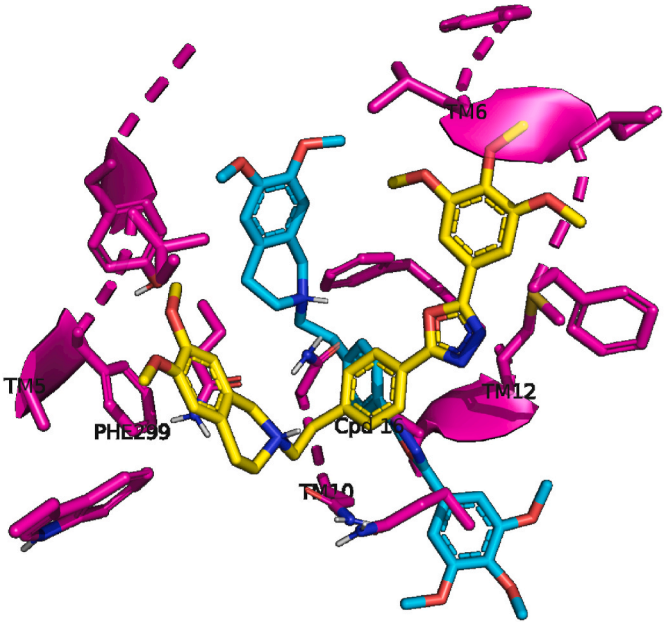

Fig. 8. Comparison between binding poses obtained through docking (cyan) and 200 ns MD (yellow) for **16**. The interacting residues are depicted in magenta and the indication of the corresponding transmembrane domain is reported.

conformations obtained by molecular docking allowed to explain the activity profile of a relevant number of compounds among the most active ones, highlighting a quite definite pattern of interaction which is shared by them. These interactions were then further characterized through molecular dynamics simulation and proved somewhat stable, at least as far as a general pose inside the cavity is concerned. For some compounds, molecular dynamics simulation was useful to give deeper characterization of the interaction with the biological target and indication regarding interactions with different transporters, providing hints which were not inferable through docking simulation. Also the in silico studies indicated compound **15** as the most interesting derivative of this series.

3. Conclusions

In this work, we described a new series of compounds able to modulate the ABC transporter proteins involved in tumor multidrug resistance (MDR). We designed and synthesized three new series of derivatives, where the amide function of the lead compounds elacridar and tariquidar was substituted with two bioisosteric groups, tetrazole and oxadiazole. In details, we designed both the 2,5- and the 1,5-disubstituted tetrazoles, and the 2,5-disubstituted-1,3,4-oxadiazoles; the heterocycles were linked to methoxy-substituted aryl moieties, that were already present in potent and efficacious P-gp dependent MDR reversers. The three series of compounds were tested on MDCK-MDR1, MDCK-MRP1 and MDCK-BCRP transfected cells overexpressing P-gp, MRP1 and BCRP, respectively, measuring the inhibition of the efflux of the pro-fluorescent probe Calcein-AM, on MDCK-MDR1 and MDCK-MRP1 cells, or the fluorescent probe Hoechst 33342 on MDCK-BCRP cells.

All compounds were able to inhibit P-gp with a high potency, reaching in most cases the medium nanomolar range or even the low nanomolar range as in the case of compounds **15** and **22** ($EC_{50} = 1.6$ nM and 3.3 nM, respectively), thus showing higher activity than lead tariquidar and elacridar. As regard SARs, P-gp inhibiting values of these compounds are mainly influenced by the nature and the substituted position of the heterocycle; in fact, 2,5-disubstituted tetrazoles and to a greater extent 2,5-disubstituted-oxadiazoles displayed excellent activity, while the 1,5-disubstituted tetrazoles turned out to be definitely less potent. Within the series, the introduction of some substituents (mainly **a** and **h**) improves the inhibitory activity of the compounds.

A partial explanation to the structure activity relationship frame towards P-gp was given through a computational study: in particular, it was possible to relate the high activity of most of the potent compounds to a common interaction pattern, involving a definite region of the internal cavity of the transporter.

Only few compounds were active on the other efflux pumps MRP1 and BCRP, however compound **15** emerged as novel P-gp/BCRP dual inhibitor, since it showed a good activity on BCRP and is an outstanding P-gp inhibitor. This is an interesting feature since P-gp and BCRP are often co-expressed in several tumors.

Co-administration of selected compounds, at 1 or 10 μM concentration, with 5 μM doxorubicin in MDCK cells, selectively overexpressing P-gp, MRP1 or BCRP, indicated that they enhanced the antiproliferative effect of doxorubicin in MDCK-MDR1 cells in a dose-dependent way, confirming their nature of P-gp modulators, and caused an increased release of LDH. Particularly, compounds **1**, **8**, **15** and **22** were the most potent in these assays.

The same selected compounds were tested on resistant HT29/DX cells, which have high levels of P-gp transporter, to move toward a setting closer to real cancers. The derivatives, which showed a very negligible cytotoxic effect (around 10%) on HT29/DX cells when used alone, markedly increased the reduction of cell viability induced by doxorubicin alone in a dose-dependent way. This effect was more pronounced in oxadiazole derivatives, reaching 64.3% for compound **18**, and confirming the trend already highlighted in the MDCK-MDR1 cell assay.

The intracellular accumulation of doxorubicin in MDCK-MDR1 and HT29/DX cells in co-administration with oxadiazole derivatives **15**–**22** was also evaluated. All compounds were able to increase intracellular

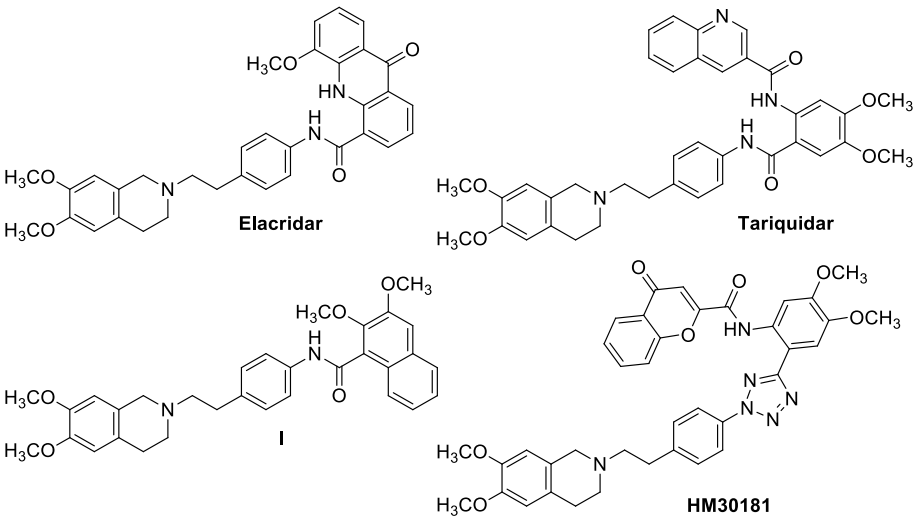

Chart 1. Elacridar, tariquidar, compound **I**, described in the previous study [34], and HM30181.

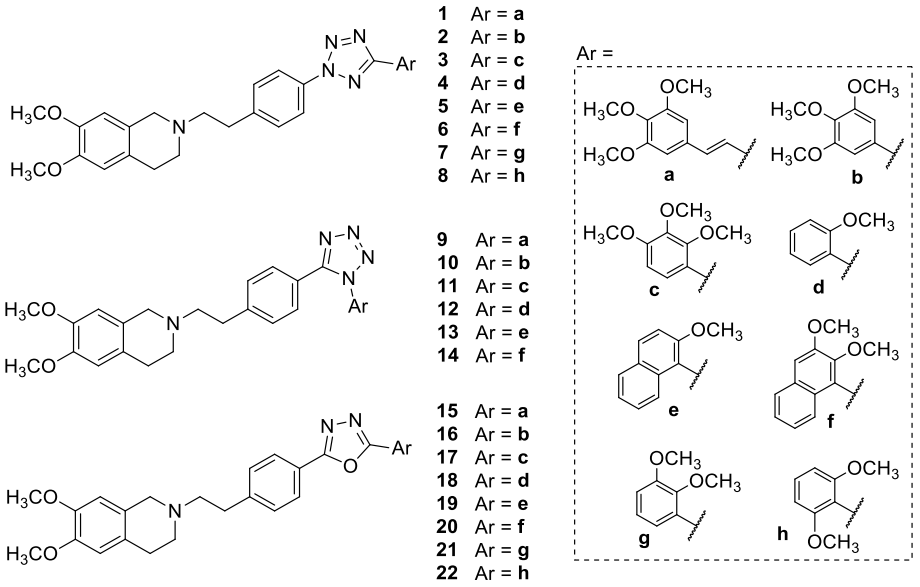

Chart 2. Structures of the synthesized 2,5- (**1**–**8**) and 1,5-disubstituted (**9-14**) tetrazoles, and of the 2,5-disubstituted-1,3,4-oxadiazoles (**15**–**22**).

doxorubicin, confirming their mechanism of action. Derivative **15** was the most potent in both these assays.

All together, these results confirm the starting hypothesis. The bioisosteric substitution of the amide group of elacridar and tariquidar allowed identifying a new set of potent oxadiazole derivatives that modulate MDR through inhibition of the P-gp efflux activity. If compared to the previously synthesized amide derivatives, the introduction of the bioisosteric heterocycles greatly enhances the activity on P-gp, introduces in two compounds a moderate inhibitory activity on MRP1 and maintains in some cases the effect on BCRP, leading to the unveiling of dual inhibitor **15**.

4. Materials and methods

4.1. Chemistry

The chemical reagents were purchased from Sigma-Aldrich (St. Louis, MI, USA). Thin layer chromatography (TLC) was performed on silica gel-aluminum backed plates (TLC silica gel 60 F_{254}, Merck) to monitor the course of the reactions, and an UV lamp (254 nm) and iodine vapor were used to visualize the TLC spots. Chromatographic separations were performed on a silica gel column by flash chromatography (silica gel 40, 0.040–0.063 mm; Merck). Yields are given after purification, unless otherwise stated. All melting points were taken on a Büchi apparatus and are uncorrected. NMR spectra were recorded at room temperature (25 °C) on a Bruker Avance 400 spectrometer (400 MHz for ^{1}H NMR, 100 MHz for ^{13}C NMR), in an appropriate solvent ($CDCl_3$, DMSO-d_6, CD_3OD). Chemical shifts (δ) are expressed in ppm referenced to TMS; spectral data are reported using the following abbreviations: s = singlet, d = doublet, dd = doublet of doublets, t = triplet, bs = broad singlet, m = multiplet, and coupling constants (J) are reported in Hz, followed by integration. Assignments of the ^{13}C signals were performed using the attached proton test (APT) technique. The solid phase extraction technique (SPE) was performed with Supelco Discovery DSC-18LT tubes (3 mL, cartridge: 500 mg), by using, as solvents, 10 mM of formic acid in mQ water:acetonitrile 80:20 (v/v) solution (solvent A), and methanol (solvent B). After conditioning the SPE-C18 cartridges with 3 mL of methanol followed by 3 mL of solvent A, the sample solutions were loaded on tubes in 10 mL of solvent A and the eluates containing the interferences were wasted. Finally, the formate

salts of purified compounds were recovered by elution of the SPE-C18 cartridges with 10 mL of solvent B. All the collected fractions were analyzed on an ESI-MS triple quadrupole (Varian 1200 L) system, in positive ion mode.

The high-resolution mass spectrometry (HRMS) analysis was performed with a Thermo Finnigan LTQ Orbitrap mass spectrometer equipped with an electrospray ionization source (ESI). The accurate mass/charge ratio measure was carried out by introducing, via syringe pump at 10 μL min-1, the sample solution (1.0 μg mL-1 in mQ water: acetonitrile 50:50), and the signal of the positive ions was acquired. The proposed experimental conditions allowed to monitoring the protonated molecules of studied compounds ($[M+H]^+$ species), that were measured with a proper dwell time to achieve 60 000 units of resolution at Full Width at Half Maximum (FWHM). The elemental composition of each compound was calculated based on its measured accurate mass/charge ratio, accepting only results with an attribution error less than 2.5 ppm and a not integer double bond/ring equivalents (RDB) value, to consider only the protonated species [60]. All compounds are >95% pure as determined by HPLC/diode-array detection (DAD) analysis: the specific analytical method used to determine purity and HPLC/DAD spectra are included in the Supplementary data. Compounds were named following IUPAC rules as applied by ChemBioDraw Ultra 14.0 software. When reactions were performed in anhydrous conditions, the mixtures were maintained under nitrogen. Free bases of final compounds **1**–**6** and **9**–**22** were transformed into the corresponding hydrochlorides as solids, by treatment with a solution of acetyl chloride (1.1 equiv.) in dry CH_3OH. The salts were crystallized from abs. ethanol/petroleum ether. Compounds **7** and **8** were obtained as formate salts after purification with SPE-C18 (see below for details).

4.1.1. General procedure for the synthesis of 2,5-substituted-2H-tetrazoles *1*–*8*

Final compounds were synthesized following the procedure described by Köhler et al. [38] with slight modifications. The aniline **39** [33] (1 equiv.) and concentrated HCl (8 equiv.) were solubilized in 1 mL of ethanol and 1 mL of water, then, in an ice-bath, a cooled solution of $NaNO_2$ (3 equiv.) in water (2.0 mL) was added. The mixture was stirred at rt for 1 h, then added dropwise, between −10 °C and −15 °C, to the proper benzenesulfonohydrazide (**31**–**38**, 1 equiv.) dissolved in pyridine (4–5 mL). When the solution arrived at rt, it was extracted three times with CH_2Cl_2: the organic phases were collected, dried over Na_2SO_4, and concentrated under reduced pressure. Finally, the residue was purified by flash chromatography, using $CH_2Cl_2/CH_3OH/NH_4OH$ 99:1:0.1 as the proper eluting system, obtaining the desired compounds as oils. TLC: $CH_2Cl_2/CH_3OH/NH_4OH$ 95:5:0.5.

4.1.1.1. *(E)-6,7-Dimethoxy-2-(4-(5-(3,4,5-trimethoxystyryl)-2H-tetrazol-2-yl)phenethyl)-1,2,3,4-tetrahydroisoquinoline (1)*.

From **39** [33] (0.083 g, 0.27 mmol) and **31** (0.10 g, 0.27 mmol), compound **1** (0.080 g, yield: 54.0%) was synthesized as a pale-yellow oil. **Free base:** ^{1}H NMR (400 MHz, $CDCl_3$) δ: 8.02 (d, J = 8.4 Hz, 2H, CH arom.); 7.73 (d, J = 16.0 Hz, 1H, C*H*═CH); 7.39 (d, J = 8.4 Hz, 2H, CH arom.); 7.10 (d, J = 16.0 Hz, 1H, CH═C*H*); 6.79 (s, 2H, CH arom.); 6.57 (s, 1H, CH arom.); 6.50 (s, 1H, CH arom.); 3.88 (s, 6H, OCH_3); 3.85 (s, 3H, OCH_3); 3.81 (s, 3H, OCH_3); 3.80 (s, 3H, OCH_3); 3.63 (s, 2H, NCH_2Ar); 2.98–2.94 (m, 2H, CH_2); 2.82–2.76 (m, 6H, CH_2) ppm. ^{13}C NMR (100 MHz, $CDCl_3$) δ: 164.17 (C); 153.50 (C); 147.61 (C); 147.28 (C); 142.42 (C); 139.16 (C); 136.79 (CH); 135.07 (C); 131.31 (C); 129.95 (CH); 126.30 (C); 126.07 (C); 119.76 (CH); 112.68 (CH); 111.38 (CH); 109.47 (CH); 104.32 (CH); 60.99 (CH_3); 59.64 (CH_2); 56.16 (CH_3); 55.95 (CH_3); 55.91 (CH_3); 55.70 (CH_2); 51.04 (CH_2); 33.65 (CH_2); 28.65 (CH_2) ppm. ESI-HRMS (m/z) calculated for $[M+H]^+$ ion species $C_{31}H_{36}N_5O_5$ = 558.2711, found 558.2706. **Hydrochloride:** pale-yellow solid; mp 226–228 °C.

4.1.1.2. *6,7-Dimethoxy-2-(4-(5-(3,4,5-trimethoxyphenyl)-2H-tetrazol-2-yl)phenethyl)-1,2,3,4-tetrahydroisoquinoline (2)*.

From **39** [33] (0.18 g, 0.57 mmol) and **32** (0.20 g, 0.57 mmol), compound **2** (0.13 g, yield: 42.8%) was synthesized as a yellow oil. **Free base:** ^{1}H NMR (400 MHz, $CDCl_3$) δ: 8.08 (d, J = 8.0 Hz, 2H, CH arom.); 7.46 (s, 2H, CH arom.); 7.42 (d, J = 8.0 Hz, 2H, CH arom.); 6.58 (s, 1H, CH arom.); 6.51 (s, 1H, CH arom.); 3.95 (s, 6H, OCH_3); 3.89 (s, 3H, OCH_3); 3.82 (s, 3H, OCH_3); 3.81 (s, 3H, OCH_3); 3.69 (s, 2H, NCH_2Ar); 3.04–2.99 (m, 2H, CH_2); 2.91–2.78 (m, 6H, CH_2) ppm. ^{13}C NMR (100 MHz, $CDCl_3$) δ: 164.98 (C); 153.71 (C); 147.62 (C); 147.30 (C); 142.55 (C); 135.12 (C); 129.91 (CH); 126.39 (C); 126.11 (C); 122.48 (C); 119.94 (CH); 111.43 (CH); 109.52 (CH); 104.17 (CH); 60.97 (CH_3); 59.64 (CH_2); 56.33 (CH_3); 55.92 (CH_3); 55.70 (CH_2); 51.03 (CH_2); 33.66 (CH_2); 28.68 (CH_2) ppm. ESI-HRMS (m/z) calculated for $[M+H]^+$ ion species $C_{29}H_{34}N_5O_5$ = 532.2554, found 532.2553. **Hydrochloride:** orange solid; mp 207–210 °C.

4.1.1.3. *6,7-Dimethoxy-2-(4-(5-(2,3,4-trimethoxyphenyl)-2H-tetrazol-2-yl)phenethyl)-1,2,3,4-tetrahydroisoquinoline (3)*.

From **39** [33] (0.15 g, 0.48 mmol) and **33** (0.17 g, 0.48 mmol), compound **3** (0.020 g, yield: 7.8%) was synthesized as an orange oil. **Free base:** ^{1}H NMR (400 MHz, $CDCl_3$) δ: 8.08 (d, J = 8.4 Hz, 2H, CH arom.); 7.78 (d, J = 8.8 Hz, 1H, CH arom.); 7.40 (d, J = 8.4 Hz, 2H, CH arom.); 6.80 (d, J = 8.8 Hz, 1H, CH arom.); 6.58 (s, 1H, CH arom.); 6.51 (s, 1H, CH arom.); 3.99 (s, 3H, OCH_3); 3.92 (s, 3H, OCH_3); 3.91 (s, 3H, OCH_3); 3.82 (s, 3H, OCH_3); 3.81 (s, 3H, OCH_3); 3.67 (s, 2H, NCH_2Ar); 3.01–2.97 (m, 2H, CH_2); 2.85–2.78 (m, 6H, CH_2) ppm. ^{13}C NMR (100 MHz, $CDCl_3$) δ: 162.97 (C); 155.60 (C); 152.65 (C); 147.86 (C); 147.49 (C); 141.62 (C); 135.39 (C); 129.90 (CH); 125.57 (C); 124.97 (CH); 119.98 (CH); 114.66 (C); 111.40 (CH); 109.48 (CH); 107.87 (CH); 61.60 (CH_3); 61.07 (CH_3); 59.06 (CH_2); 56.12 (CH_3); 55.97 (CH_3); 55.93 (CH_3); 55.19 (CH_2); 50.77 (CH_2); 33.18 (CH_2); 27.96 (CH_2) ppm. ESI-HRMS (m/z) calculated for $[M+H]^+$ ion species $C_{29}H_{34}N_5O_5$ = 532.2554, found 532.2554. **Hydrochloride:** yellow solid; mp 202–204 °C.

4.1.1.4. *6,7-Dimethoxy-2-(4-(5-(2-methoxyphenyl)-2H-tetrazol-2-yl)phenethyl)-1,2,3,4-tetrahydroisoquinoline (4)*.

From **39** [33] (0.10 g, 0.32 mmol) and **34** (0.093 g, 0.32 mmol), compound **4** (0.11 g, yield: 73.0%) was synthesized as a yellow oil. **Free base:** ^{1}H NMR (400 MHz, $CDCl_3$) δ: 8.07 (d, J = 8.4 Hz, 2H, CH arom.); 8.00 (d, J = 7.6 Hz, 1H, CH arom.); 7.43 (t, J = 7.6 Hz, 1H, CH arom.); 7.39 (d, J = 8.4 Hz, 2H, CH arom.); 7.08–7.03 (m, 2H, CH arom.); 6.57 (s, 1H, CH arom.); 6.51 (s, 1H, CH arom.); 3.92 (s, 3H, OCH_3); 3.81 (s, 3H, OCH_3); 3.80 (s, 3H, OCH_3); 3.63 (s, 2H, NCH_2Ar); 2.98–2.93 (m, 2H, CH_2); 2.82–2.75 (m, 6H, CH_2) ppm. ^{13}C NMR (100 MHz, $CDCl_3$) δ: 163.37 (C); 157.67 (C); 147.61 (C); 147.29 (C); 142.23 (C); 135.25 (C); 131.77 (CH); 130.85 (CH); 129.85 (CH); 126.24 (C); 126.03 (C); 120.79 (CH); 120.03 (CH); 116.34 (C); 111.96 (CH); 111.40 (CH); 109.50 (CH); 59.57 (CH_2); 56.05 (CH_3); 55.93 (CH_3); 55.61 (CH_2); 50.98 (CH_2); 33.57 (CH_2); 28.57 (CH_2) ppm. ESI-HRMS (m/z) calculated for $[M+H]^+$ ion species $C_{27}H_{30}N_5O_3$ = 472.2343, found 472.2343. **Hydrochloride:** yellow solid; mp 206–209 °C.

4.1.1.5. *6,7-Dimethoxy-2-(4-(5-(2-methoxynaphthalen-1-yl)-2H-tetrazol-2-yl)phenethyl)-1,2,3,4-tetrahydroisoquinoline (5)*.

From **39** [33] (0.10 g, 0.32 mmol) and **35** (0.11 g, 0.32 mmol), compound **5** (0.080 g, yield: 48.0%) was synthesized as a yellow oil. **Free base:** ^{1}H NMR (400 MHz, $CDCl_3$) δ: 8.14 (d, J = 8.4 Hz, 2H, CH arom.); 7.98 (d, J = 9.2 Hz, 1H, CH arom.); 7.81 (d, J = 8.0 Hz, 1H, CH arom.); 7.56 (d, J = 8.0 Hz, 1H, CH arom.); 7.42–7.32 (m, 5H, CH arom.); 6.58 (s, 1H, CH arom.); 6.51 (s, 1H, CH arom.); 3.89 (s, 3H, OCH_3); 3.82 (s, 3H, OCH_3); 3.81 (s, 3H, OCH_3); 3.63 (s, 2H, NCH_2Ar); 2.99–2.95 (m, 2H, CH_2); 2.85–2.75 (m, 6H, CH_2) ppm. ^{13}C NMR (100 MHz, $CDCl_3$) δ: 161.48 (C); 156.53 (C); 147.58 (C); 147.25 (C); 142.37 (C); 135.32 (C); 133.56 (C); 132.38 (CH); 129.95 (CH); 128.75 (C); 128.15 (CH); 127.58 (CH); 126.27 (C); 126.04 (C); 124.14 (CH); 124.07 (CH); 120.01 (CH); 113.18 (CH); 111.33 (CH);

109.42 (CH); 59.71 (CH_2); 56.82 (CH_3); 55.92 (CH_3); 55.70 (CH_2); 51.05 (CH_2); 33.67 (CH_2); 28.65 (CH_2) ppm. ESI-HRMS (*m/z*) calculated for $[M+H]^+$ ion species $C_{31}H_{32}N_5O_3$ = 522.2500, found 522.2499. **Hydrochloride:** yellow solid; mp 186–188 °C.

*4.1.1.6. 2-(4-(5-(2,3-Dimethoxynaphthalen-1-yl)-2H-tetrazol-2-yl)phenethyl)-6,7-dimethoxy-1,2,3,4-tetrahydroisoquinoline (**6**).* From **39** [33] (0.10 g, 0.32 mmol) and **36** (0.12 g, 0.32 mmol), compound **6** (0.080 g, yield: 45.4%) was synthesized as a yellow oil. **Free base:** ^{1}H NMR (400 MHz, $CDCl_3$) *δ*: 8.14 (d, *J* = 8.4 Hz, 2H, CH arom.); 7.74 (d, *J* = 8.0 Hz, 1H, CH arom.); 7.59 (d, *J* = 8.0 Hz, 1H, CH arom.); 7.42 (d, *J* = 8.4 Hz, 2H, CH arom.); 7.39 (t, *J* = 8.0 Hz, 1H, CH arom.); 7.32–7.28 (m, 2H, CH arom.); 6.58 (s, 1H, CH arom.); 6.52 (s, 1H, CH arom.); 4.00 (s, 3H, OCH_3); 3.92 (s, 3H, OCH_3); 3.82 (s, 3H, OCH_3); 3.81 (s, 3H, OCH_3); 3.64 (s, 2H, NCH_2Ar); 3.01–2.95 (m, 2H, CH_2); 2.83–2.76 (m, 6H, CH_2) ppm. ^{13}C NMR (100 MHz, $CDCl_3$) *δ*: 161.27 (C); 151.96 (C); 149.44 (C); 147.66 (C); 147.34 (C); 142.55 (C); 135.29 (C); 131.19 (C); 129.97 (CH); 128.02 (C); 126.81 (CH); 126.45 (C); 126.16 (C); 125.71 (CH); 124.97 (CH); 124.75 (CH); 119.95 (CH); 117.84 (C); 111.50 (CH); 109.80 (CH); 109.60 (CH); 62.26 (CH_3); 59.65 (CH_2); 55.95 (CH_3); 55.83 (CH_3); 55.72 (CH_2); 51.04 (CH_2); 33.67 (CH_2); 28.69 (CH_2) ppm. ESI-HRMS (*m/z*) calculated for $[M+H]^+$ ion species $C_{32}H_{34}N_5O_4$ = 552.2605, found 552.2604. **Hydrochloride:** yellow solid; mp 203–205 °C.

*4.1.1.7. 2-(4-(5-(2,3-Dimethoxyphenyl)-2H-tetrazol-2-yl) phenethyl)-6,7-dimethoxy-1,2,3,4-tetrahydroisoquinoline (**7**).* From **39** [33] (0.070 g, 0.22 mmol) and **37** (0.072 g, 0.22 mmol), the mixture was first purified by flash chromatography, then with SPE-C18, obtaining the formate salt of compound **7** (0.011 g, yield: 9.8%). **Free base:** ^{1}H NMR (400 MHz, $CDCl_3$) *δ*: 8.12 (d, *J* = 8.4 Hz, 2H, CH arom); 7.64 (d, *J* = 7.6 Hz, 1H, CH arom.); 7.44 (d, *J* = 8.4 Hz, 2H, CH arom.); 7.20 (t, *J* = 7.6 Hz, 1H, CH arom.); 7.07 (d, *J* = 7.6 Hz, 1H, CH arom.); 6.61 (s, 1H, CH arom.); 6.54 (s, 1H, CH arom.); 4.01 (s, 3H, OCH_3); 3.94 (s, 3H, OCH_3); 3.85 (s, 3H, OCH_3); 3.84 (s, 3H, OCH_3); 3.67 (s, 2H, NCH_2Ar); 3.03–2.99 (m, 2H, CH_2); 2.88–2.76 (m, 6H, CH_2) ppm. ESI-HRMS (*m/z*) calculated for $[M+H]^+$ ion species $C_{28}H_{32}N_5O_4$ = 502.2449, found 502.2442. **Formate:** yellow solid; mp 124–126 °C. ^{1}H NMR (400 MHz, CD_3OD) *δ*: 8.14 (d, *J* = 8.4 Hz, 2H, CH arom.); 7.60 (d, *J* = 8.4 Hz, 2H, CH arom.); 7.55 (d, *J* = 7.6 Hz, 1H, CH arom.); 7.26–7.19 (m, 2H, CH arom.); 6.77 (s, 1H, CH arom.); 6.73 (s, 1H, CH arom.); 4.26 (s, 2H, NCH_2Ar); 3.93 (s, 3H, OCH_3); 3.92 (s, 3H, OCH_3); 3.79 (s, 6H, OCH_3); 3.46–3.35 (m, 4H, CH_2); 3.27–3.21 (m, 2H, CH_2); 3.11–3.06 (m, 2H, CH_2) ppm.

*4.1.1.8. 2-(4-(5-(2,6-Dimethoxyphenyl)-2H-tetrazol-2-yl) phenethyl)-6,7-dimethoxy-1,2,3,4-tetrahydroisoquinoline (**8**).* From **39** [33] (0.070 g, 0.22 mmol) and **38** (0.072 g, 0.22 mmol), the mixture was first purified by flash chromatography, then with SPE-C18, obtaining the formate salt of compound **8** (0.018 g, yield: 16.0%). **Free base:** ^{1}H NMR (400 MHz, $CDCl_3$) *δ*: 8.12 (d, *J* = 8.0 Hz, 2H, CH arom.); 7.44–7.40 (m, 3H, CH arom.); 6.67 (d, *J* = 8.8 Hz, 2H, CH arom.); 6.61 (s, 1H, CH arom.); 6.54 (s, 1H, CH arom); 3.85 (s, 3H, OCH_3); 3.84 (s, 3H, OCH_3); 3.77 (s, 6H, OCH_3); 3.66 (s, 2H, NCH_2Ar); 3.02–2.97 (m, 2H, CH_2); 2.86–2.79 (m, 6H, CH_2) ppm. ESI-HRMS (*m/z*) calculated for $[M+H]^+$ ion species $C_{28}H_{32}N_5O_4$ = 502.2449, found 502.2445. **Formate:** yellow solid; mp 129–131 °C. ^{1}H NMR (400 MHz, CD_3OD) *δ*: 8.11 (d, *J* = 8.0 Hz, 2H, CH arom.); 7.59 (d, *J* = 8.0 Hz, 2H, CH arom.); 7.49 (t, *J* = 8.4 Hz, 1H, CH arom); 6.80–6.76 (m, 4H, CH arom.); 4.37 (s, 2H, NCH_2Ar); 3.80 (s, 3H, OCH_3); 3.79 (s, 3H, OCH_3); 3.75 (s, 6H, OCH_3); 3.56–3.45 (m, 4H, CH_2); 3.30–3.24 (m, 2H, CH_2); 3.14–3.09 (m, 2H, CH_2) ppm.

*4.1.2. General procedure for the synthesis of 1,5-substituted-1H-tetrazoles **9**–**14***

The proper tosyl derivative (**61**–**66**, 1 equiv.) was dissolved in dry CH_3CN, then Et_3N (6 equiv.) and 6,7-dimethoxy-1,2,3,4-tetrahydroisoquinoline hydrochloride (1.2 equiv.) were added. The reaction was refluxed overnight, then cooled to rt and the solvent was removed under reduced pressure. The mixture was treated with CH_2Cl_2, and the organic layer was washed twice with water, dried over Na_2SO_4, and concentrated under reduced pressure. The residue was purified by flash chromatography using the proper eluting system, yielding the desired compound as an oil.

*4.1.2.1. (E)-6,7-Dimethoxy-2-(4-(5-(3,4,5-trimethoxystyryl)-1H-tetrazol-1-yl)phenethyl)-1,2,3,4-tetrahydroisoquinoline (**9**).* From **61** (0.034 g, 0.064 mmol) and 6,7-dimethoxy-1,2,3,4-tetrahydroisoquinoline hydrochloride (0.018 g, 0.077 mmol) in 4.0 mL of dry CH_3CN, compound **9** (0.0065 g, yield: 18.1%) was synthesized as a pale-yellow oil. **Free base:** Chromatographic eluent: $CH_2Cl_2/CH_3OH/NH_4OH$ 97:3:0.3. ^{1}H NMR (400 MHz, $CDCl_3$) *δ*: 7.90 (d, *J* = 16.0 Hz, 1H, C*H*═CH); 7.52 (d, *J* = 8.0 Hz, 2H, CH arom.); 7.46 (d, *J* = 8.0 Hz, 2H, CH arom.); 6.72 (s, 2H, CH arom.); 6.67 (d, *J* = 16.0 Hz, 1H, CH═C*H*); 6.62 (s, 1H, CH arom.); 6.55 (s, 1H, CH arom.); 3.90–3.85 (m, 11H, OCH_3 and NCH_2Ar); 3.85 (s, 3H, OCH_3); 3.84 (s, 3H, OCH_3); 3.33–3.22 (m, 2H, CH_2); 3.20–2.98 (m, 6H, CH_2) ppm.^{13}C NMR (100 MHz, $CDCl_3$) *δ*: 153.58 (C); 152.35 (C); 147.67 (C); 147.30 (C); 143.00 (C); 141.65 (CH); 141.54 (CH); 130.43 (CH); 130.22 (C); 126.00 (C); 125.45 (CH); 125.32 (CH); 111.30 (CH); 109.32 (CH); 106.60 (CH); 105.28 (CH); 105.19 (CH); 61.00 (CH_3); 59.42 (CH_2); 56.38 (CH_3); 56.02 (CH_3); 55.99 (CH_3); 55.80 (CH_2); 50.26 (CH_2); 29.70 (CH_2); 25.65 (CH_2) ppm. ESI-HRMS (*m/z*) calculated for $[M+H]^+$ ion species $C_{31}H_{36}N_5O_5$ = 558.2711, found 558.2709. **Hydrochloride:** pale yellow solid; mp 170–172 °C.

*4.1.2.2. 6,7-Dimethoxy-2-(4-(5-(3,4,5-trimethoxyphenyl)-1H-tetrazol-1-yl)phenethyl)-1,2,3,4-tetrahydroisoquinoline (**10**).* From **62** (0.080 g, 0.16 mmol) and 6,7-dimethoxy-1,2,3,4-tetrahydroisoquinoline hydrochloride (0.043 g, 0.19 mmol) in 5.0 mL of dry CH_3CN, compound **10** (0.050 g, yield: 60.0%) was synthesized as a pale-yellow oil. **Free base:** Chromatographic eluent: $CH_2Cl_2/CH_3OH/NH_4OH$ 97:3:0.3. ^{1}H NMR (400 MHz, $CDCl_3$) *δ*: 7.40 (d, *J* = 8.4 Hz, 2H, CH arom.); 7.31 (d, *J* = 8.4 Hz, 2H, CH arom.); 6.73 (s, 2H, CH arom.); 6.56 (s, 1H, CH arom.); 6.49 (s, 1H, CH arom.); 3.83 (s, 3H, OCH_3); 3.81 (s, 3H, OCH_3); 3.80 (s, 3H, OCH_3); 3.63 (s, 2H, NCH_2Ar); 3.60 (s, 6H, OCH_3); 3.02–2.95 (m, 2H, CH_2); 2.82–2.75 (m, 6H, CH_2) ppm. ^{13}C NMR (100 MHz, $CDCl_3$) *δ*: 153.42 (C); 153.37 (C); 147.70 (C); 147.36 (C); 143.41 (C); 132.84 (C); 130.19 (CH); 125.85 (C); 125.75 (CH); 118.36 (C); 111.34 (CH); 109.39 (CH); 106.17 (CH); 60.97 (CH_3); 59.37 (CH_2); 55.98 (CH_3); 55.95 (CH_3); 55.91 (CH_3); 55.55 (CH_2); 50.90 (CH_2); 33.41 (CH_2); 28.46 (CH_2) ppm. ESI-HRMS (*m/z*) calculated for $[M+H]^+$ ion species $C_{29}H_{34}N_5O_5$ = 532.2554, found 532.2556. **Hydrochloride:** pale yellow solid; mp 180–183 °C.

*4.1.2.3. 6,7-Dimethoxy-2-(4-(5-(2,3,4-trimethoxyphenyl)-1H-tetrazol-1-yl)phenethyl)-1,2,3,4-tetrahydroisoquinoline (**11**).* From **63** (0.19 g, 0.37 mmol) and 6,7-dimethoxy-1,2,3,4-tetrahydroisoquinoline hydrochloride (0.10 g, 0.44 mmol) in 8.0 mL of dry CH_3CN, compound **11** (0.080 g, yield: 40.5%) was synthesized as a pale-yellow oil. **Free base:** Chromatographic eluent: $CH_2Cl_2/CH_3OH/NH_4OH$ 96:4:0.4. ^{1}H NMR (400 MHz, $CDCl_3$) *δ*: 7.25 (d, *J* = 8.8 Hz, 2H, CH arom.); 7.22 (d, *J* = 8.8 Hz, 2H, CH arom.); 7.18 (d, *J* = 8.4 Hz, 1H, CH arom.); 6.71 (d, *J* = 8.4 Hz, 1H, CH arom.); 6.55 (s, 1H, CH arom.); 6.47 (s, 1H, CH arom.); 3.87 (s, 3H, OCH_3); 3.79 (s, 3H, OCH_3); 3.78 (s, 3H, OCH_3); 3.67 (s, 3H, OCH_3); 3.58 (s, 2H, NCH_2Ar); 3.36 (s, 3H, OCH_3); 2.91–2.86 (m, 2H, CH_2); 2.80–2.67 (m, 6H, CH_2) ppm. ^{13}C NMR (100 MHz, $CDCl_3$) *δ*: 156.66 (C); 151.73 (C); 151.52 (C); 147.59 (C); 147.25 (C); 142.30 (C); 133.24 (C); 129.71 (CH); 126.21 (C); 125.99 (CH); 123.38 (CH); 111.33 (CH); 110.73 (C); 109.40 (CH); 107.25 (CH); 60.87 (CH_3); 60.63 (CH_3); 59.56 (CH_2); 56.12 (CH_3); 55.94 (CH_3); 55.90 (CH_3); 55.63 (CH_2); 50.99 (CH_2); 33.53 (CH_2); 28.61 (CH_2) ppm. ESI-HRMS (*m/z*) calculated for $[M+H]^+$ ion species $C_{29}H_{34}N_5O_5$ = 532.2554, found 532.2548. **Hydrochloride:** pale-yellow solid; mp 217–219 °C.

*4.1.2.4. 6,7-Dimethoxy-2-(4-(5-(2-methoxyphenyl)-1H-tetrazol-1-yl)phenethyl)-1,2,3,4-tetrahydroisoquinoline (**12**).* From **64** (0.060 g, 0.13 mmol) and 6,7-dimethoxy-1,2,3,4-tetrahydroisoquinoline hydrochloride (0.037 g, 0.16 mmol) in 5.0 mL of dry CH_3CN, compound **12** (0.030 g, yield: 47.9%) was synthesized as a pale-yellow oil. **Free base:** Chromatographic eluent: $CH_2Cl_2/CH_3OH/NH_4OH$ 96:4:0.4. ^{1}H NMR (400 MHz, $CDCl_3$) δ: 7.57 (d, J = 8.0 Hz, 1H, CH arom.); 7.45 (t, J = 8.0 Hz, 1H, CH arom.); 7.24 (d, J = 8.0 Hz, 2H, CH arom.); 7.19 (d, J = 8.0 Hz, 2H, CH arom.); 7.06 (t, J = 8.0 Hz, 1H, CH arom.); 6.76 (d, J = 8.0 Hz, 1H, CH arom.); 6.56 (s, 1H, CH arom.); 6.48 (s, 1H, CH arom.); 3.81 (s, 3H, OCH_3); 3.80 (s, 3H, OCH_3); 3.58 (s, 2H, NCH_2Ar); 3.25 (s, 3H, OCH_3); 2.91–2.87 (m, 2H, CH_2); 2.80–2.68 (m, 6H, CH_2) ppm. ^{13}C NMR (100 MHz, $CDCl_3$) δ: 156.66 (C); 152.04 (C); 147.67 (C); 147.33 (C); 142.19 (C); 133.63 (C); 132.96 (CH); 131.57 (CH); 129.49 (CH); 126.38 (C); 126.11 (C); 123.16 (CH); 121.14 (CH); 113.60 (C); 111.44 (CH); 109.53 (CH); 59.51 (CH_2); 55.98 (CH_3); 55.94 (CH_3); 55.67 (CH_2); 54.85 (CH_3); 50.96 (CH_2); 33.54 (CH_2); 28.67 (CH_2) ppm. ESI-HRMS (*m/z*) calculated for $[M+H]^+$ ion species $C_{27}H_{30}N_5O_3$ = 472.2343, found 472.2345. **Hydrochloride:** pale yellow solid; mp 168–170 °C.

*4.1.2.5. 6,7-Dimethoxy-2-(4-(5-(2-methoxynaphthalen-1-yl)-1H-tetrazol-1-yl)phenethyl)-1,2,3,4-tetrahydroisoquinoline (**13**).* From **65** (0.070 g, 0.14 mmol) and 6,7-dimethoxy-1,2,3,4-tetrahydroisoquinoline hydrochloride (0.039 g, 0.17 mmol) in 5.0 mL of dry CH_3CN, compound **13** (0.030 g, yield: 41.1%) was synthesized as a yellow oil. **Free base:** Chromatographic eluent: ethyl acetate 100. TLC: $CH_2Cl_2/CH_3OH/NH_4OH$ 95:5:0.5. ^{1}H NMR (400 MHz, $CDCl_3$) δ: 8.00 (d, J = 9.2 Hz, 1H, CH arom.); 7.84 (d, J = 8.0 Hz, 1H, CH arom.); 7.53 (d, J = 8.0 Hz, 1H, CH arom.); 7.49 (t, J = 8.0 Hz, 1H, CH arom.); 7.41 (t, J = 8.0 Hz, 1H, CH arom.); 7.21–7.14 (m, 5H, CH arom.); 6.58 (s, 1H, CH arom.); 6.49 (s, 1H, CH arom.); 3.83 (s, 3H, OCH_3); 3.82 (s, 3H, OCH_3); 3.64 (s, 2H, NCH_2Ar); 3.53 (s, 3H, OCH_3); 2.93–2.88 (m, 2H, CH_2); 2.85–2.72 (m, 6H, CH_2) ppm. ^{13}C NMR (100 MHz, $CDCl_3$) δ: 155.65 (C); 150.53 (C); 147.59 (C); 147.25 (C); 142.30 (C); 133.50 (CH); 132.98 (C); 132.86 (C); 129.51 (CH); 128.69 (C); 128.39 (CH); 128.32 (CH); 126.31 (C); 126.05 (C); 124.56 (CH); 123.58 (CH); 123.20 (CH); 112.47 (CH); 111.36 (CH); 109.44 (CH); 106.57 (C); 59.40 (CH_2); 55.93 (CH_3); 55.63 (CH_2); 50.92 (CH_2); 33.49 (CH_2); 28.62 (CH_2) ppm. ESI-HRMS (*m/z*) calculated for $[M+H]^+$ ion species $C_{31}H_{32}N_5O_3$ = 522.2500, found 522.2500. **Hydrochloride:** yellow solid; mp 169–171 °C.

*4.1.2.6. 2-(4-(5-(2,3-Dimethoxynaphthalen-1-yl)-1H-tetrazol-1-yl)phenethyl)-6,7-dimethoxy-1,2,3,4-tetrahydroisoquinoline (**14**).* From **66** (0.032 g, 0.060 mmol) and 6,7-dimethoxy-1,2,3,4-tetrahydroisoquinoline hydrochloride (0.016 g, 0.072 mmol) in 3.0 mL of dry CH_3CN, compound **14** (0.013 g, yield: 40.8%) was synthesized as a yellow oil. **Free base:** Chromatographic eluent: $CH_2Cl_2/CH_3OH/NH_4OH$ 97:3:0.3. ^{1}H NMR (400 MHz, $CDCl_3$) δ: 7.75 (d, J = 8.0 Hz, 1H, CH arom.); 7.42 (t, J = 8.0 Hz, 1H, CH arom.); 7.36–7.28 (m, 2H, CH arom.); 7.24 (d, J = 8.4 Hz, 2H, CH arom.); 7.19 (d, J = 8.0 Hz, 1H, CH arom.); 7.16 (d, J = 8.4 Hz, 2H, CH arom.); 6.57 (s, 1H, CH arom.); 6.49 (s, 1H, CH arom.); 3.97 (s, 3H, OCH_3); 3.82 (s, 3H, OCH_3); 3.81 (s, 3H, OCH_3); 3.66 (s, 3H, OCH_3); 3.60 (s, 2H, NCH_2Ar); 2.88–2.66 (m, 8H, CH_2) ppm. ^{13}C NMR (100 MHz, $CDCl_3$) δ: 151.35 (C); 150.19 (C); 148.79 (C); 147.82 (C); 147.44 (C); 141.87 (C); 132.49 (C); 130.97 (C); 129.79 (CH); 127.57 (C); 126.99 (CH); 126.16 (CH); 125.69 (CH); 125.51 (C); 123.82 (CH); 123.50 (CH); 114.30 (C); 111.32 (CH); 110.62 (CH); 109.39 (CH); 61.64 (CH_3); 58.84 (CH_2); 55.95 (CH_3); 55.91 (CH_3); 55.79 (CH_3); 55.12 (CH_2); 50.72 (CH_2); 33.04 (CH_2); 27.90 (CH_2) ppm. ESI-HRMS (*m/z*) calculated for $[M+H]^+$ ion species $C_{32}H_{34}N_5O_4$ = 552.2605, found 552.2605. **Hydrochloride:** yellow solid; mp 185–188 °C.

*4.1.3. General procedure for the synthesis of 2,5-substituted-1,3,4-oxadiazole compounds **15**–**22***

Final compounds were synthesized following the procedure described by Stabile et al. [40] with slight modifications. The hydrazide **71** (1 equiv.) and the proper carboxylic acid (1 equiv.) were dissolved in dry CH_3CN, then at 0 °C DIPEA (3 equiv.) and HATU (1.45 equiv.) were added in this order. The mixture was stirred 10 min at 0 °C, then at rt for 4 h. When all the acid is consumed (monitored by TLC), DIPEA (2 equiv.) and *p*-toluenesulfonyl chloride (3 equiv.) were added and the reaction is maintained at rt for 16 h. Then the solvent is removed under reduced pressure, and the mixture was treated with CH_2Cl_2. The organic layer was washed twice with water and with a saturated solution of $NaHCO_3$, dried over Na_2SO_4, and concentrated under vacuum. The residue was purified by flash chromatography using the proper eluting system, then triturated with Et_2O, obtaining the desired compounds as oils.

*4.1.3.1. (E)-2-(4-(2-(6,7-dimethoxy-3,4-dihydroisoquinolin-2(1H)-yl)ethyl)phenyl)-5-(3,4,5-trimethoxystyryl)-1,3,4-oxadiazole (**15**).* From **71** (0.070 g, 0.20 mmol) and (*E*)-3-(3,4,5-trimethoxyphenyl)acrylic acid (0.045 g, 0.20 mmol) in 2.5 mL of dry CH_3CN, compound **15** (0.020 g, yield 18.2%) was synthesized as a yellow oil. **Free base:** Chromatographic eluent: $CH_2Cl_2/CH_3OH/NH_4OH$ 95:5:0.5. ^{1}H NMR (400 MHz, $CDCl_3$) δ: 8.04 (d, J = 8.4 Hz, 2H, CH arom.); 7.54 (d, J = 16.4 Hz, 1H, C*H*═CH); 7.41 (d, J = 8.4 Hz, 2H, CH arom.); 7.02 (d, J = 16.4 Hz, 1H, CH═C*H*); 6.81 (s, 2H, CH arom.); 6.61 (s, 1H, CH arom.); 6.53 (s, 1H, CH arom.); 3.92 (s, 6H, OCH_3); 3.90 (s, 3H, OCH_3); 3.87 (s, 2H, NCH_2); 3.85 (s, 3H, OCH_3); 3.84 (s, 3H, OCH_3); 3.12–3.06 (m, 2H, CH_2); 3.04–2.90 (m, 6H, CH_2) ppm. ^{13}C NMR (100 MHz, $CDCl_3$) δ: 164.18 (C); 163.95 (C); 153.60 (C); 148.11 (C); 147.70 (C); 143.54 (C); 138.79 (CH); 130.35 (C); 129.56 (CH); 127.20 (CH); 125.00 (C); 122.08 (C); 111.34 (CH); 109.45 (CH); 109.32 (CH); 104.72 (CH); 61.02 (CH_3); 57.95 (CH_2); 56.22 (CH_3); 55.97 (CH_3); 54.31 (CH_2); 50.12 (CH_2); 32.87 (CH_2); 26.95 (CH_2) ppm. ESI-HRMS (*m/z*) calculated for $[M+H]^+$ ion species $C_{32}H_{36}N_3O_6$ = 558.2599, found 558.2595. **Hydrochloride:** yellow solid; mp 222–224 °C.

*4.1.3.2. 2-(4-(2-(6,7-dimethoxy-3,4-dihydroisoquinolin-2(1H)-yl)ethyl)phenyl)-5-(3,4,5-trimethoxyphenyl)-1,3,4-oxadiazole (**16**).* From **71** (0.070 g, 0.20 mmol) and 3,4,5-trimethoxybenzoic acid (0.042 g, 0.20 mmol) in 2.5 mL of dry CH_3CN, compound **16** (0.025 g, yield 23.8%) was synthesized as an orange oil. **Free base:** Chromatographic eluent: ethyl acetate/CH_3OH 99:1. TLC: $CH_2Cl_2/CH_3OH/NH_4OH$ 95:5:0.5. ^{1}H NMR (400 MHz, $CDCl_3$) δ: 8.06 (d, J = 8.0 Hz, 2H, CH arom.); 7.41 (d, J = 8.0 Hz, 2H, CH arom.); 7.35 (s, 2H, CH arom.); 6.60 (s, 1H, CH arom.); 6.53 (s, 1H, CH arom.); 3.97 (s, 6H, OCH_3); 3.93 (s, 3H, OCH_3); 3.84 (s, 3H, OCH_3); 3.83 (s, 3H, OCH_3); 3.71 (s, 2H, NCH_2Ar); 3.08-3.00 (m, 2H, CH_2); 2.91-2.81 (m, 6H, CH_2) ppm. ^{13}C NMR (100 MHz, $CDCl_3$) δ: 164.55 (C); 164.38 (C); 153.72 (C); 147.76 (C); 147.41 (C); 144.40 (C); 141.20 (C); 129.49 (CH); 127.09 (CH); 125.80 (C); 121.89 (C); 119.08 (C); 111.40 (CH); 109.48 (CH); 104.25 (CH); 61.04 (CH_3); 59.21 (CH_2); 56.44 (CH_3); 55.97 (CH_3); 55.93 (CH_3); 55.41 (CH_2); 50.89 (CH_2); 33.80 (CH_2); 28.29 (CH_2) ppm. ESI-HRMS (*m/z*) calculated for $[M+H]^+$ ion species $C_{30}H_{34}N_3O_6$ = 532.2442, found 532.2436. **Hydrochloride:** pale-yellow solid; mp 245–248 °C.

*4.1.3.3. 2-(4-(2-(6,7-dimethoxy-3,4-dihydroisoquinolin-2(1H)-yl)ethyl)phenyl)-5-(2,3,4-trimethoxyphenyl)-1,3,4-oxadiazole (**17**).* From **71** (0.070 g, 0.20 mmol) and 2,3,4-trimethoxybenzoic acid (0.042 g, 0.20 mmol) in 2.5 mL of dry CH_3CN, compound **17** (0.030 g, yield 29.0%) was synthesized as a yellow oil. **Free base:** Chromatographic eluent: ethyl acetate/CH_3OH 90:10. TLC: $CH_2Cl_2/CH_3OH/NH_4OH$ 90:10:1. ^{1}H NMR (400 MHz, $CDCl_3$) δ: 8.04 (d, J = 8.4 Hz, 2H, CH arom.); 7.75 (d, J = 8.8 Hz, 1H, CH arom.); 7.40 (d, J = 8.4 Hz, 2H, CH arom.); 6.81 (d, J = 8.8 Hz, 1H, CH arom.); 6.60 (s, 1H, CH arom.); 6.53 (s, 1H, CH arom.); 4.04 (s, 3H, OCH_3); 3.94 (s, 3H, OCH_3); 3.93 (s, 3H, OCH_3); 3.84 (s, 3H, OCH_3); 3.83 (s, 3H, OCH_3); 3.68 (s, 2H, NCH_2Ar); 3.03–2.97 (m, 2H, CH_2); 2.88–2.79 (m, 6H, CH_2) ppm. ^{13}C NMR (100 MHz, $CDCl_3$) δ: 164.32 (C); 162.87 (C); 156.64 (C); 152.83 (C); 147.68 (C); 147.35 (C);

144.26 (C); 143.12 (C); 129.46 (CH); 126.96 (CH); 125.92 (C); 124.97 (CH); 122.11 (C); 111.49 (C); 111.41 (CH); 109.50 (CH); 107.90 (CH); 61.68 (CH_3); 61.06 (CH_3); 59.36 (CH_2); 56.18 (CH_3); 55.95 (CH_3); 55.92 (CH_3); 55.50 (CH_2); 50.93 (CH_2); 33.86 (CH_2); 28.41 (CH_2) ppm. ESI-HRMS (*m/z*) calculated for $[M+H]^+$ ion species $C_{30}H_{34}N_3O_6$ = 532.2442, found 532.2440. **Hydrochloride:** yellow solid; mp 204–206 °C.

*4.1.3.4. 2-(4-(2-(6,7-dimethoxy-3,4-dihydroisoquinolin-2(1H)-yl)ethyl) phenyl)-5-(2-methoxyphenyl)-1,3,4-oxadiazole (**18**).* From **71** (0.080 g, 0.22 mmol) and 2-methoxybenzoic acid (0.034 g, 0.22 mmol) in 2.5 mL of dry CH_3CN, compound **18** (0.050 g, yield 47.1%) was synthesized as a yellow oil. **Free base:** Chromatographic eluent: ethyl acetate/CH_3OH 90:10. TLC: $CH_2Cl_2/CH_3OH/NH_4OH$ 90:10:1. ^1H NMR (400 MHz, $CDCl_3$) δ: 8.06 (d, J = 8.0 Hz, 2H, CH arom.); 8.00 (d, J = 7.6 Hz, 1H, CH arom.); 7.51 (t, J = 7.6 Hz, 1H, CH arom.); 7.40 (d, J = 8.0 Hz, 2H, CH arom.); 7.11–7.05 (m, 2H, CH arom.); 6.60 (s, 1H, CH arom.); 6.53 (s, 1H, CH arom.); 3.99 (s, 3H, OCH_3); 3.84 (s, 3H, OCH_3); 3.83 (s, 3H, OCH_3); 3.70 (s, 2H, NCH_2Ar); 3.05–2.99 (m, 2H, CH_2); 2.91–2.82 (m, 6H, CH_2) ppm. ^{13}C NMR (100 MHz, $CDCl_3$) δ: 163.22 (C); 157.91 (C); 147.80 (C); 147.44 (C); 144.02 (C); 133.02 (CH); 130.43 (CH); 129.42 (CH); 127.09 (CH); 125.73 (C); 122.18 (C); 120.76 (CH); 112.04 (CH); 111.43 (CH); 109.54 (CH); 59.05 (CH_2); 56.04 (CH_3) 55.97 (CH_3); 55.93 (CH_3); 55.24 (CH_2); 50.76 (CH_2); 33.63 (CH_2); 28.09 (CH_2) ppm. ESI-HRMS (*m/z*) calculated for $[M+H]^+$ ion species $C_{28}H_{30}N_3O_4$ = 472.2231, found 472.2226. **Hydrochloride:** yellow solid; mp 197–199 °C.

*4.1.3.5. 2-(4-(2-(6,7-dimethoxy-3,4-dihydroisoquinolin-2(1H)-yl)ethyl) phenyl)-5-(2-methoxynaphthalen-1-yl)-1,3,4-oxadiazole (**19**).* From **71** (0.065 g, 0.18 mmol) and **47** [34] (0.036 g, 0.18 mmol) in 3.0 mL of dry CH_3CN, compound **19** (0.030 g, yield 20.9%) was synthesized as a yellow oil. **Free base:** Chromatographic eluent: ethyl acetate/CH_3OH 93:7. ^1H NMR (400 MHz, $CDCl_3$) δ: 8.08 (d, J = 8.0 Hz, 2H, CH arom.); 8.05 (d, J = 9.2 Hz, 1H, CH arom.); 7.91 (d, J = 8.4 Hz, 1H, CH arom.); 7.84 (d, J = 8.4 Hz, 1H, CH arom.); 7.50 (t, J = 8.4 Hz, 1H, CH arom.); 7.42–7.35 (m, 4H, CH arom.); 6.60 (s, 1H, CH arom.); 6.53 (s, 1H, CH arom.); 3.97 (s, 3H, OCH_3); 3.84 (s, 3H, OCH_3); 3.83 (s, 3H, OCH_3); 3.71 (s, 2H, NCH_2Ar); 3.05–3.00 (m, 2H, CH_2); 2.91–2.82 (m, 6H, CH_2) ppm. ^{13}C NMR (100 MHz, $CDCl_3$) δ: 165.35 (C); 161.50 (C); 157.37 (C); 147.93 (C); 147.55 (C); 133.65 (CH); 133.08 (C); 129.48 (CH); 128.63 (C); 128.23 (CH); 127.23 (CH); 124.42 (CH); 124.10 (CH); 122.35 (C); 112.88 (CH); 111.41 (CH); 109.50 (CH); 58.88 (CH_2); 56.77 (CH_3); 55.98 (CH_3); 55.94 (CH_3); 55.09 (CH_2); 50.72 (CH_2); 33.47 (CH_2); 27.84 (CH_2) ppm. ESI-HRMS (*m/z*) calculated for $[M+H]^+$ ion species $C_{32}H_{32}N_3O_4$ = 522.2387, found 522.2383. **Hydrochloride:** yellow solid; mp 163–165 °C.

*4.1.3.6. 2-(4-(2-(6,7-dimethoxy-3,4-dihydroisoquinolin-2(1H)-yl)ethyl) phenyl)-5-(2,3-dimethoxynaphthalen-1-yl)-1,3,4-oxadiazole (**20**).* From **71** (0.065 g, 0.18 mmol) and **48** [34] (0.042 g, 0.18 mmol) in 3.0 mL of dry CH_3CN, compound **20** (0.020 g, yield 20.1%) was synthesized as a yellow oil. **Free base:** Chromatographic eluent: ethyl acetate/CH_3OH 90:10. ^1H NMR (400 MHz, $CDCl_3$) δ: 8.08 (d, J = 8.4 Hz, 2H, CH arom.); 7.93 (d, J = 8.0 Hz, 1H, CH arom.); 7.77 (d, J = 8.0 Hz, 1H, CH arom.); 7.46–7.37 (m, 5H, CH arom.); 6.60 (s, 1H, CH arom.); 6.54 (s, 1H, CH arom.); 4.04 (s, 3H, OCH_3); 3.99 (s, 3H, OCH_3); 3.84 (s, 6H, OCH_3); 3.69 (s, 2H, NCH_2Ar); 3.04–2.98 (m, 2H, CH_2); 2.90–2.78 (m, 6H, CH_2) ppm. ^{13}C NMR (100 MHz, $CDCl_3$) δ: 165.43 (C); 161.03 (C); 151.62 (C); 150.11 (C); 147.64 (C); 147.31 (C); 144.62 (C); 131.06 (C); 129.55 (CH); 127.32 (C); 127.15 (CH); 126.88 (CH); 126.08 (CH); 125.95 (C); 125.60 (CH); 124.63 (CH); 121.97 (C); 111.35 (CH); 110.93 (CH); 109.46 (CH); 62.24 (CH_3); 59.49 (CH_2); 55.91 (CH_3); 55.61 (CH_2); 51.01 (CH_2); 33.95 (CH_2); 28.52 (CH_2) ppm. ESI-HRMS (*m/z*) calculated for $[M+H]^+$ ion species $C_{33}H_{34}N_3O_5$ = 552.2493, found 552.2491. **Hydrochloride:** yellow solid; mp 157–160 °C.

*4.1.3.7. 2-(4-(2-(6,7-dimethoxy-3,4-dihydroisoquinolin-2(1H)-yl)ethyl) phenyl)-5-(2,3-dimethoxyphenyl)-1,3,4-oxadiazole (**21**).* From **71** (0.060 g, 0.17 mmol) and 2,3-dimethoxybenzoic acid (0.025 g, 0.17 mmol) in 3.0 mL of dry CH_3CN, compound **21** (0.020 g, yield 23.6%) was synthesized as a yellow oil. **Free base:** Chromatographic eluent: ethyl acetate/CH_3OH 90:10. ^1H NMR (400 MHz, $CDCl_3$) δ: 8.03 (d, J = 8.0 Hz, 2H, CH arom.); 7.60 (d, J = 7.6 Hz, 1H, CH arom.); 7.40 (d, J = 8.0 Hz, 2H, CH arom.); 7.20 (t, J = 7.6 Hz, 1H, CH arom.); 7.10 (d, J = 7.6 Hz, 1H, CH arom.); 6.60 (s, 1H, CH arom.); 6.55 (s, 1H, CH arom.); 4.01 (s, 3H, OCH_3); 3.94 (s, 3H, OCH_3); 3.85–3.83 (m, 8H, OCH_3 and NCH_2Ar); 3.12–3.01 (m, 6H, CH_2); 2.97–2.90 (m, 2H, CH_2) ppm. ^{13}C NMR (100 MHz, $CDCl_3$) δ: 164.62 (C); 163.02 (C); 153.75 (C); 148.10 (C); 147.68 (C); 143.06 (C); 129.67 (CH); 129.46 (CH); 127.19 (CH); 124.72 (C); 123.54 (C); 122.28 (C); 121.52 (CH); 121.36 (CH); 118.65 (C); 111.31 (CH); 111.09 (CH); 109.48 (CH); 109.29 (CH); 58.09 (CH_2); 56.05 (CH_3); 55.57 (CH_3); 50.41 (CH_2); 32.71 (CH_2); 26.94 (CH_2) ppm. ESI-HRMS (*m/z*) calculated for $[M+H]^+$ ion species $C_{29}H_{32}N_3O_5$ = 502.2336, found 502.2333. **Hydrochloride:** yellow solid; mp 174–176 °C.

*4.1.3.8. 2-(4-(2-(6,7-dimethoxy-3,4-dihydroisoquinolin-2(1H)-yl)ethyl) phenyl)-5-(2,6-dimethoxyphenyl)-1,3,4- oxadiazole (**22**).* From **71** (0.080 g, 0.22 mmol) and 2,6-dimethoxybenzoic acid (0.041 g, 0.22 mmol) in 3.0 mL of dry CH_3CN, compound **22** (0.020 g, yield 17.7%) was synthesized as a yellow oil. **Free base:** Chromatographic eluent: $CH_2Cl_2/CH_3OH/NH_4OH$ 97:3:0.3. ^1H NMR (400 MHz, $CDCl_3$) δ: 8.04 (d, J = 8.0 Hz, 2H, CH arom.); 7.45 (t, J = 7.6 Hz, 1H, CH arom.); 7.38 (d, J = 8.0 Hz, 2H, CH arom.); 6.64 (d, J = 7.6 Hz, 2H, CH arom.); 6.60 (s, 1H, CH arom.); 6.54 (s, 1H, CH arom.); 3.84 (s, 6H, OCH_3); 3.81 (s, 6H, OCH_3); 3.66 (s, 2H, NCH_2Ar); 3.01–2.96 (m, 2H, CH_2); 2.85–2.78 (m, 6H, CH_2) ppm. ESI-HRMS (*m/z*) calculated for $[M+H]^+$ ion species $C_{29}H_{32}N_3O_5$ = 502.2336, found 502.2331. **Hydrochloride:** yellow solid; mp 187–189 °C.

*4.1.4. General procedure for the synthesis of esters **25** and **26***

2,3-Dimethoxybenzoic acid or 2,6-dimethoxybenzoic acid (1 equiv.) were dissolved in 4.0 mL of dry methanol, and $SOCl_2$ (1 equiv.) was added. The mixture was refluxed for 5 h, then the solvent was removed under vacuum. The residue was treated twice with cyclohexane, and the solvent was removed under reduce pressure, obtaining the desired esters.

*4.1.4.1. Methyl 2,3-dimethoxybenzoate (**25**).* From 2,3-dimethoxybenzoic acid (0.25 g, 1.37 mmol), compound **25** (0.21 g, yield: 78.1%) was obtained as a white solid. TLC: CH_2Cl_2/CH_3OH 92:8. Mp: 47–49 °C. ^1H NMR (400 MHz, $CDCl_3$) δ: 7.30 (dd, J = 7.2, 2.4 Hz, 1H, CH arom.); 7.09–7.03 (m, 2H, CH arom.); 3.89 (s, 6H, OCH_3); 3.86 (s, 3H, OCH_3) ppm.

*4.1.4.2. Methyl 2,6-dimethoxybenzoate (**26**).* From 2,6-dimethoxybenzoic acid (0.25 g, 1.37 mmol), compound **26** (0.25 g, yield: 93.0%) was obtained as a white solid. TLC: CH_2Cl_2/CH_3OH 95:5. Mp: 86–88 °C. ^1H NMR (400 MHz, $CDCl_3$) δ: 7.28 (t, J = 8.4 Hz, 1H, CH arom.); 6.55 (d, J = 8.4 Hz, 2H, CH arom.); 3.90 (s, 3H, OCH_3); 3.81 (s, 6H, OCH_3) ppm.

*4.1.5. General procedure for the synthesis of alcohols **27** and **28***

A solution of the ester **25** or **26** (1 equiv.) in dry THF was cooled to 0 °C, then $LiAlH_4$ (3 equiv.) was added. The reaction was stirred for 5 min at 0 °C and 3 h at rt; then, the mixture was cooled to 0 °C and cold water and 3.0 mL of a 10% NaOH solution were added. The mixture was diluted with 10.0 mL of diethyl ether and filtered under vacuum. The liquid layer was concentrated under vacuum, treated with water and extracted with ethyl acetate. The organic layer was dried over Na_2SO_4,

and concentrated under vacuum, leading to the proper alcohols.

*4.1.5.1. (2,3-dimethoxyphenyl)methanol (**27**).* From **25** (0.21 g, 1.07 mmol) in 3.0 mL of dry THF, compound **27** (0.170 mg, yield 94.4%) was obtained as a pale-yellow solid. TLC: hexane/ethyl acetate 50:50. Mp: 46–48 °C. ^{1}H NMR (400 MHz, $CDCl_3$) δ: 7.03 (t, J = 8.0 Hz, 1H, CH arom.), 6.92 (d, J = 8.0 Hz, 1H, CH arom.), 6.87 (d, J = 8.0 Hz, 1H, CH arom.), 4.68 (s, 2H, CH_2OH), 3.87 (s, 3H, OCH_3), 3.86 (s, 3H, OCH_3), 2.43 (bs, 1H, OH) ppm.

*4.1.5.2. (2,6-dimethoxyphenyl)methanol (**28**).* From **26** (0.084 g, 0.43 mmol) in 3.0 mL of dry THF, compound **28** (0.058 g, yield 80.6%) was obtained as a pale-yellow solid. TLC: hexane/ethyl acetate 50:50. Mp: 54–56 °C. ^{1}H NMR (400 MHz, $CDCl_3$) δ: 7.20 (t, J = 8.4 Hz, 1H, CH arom), 6.50 (d, J = 8.4 Hz, 2H, CH arom), 4.80 (s, 2H, CH_2OH), 3.82 (s, 6H, OCH_3), 2.54 (bs, 1H, OH) ppm.

*4.1.6. General procedure for the synthesis of aldehydes **24, 29** and **30***

To a suspension of pyridinium chlorochromate (1.5 equiv.) and Celite (0.34 g) in dry CH_2Cl_2, the proper alcohol ((3,4,5-trimethoxyphenyl)methanol, **27** or **28** (1 equiv.)) was added. The mixture was stirred at rt for 5 h, then it was cooled to rt, filtered under vacuum, and concentrated under reduced pressure. The residue was purified by flash chromatography, using the proper eluting system, to obtain the desired aldehydes.

*4.1.6.1. 3,4,5-trimethoxybenzaldehyde (**24**).* From (3,4,5-trimethoxyphenyl)methanol (0.30 g, 1.51 mmol), compound **24** (0.23 g, yield 77.6%) was synthesized as a white solid. Chromatographic eluent: CH_2Cl_2/CH_3OH 99:1. Mp: 72–74 °C. ^{1}H NMR (400 MHz, $CDCl_3$) δ: 9.84 (s, 1H, CHO); 7.10 (s, 2H, CH arom.); 3.92 (s, 6H, OCH_3); 3.91 (s, 3H, OCH_3) ppm.

*4.1.6.2. 2,3-dimethoxybenzaldehyde (**29**).* From **27** (0.17 g, 1.01 mmol), compound **29** (0.16 g, yield 95.3%) was synthesized as a white solid. Chromatographic eluent: hexane/ethyl acetate 50:50. Mp: 50–52 °C. ^{1}H NMR (400 MHz, $CDCl_3$) δ: 10.41 (s, 1H, CHO); 7.40 (dd, J = 6.8, 2.4 Hz, 1H, CH arom.); 7.15–7.09 (m, 2H, CH arom.); 3.97 (s, 3H, OCH_3); 3.89 (s, 3H, OCH_3) ppm.

*4.1.6.3. 2,6-dimethoxybenzaldehyde (**30**).* From **28** (0.14 g, 0.83 mmol), compound **30** (0.11 g, yield 79.5%) was obtained as a white solid. Chromatographic eluent: hexane/ethyl acetate 50:50. Mp: 95–97 °C. ^{1}H NMR (400 MHz, $CDCl_3$) δ: 10.50 (s, 1H, CHO); 7.44 (t, J = 8.4 Hz, 1H, CH arom.); 6.57 (d, J = 8.4 Hz, 2H, CH arom.); 3.89 (s, 6H, OCH_3) ppm.

*4.1.7. General procedure for the synthesis of methoxy-substituted aryl benzenesulfonohydrazides **31–38***

Following the procedure described by Gujarati et al. [61] with slight modifications, the proper aldehyde (1 equiv.) and benzenesulfonyl hydrazide (1 equiv.) were suspended in the adequate amount of ethanol and the mixture was stirred at rt for 3 h. Upon completion of the reaction, the precipitate was filtered and dried under vacuum. Otherwise, if the desired compound did not precipitate, the solvent was removed under reduced pressure and the residue was purified by flash chromatography using the proper eluting system, yielding the benzenesulfonohydrazides as pure solids/oils.

*4.1.7.1. (E)-N'-((E)-3-(3,4,5-trimethoxyphenyl)allylidene)benzenesulfonohydrazide (**31**).* From **23** [33] (0.090 g, 0.40 mmol) and benzenesulfonyl hydrazide (0.084 g, 0.49 mmol) in 3.0 mL of ethanol, compound **31** (0.10 g, yield 65.7%) was obtained as a yellow oil. Chromatographic eluent: CH_2Cl_2/CH_3OH 99:1. TLC: $CH_2Cl_2/CH_3OH/NH_4OH$ 95:5:0.5. ^{1}H NMR (400 MHz, $CDCl_3$) δ: 8.33 (bs, 1H, NH); 7.94 (d, J = 7.6 Hz, 2H, CH arom.); 7.59–7.46 (m, 4H, CH arom. and CH); 6.72 (d, J = 8.4 Hz, 1H, CH); 6.69 (s, 1H, CH); 6.60 (s, 2H, CH arom.); 3.81 (s, 9H, OCH_3) ppm.

*4.1.7.2. (E)-N'-(3,4,5-trimethoxybenzylidene)benzenesulfonohydrazide (**32**).* From **24** (0.23 g, 1.17 mmol) and benzenesulfonyl hydrazide (0.20 g, 1.17 mmol) in 8.0 mL of ethanol, compound **32** (0.34 g, yield 83.0%) precipitated as a pure white solid. TLC: $CH_2Cl_2/CH_3OH/NH_4OH$ 93:7:0.7. Mp: 181–183 °C. ^{1}H NMR (400 MHz, $CDCl_3$) δ: 7.95 (d, J = 7.2 Hz, 2H, CH arom.); 7.86 (bs, 1H, NH); 7.67 (s, 1H, CH); 7.57 (t, J = 7.2 Hz, 1H, CH arom.); 7.49 (t, J = 7.2 Hz, 2H, CH arom.); 6.78 (s, 2H, CH arom.); 3.83 (s, 6H, OCH_3); 3.82 (s, 3H, OCH_3) ppm.

*4.1.7.3. (E)-N'-(2,3,4-trimethoxybenzylidene)benzenesulfonohydrazide (**33**).* From 2,3,4-trimethoxy-1-benzaldehyde (0.29 g, 1.48 mmol) and benzenesulfonyl hydrazide (0.25 g, 1.48 mmol) in 8.0 mL of ethanol, compound **33** (0.45 g, yield 86.9%) precipitated as a pure yellow solid. TLC: $CH_2Cl_2/CH_3OH/NH_4OH$ 93:7:0.7. Mp: 178–180 °C. ^{1}H NMR (400 MHz, $CDCl_3$) δ: 7.99–7.94 (m, 3H, CH arom. and CH); 7.88 (bs, 1H, NH); 7.53–7.47 (m, 4H, CH arom.); 6.64 (d, J = 8.4 Hz, 1H, CH arom.); 3.83 (s, 3H, OCH_3); 3.81 (s, 3H, OCH_3); 3.79 (s, 3H, OCH_3) ppm.

*4.1.7.4. (E)-N'-(2-methoxybenzylidene)benzenesulfonohydrazide (**34**).* From 2-methoxybenzaldehyde (0.09 mL, 0.73 mmol) and benzenesulfonyl hydrazide (0.13 g, 0.73 mmol) in 6.0 mL of ethanol, compound **34** (0.17 g, yield 79.8%) was obtained as a white solid. Chromatographic eluent: CH_2Cl_2/CH_3OH 99:1. Mp: 184–187 °C. ^{1}H NMR (400 MHz, $CDCl_3$) δ: 8.19 (s, 1H, CH); 7.99 (d, J = 8.4 Hz, 2H, CH arom.); 7.82 (d, J = 8.4 Hz, 1H, CH arom.); 7.59–7.48 (m, 3H, CH arom.); 7.33 (t, J = 8.4 Hz, 1H, CH arom.); 6.93 (t, J = 8.4 Hz, 1H, CH arom.); 6.85 (d, J = 8.4 Hz, 1H, CH arom.); 3.80 (s, 3H, OCH_3) ppm.

*4.1.7.5. (E)-N'-((2-methoxynaphthalen-1-yl)methylene)benzenesulfonohydrazide (**35**).* From 2-methoxy-1-naphthaldehyde (0.20 g, 1.07 mmol) and benzenesulfonyl hydrazide (0.18 g, 1.07 mmol) in 5.0 mL of ethanol, compound **35** (0.36 g, yield 98.8%) precipitated as a pale-yellow solid. TLC: $CH_2Cl_2/CH_3OH/NH_4OH$ 95:5:0.5. Mp: 150–152 °C. ^{1}H NMR (400 MHz, DMSO-d_6) δ: 8.53–8.49 (m, 2H, CH arom. and CH); 7.95 (d, J = 9.2 Hz, 1H, CH arom.); 7.93–7.87 (m, 2H, CH arom.); 7.81 (d, J = 7.6 Hz, 1H, CH arom.); 7.67–7.58 (m, 3H, CH arom.); 7.40 (d, J = 9.2 Hz, 1H, CH arom.); 7.38–7.31 (m, 2H, CH arom.); 3.88 (s, 3H, OCH_3) ppm.

*4.1.7.6. (E)-N'-((2,3-dimethoxynaphthalen-1-yl)methylene)benzenesulfonohydrazide (**36**).* From 2,3-dimethoxy-1-naphthaldehyde (0.20 g, 0.92 mmol) and benzenesulfonyl hydrazide (0.16 g, 0.92 mmol) in 5.0 mL of ethanol, compound **36** (0.34 g, yield 99.2%) was obtained as a white solid. Chromatographic eluent: $CH_2Cl_2/CH_3OH/NH_4OH$ 99:1:0.1. Mp: 142–144 °C. ^{1}H NMR (400 MHz, DMSO-d_6) δ: 8.46–8.42 (m, 2H, CH arom. and CH); 7.93–7.86 (m, 2H, CH arom.); 7.77 (d, J = 7.6 Hz, 1H, CH arom.); 7.67–7.59 (m, 3H, CH arom.); 7.44 (s, 1H, CH arom.); 7.36 (t, J = 7.6 Hz, 1H, CH arom.); 7.27 (t, J = 7.6 Hz, 1H, CH arom.); 3.88 (s, 3H, OCH_3); 3.72 (s, 3H, OCH_3) ppm.

*4.1.7.7. (E)-N'-(2,3-dimethoxybenzylidene)benzenesulfonohydrazide (**37**).* From **29** (0.10 g, 0.60 mmol) and benzenesulfonyl hydrazide (0.10 g, 0.60 mmol) in 8.0 mL of ethanol, compound **37** (0.15 g, yield 77.8%) was synthesized as a pale-yellow oil. TLC: $CH_2Cl_2/CH_3OH/NH_4OH$ 95:5:0.5. ^{1}H NMR (400 MHz, $CDCl_3$) δ: 8.63 (bs, 1H, NH); 8.14 (s, 1H, CH); 7.97 (d, J = 8.0 Hz, 2H, CH arom.); 7.56–7.48 (m, 3H, CH arom.); 7.38 (d, J = 8.0 Hz, 1H, CH arom.); 7.00 (t, J = 8.0 Hz, 1H, CH arom.); 6.89 (d, J = 8.0 Hz, 1H, CH arom.); 3.82 (s, 3H, OCH_3); 3.75 (s, 3H, OCH_3) ppm.

*4.1.7.8. (E)-N'-(2,6-dimethoxybenzylidene)benzenesulfonohydrazide (**38**).* From **30** (0.11 g, 0.66 mmol) and benzenesulfonyl hydrazide (0.11 g, 0.66 mmol) in 8.0 mL of ethanol, compound **38** (0.10 g, yield 47.2%) precipitated as a yellow solid. TLC: $CH_2Cl_2/CH_3OH/NH_4OH$ 95:5:0.5. Mp: 129–132 °C. ^{1}H NMR (400 MHz, $CDCl_3$) δ: 8.18 (s, 1H, CH); 8.01 (d, J = 8.0 Hz, 2H, CH arom); 7.56–7.47 (m, 3H, CH arom); 7.27 (t, J = 8.4 Hz, 1H, CH arom); 6.53 (d, J = 8.4 Hz, 2H, CH arom.); 3.82 (s, 6H, OCH_3) ppm.

*4.1.8. Methyl 2-(4-aminophenyl)acetate (**40**)*

To a solution of 2-(4-aminophenyl)acetic acid (1.00 g, 6.61 mmol) in 20.0 mL of dry methanol, $SOCl_2$ (0.48 mL, 6.61 mmol) was added. The reaction mixture was refluxed for 3 h, then cooled to rt and the solvent was removed under reduced pressure. The residue was treated twice with cyclohexane and the solvent was removed under vacuum. The mixture was dissolved in CH_2Cl_2 and the organic phase was washed twice with Na_2CO_3, dried over Na_2SO_4 and concentrated under reduced pressure, obtaining **40** (1.08 g, yield: 99.0%) as a brown oil. TLC: CH_2Cl_2/CH_3OH 90:10. ^{1}H NMR (400 MHz, $CDCl_3$) δ: 7.03 (d, J = 7.6 Hz, 2H, CH arom.); 6.60 (d, J = 7.6 Hz, 2H, CH arom.); 3.64 (s, 3H, OCH_3); 3.55 (bs, 2H, NH_2); 3.48 (s, 2H, CH_2) ppm.

*4.1.9. General procedure for the synthesis of amides **41**–**45***

To a solution of the proper carboxylic acid (1 equiv.) in the adequate amount of $CHCl_3$ (free of ethanol), $SOCl_2$ (10 equiv.) was added. The mixture was refluxed for 5 h, then it was cooled to rt, and the solvent was removed under reduced pressure. The residue was treated twice with cyclohexane and the solvent was removed under vacuum. The obtained acyl chloride was dissolved in the adequate amount of $CHCl_3$ (free of ethanol) and **40** (1 equiv.) was added: the reaction was stirred at rt for 18 h, then treated with CH_2Cl_2. The organic layer was washed with 1 N HCl, then four times with a saturated solution of $NaHCO_3$, dried over Na_2SO_4, and concentrated under reduced pressure. The desired compounds were obtained as pure oils/solids, or the residue was purified by flash chromatography using the proper eluting system.

*4.1.9.1. (E)-methyl 2-(4-(3-(3,4,5-trimethoxyphenyl)acrylamido)phenyl) acetate (**41**).* From (*E*)-3-(3,4,5-trimethoxyphenyl)acrylic acid (0.58 g, 2.43 mmol) and **40** (0.40 g, 2.43 mmol), compound **41** (0.76 g, yield 84.3%) was obtained as a pure yellow oil. TLC: $CH_2Cl_2/CH_3OH/NH_4OH$ 95:5:0.5. ^{1}H NMR (400 MHz, $CDCl_3$) δ: 8.13 (bs, 1H, NH); 7.62 (d, J = 16.0 Hz, 1H, C*H*═CH); 7.58 (d, J = 8.4 Hz, 2H, CH arom.); 7.20 (d, J = 8.4 Hz, 2H, CH arom.); 6.68 (s, 2H, CH arom.); 6.54 (d, J = 16.0 Hz, 1H, CH═C*H*); 3.85 (s, 3H, OCH_3); 3.78 (s, 6H, OCH_3); 3.67 (s, 3H, OCH_3); 3.57 (s, 2H, CH_2) ppm.

*4.1.9.2. Methyl 2-(4-(3,4,5-trimethoxybenzamido)phenyl)acetate (**42**).* From 3,4,5-trimethoxybenzoic acid (0.26 g, 1.21 mmol) and **40** (0.20 g, 1.21 mmol), compound **42** (0.41 g, yield 94.3%) was obtained as a yellow solid. Chromatographic eluent: $CH_2Cl_2/CH_3OH/NH_4OH$ 98:2:0.2. ^{1}H NMR (400 MHz, $CDCl_3$) δ: 8.24 (bs, 1H, NH); 7.54 (d, J = 8.4 Hz, 2H, CH arom.); 7.18 (d, J = 8.4 Hz, 2H, CH arom.); 7.01 (s, 2H, CH arom.); 3.82 (s, 3H, OCH_3); 3.78 (s, 6H, OCH_3); 3.64 (s, 3H, OCH_3); 3.55 (s, 2H, CH_2) ppm.

*4.1.9.3. Methyl 2-(4-(2,3,4-trimethoxybenzamido)phenyl)acetate (**43**).* From 2,3,4-trimethoxybenzoic acid (0.26 g, 1.21 mmol) and **40** (0.20 g, 1.21 mmol), compound **43** (0.29 g, yield 66.7%) was obtained as a yellow solid. Chromatographic eluent: $CH_2Cl_2/CH_3OH/NH_4OH$ 98:2:0.2. ^{1}H NMR (400 MHz, $CDCl_3$) δ: 9.92 (bs, 1H, NH); 7.93 (d, J = 9.2 Hz, 1H, CH arom.); 7.60 (d, J = 8.4 Hz, 2H, CH arom.); 7.23 (d, J = 8.4 Hz, 2H, CH arom.); 6.78 (d, J = 9.2 Hz, 1H, CH arom.); 4.01 (s, 3H, OCH_3); 3.88 (s, 3H, OCH_3); 3.86 (s, 3H, OCH_3); 3.64 (s, 3H, OCH_3); 3.57 (s, 2H, CH_2) ppm.

*4.1.9.4. Methyl 2-(4-(2-methoxybenzamido)phenyl)acetate (**44**).* From 2-methoxybenzoic acid (0.16 g, 1.05 mmol) and **40** (0.17 g, 1.05 mmol), compound **44** (0.23 g, yield 73.3%) was obtained as a pale-yellow solid. Chromatographic eluent: $CH_2Cl_2/CH_3OH/NH_4OH$ 97:3:0.3. ^{1}H NMR (400 MHz, $CDCl_3$) δ: 9.75 (bs, 1H, NH); 8.23 (d, J = 7.6 Hz, 1H, CH arom.); 7.60 (d, J = 8.4 Hz, 2H, CH arom.); 7.44 (t, J = 7.6 Hz, 1H, CH arom.); 7.23 (d, J = 8.4 Hz, 2H, CH arom.); 7.07 (t, J = 7.6 Hz, 1H, CH arom.); 6.97 (d, J = 7.6 Hz, 1H, CH arom.); 3.98 (s, 3H, OCH_3); 3.65 (s, 3H, OCH_3); 3.57 (s, 2H, CH_2) ppm.

*4.1.9.5. Methyl 2-(4-(2-methoxy-1-naphthamido)phenyl)acetate (**45**).* From **47** [34] (0.40 g, 1.98 mmol) and **40** (0.33 g, 1.98 mmol), **45** (0.38 g, yield 55.0%) was obtained as a yellow solid. Chromatographic eluent: $CH_2Cl_2/CH_3OH/NH_4OH$ 98:2:0.2. ^{1}H NMR (400 MHz, $CDCl_3$) δ: 8.00 (d, J = 8.4 Hz, 1H, CH arom.); 7.91–7.83 (m, 2H, CH arom. and NH); 7.78 (d, J = 8.4 Hz, 1H, CH arom.); 7.66 (d, J = 8.4 Hz, 2H, CH arom.); 7.47 (t, J = 8.4 Hz, 1H, CH arom.); 7.37 (t, J = 8.4 Hz, 1H, CH arom.); 7.28–7.24 (m, 3H, CH arom.); 3.94 (s, 3H, OCH_3); 3.68 (s, 3H, OCH_3); 3.60 (s, 2H, CH_2) ppm.

*4.1.10. Methyl 2-(4-(2,3-dimethoxy-1-naphthamido)phenyl)acetate (**46**)*

In an ice-bath, to a solution of **48** [34] (0.40 g, 1.98 mmol) and **40** (0.33 g, 1.98 mmol) in 15.0 mL of dry CH_2Cl_2, DMAP (0.16 g, 1.27 mmol) and EDC hydrochloride (0.55 g, 2.87 mmol) were added in this order. The reaction mixture was stirred at 0 °C for 1 h, then at rt for 48 h. The mixture was treated with CH_2Cl_2, and the organic layer was washed twice with water and 1 N HCl, then four times with a saturated solution of $NaHCO_3$, dried over Na_2SO_4 and concentrated under reduced pressure. The residue was purified by flash chromatography, using hexane/ethyl acetate 60:40 as the proper eluting system, and **46** (0.11 g, yield 18.3%) was obtained as a pale-yellow solid. ^{1}H NMR (400 MHz, $CDCl_3$) δ: 8.12 (bs, 1H, NH); 7.97 (d, J = 8.0 Hz, 1H, CH arom.); 7.73–7.65 (m, 3H, CH arom.); 7.44–7.36 (m, 2H, CH arom.); 7.30 (d, J = 8.4 Hz, 2H, CH arom.); 7.02 (s, 1H, CH arom.); 3.93 (s, 3H, OCH_3); 3.80 (s, 3H, OCH_3); 3.69 (s, 3H, OCH_3); 3.62 (s, 2H, CH_2) ppm.

*4.1.11. (E)-methyl 2-(4-(5-(3,4,5-trimethoxystyryl)-1H-tetrazol-1-yl) phenyl)acetate (**49**)*

Following the procedure reported by Li et al. [62] with slight modifications, **41** (0.090 g, 0.24 mmol) and dry pyridine (0.12 mL, 1.45 mmol) were dissolved in 3.6 mL of dry CH_2Cl_2, then PCl_5 (0.15 g, 0.73 mmol) was added. The suspension was refluxed for 3 h, then the solvent was removed under reduced pressure. In an ice bath, the solution of the obtained imidoyl chloride in 4.0 mL dry DMF was added dropwise to a stirring suspension of NaN_3 (0.11 g, 1.70 mmol) in 1.0 mL of dry DMF. The reaction was maintained at rt overnight, then cooled to 0 °C and treated with 6.0 mL of water. The mixture was extracted with CH_2Cl_2, and the organic layer was washed with brine, dried over Na_2SO_4, and concentrated under vacuum. Finally, the residue was purified by flash chromatography using CH_2Cl_2/CH_3OH 97:3 as eluent, obtaining **49** (0.060 g, yield 60.5%) as a pale-yellow solid. TLC: cyclohexane/ethyl acetate 20:80. ^{1}H NMR (400 MHz, $CDCl_3$) δ: 7.85 (d, J = 16.0 Hz, 1H, C*H*═CH); 7.51 (d, J = 8.0 Hz, 2H, CH arom.); 7.47 (d, J = 8.0 Hz, 2H, CH arom.); 6.70 (s, 2H, CH arom.); 6.66 (d, J = 16.0 Hz, 1H, CH═C*H*); 3.85 (s, 6H, OCH_3); 3.84 (s, 3H, OCH_3); 3.75 (s, 2H, CH_2); 3.72 (s, 3H, OCH_3) ppm.

*4.1.12. General procedure for the synthesis of tetrazoles **50**–**54***

Following the procedure reported by Jedhe et al. [63], in an ice bath the proper amide (**42**–**46**, 1 equiv.) was dissolved in the adequate amount of dry CH_2Cl_2 (4–8 mL), then dry pyridine (5 equiv.) and oxalyl chloride (3 equiv.) were added dropwise in this order: the suspension was stirred at rt for 24 h, then the solvent was removed under reduced pressure. The solution of the obtained imidoyl chloride in dry DMF (6–8 mL) was added dropwise to a suspension of NaN_3 (7 equiv.) in 1 mL of

dry DMF. The mixture was stirred at 60 °C overnight, then cooled to rt and treated with CH_2Cl_2: the organic layer was washed with brine, dried over Na_2SO_4 and concentrated under vacuum. Finally, the residue was purified by flash chromatography using cyclohexane/ethyl acetate 60:40 as the proper eluting system, yielding the desired tetrazole derivatives as oils or solids.

*4.1.12.1. Methyl 2-(4-(5-(3,4,5-trimethoxyphenyl)-1H-tetrazol-1-yl) phenyl)acetate (**50**).* From **42** (0.25 g, 0.70 mmol) and NaN_3 (0.32 g, 4.87 mmol), **50** (0.14 g, yield 52.3%) was obtained as a white solid. ^{1}H NMR (400 MHz, $CDCl_3$) δ: 7.43 (d, J = 8.4 Hz, 2H, CH arom.); 7.36 (d, J = 8.4 Hz, 2H, CH arom.); 6.73 (s, 2H, CH arom.); 3.83 (s, 3H, OCH_3); 3.70 (s, 2H, CH_2); 3.68 (s, 3H, OCH_3); 3.63 (s, 6H, OCH_3) ppm.

*4.1.12.2. Methyl 2-(4-(5-(2,3,4-trimethoxyphenyl)-1H-tetrazol-1-yl) phenyl)acetate (**51**).* From **43** (0.30 g, 0.83 mmol) and NaN_3 (0.38 g, 5.84 mmol), **51** (0.24 g, yield 74.8%) was obtained as a pale-yellow solid. ^{1}H NMR (400 MHz, $CDCl_3$) δ: 7.30 (d, J = 8.8 Hz, 2H, CH arom.); 7.27 (d, J = 8.8 Hz, 2H, CH arom.); 7.18 (d, J = 8.8 Hz, 1H, CH arom.); 6.72 (d, J = 8.8 Hz, 1H, CH arom.); 3.87 (s, 3H, OCH_3); 3.68 (s, 3H, OCH_3); 3.63 (s, 3H, OCH_3); 3.61 (s, 2H, CH_2); 3.40 (s, 3H, OCH_3) ppm.

*4.1.12.3. Methyl 2-(4-(5-(2-methoxyphenyl)-1H-tetrazol-1-yl)phenyl)acetate (**52**).* From **44** (0.15 g, 0.50 mmol) and NaN_3 (0.23 g, 3.51 mmol), **52** (0.090 g, yield 61.5%) was obtained as a white solid. ^{1}H NMR (400 MHz, $CDCl_3$) δ: 7.56 (d, J = 7.6 Hz, 1H, CH arom.); 7.43 (t, J = 7.6 Hz, 1H, CH arom.); 7.26 (d, J = 8.4 Hz, 2H, CH arom.); 7.21 (d, J = 8.4 Hz, 2H, CH arom.); 7.04 (t, J = 7.6 Hz, 1H, CH arom.); 6.79 (d, J = 7.6 Hz, 1H, CH arom.); 3.65 (s, 3H, OCH_3); 3.63 (s, 2H, CH_2); 3.28 (s, 3H, OCH_3) ppm. ^{13}C NMR (100 MHz, $CDCl_3$) δ: 171.29 (C); 156.56 (C); 152.10 (C); 135.54 (C); 134.60 (C); 133.15 (CH); 131.57 (CH); 130.24 (CH); 123.23 (CH); 121.20 (CH); 113.32 (C); 111.52 (CH); 54.84 (CH_3); 52.19 (CH_3); 40.52 (CH_2) ppm.

*4.1.12.4. Methyl 2-(4-(5-(2-methoxynaphthalen-1-yl)-1H-tetrazol-1-yl) phenyl)acetate (**53**).* From **45** (0.28 g, 0.80 mmol) and NaN_3 (0.36 g, 5.62 mmol), **53** (0.070 g, yield 23.3%) was obtained as a pale-yellow oil. ^{1}H NMR (400 MHz, $CDCl_3$) δ: 8.01 (d, J = 9.2 Hz, 1H, CH arom.); 7.85 (d, J = 8.0 Hz, 1H, CH arom.); 7.56 (d, J = 8.0 Hz, 1H, CH arom.); 7.49 (t, J = 8.0 Hz, 1H, CH arom.); 7.42 (t, J = 8.0 Hz, 1H, CH arom.); 7.26–7.17 (m, 5H, CH arom.); 3.66 (s, 3H, OCH_3); 3.59 (s, 2H, CH_2); 3.54 (s, 3H, OCH_3) ppm.

*4.1.12.5. Methyl 2-(4-(5-(2,3-dimethoxynaphthalen-1-yl)-1H-tetrazol-1-yl)phenyl)acetate (**54**).* From **46** (0.10 g, 0.26 mmol) and NaN_3 (0.12 g, 1.82 mmol), **54** (0.035 g, yield 32.7%) was obtained as a yellow oil. ^{1}H NMR (400 MHz, $CDCl_3$) δ: 7.75 (d, J = 8.0 Hz, 1H, CH arom.); 7.42 (t, J = 8.0 Hz, 1H, CH arom.); 7.34–7.27 (m, 4H, CH arom.); 7.22–7.17 (m, 3H, CH arom.); 3.97 (s, 3H, OCH_3); 3.66 (s, 3H, OCH_3); 3.63 (s, 3H, OCH_3); 3.55 (s, 2H, CH_2) ppm.

*4.1.13. (E)-2-(4-(5-(3,4,5-Trimethoxystyryl)-1H-tetrazol-1-yl)phenyl) ethanol (**55**)*

A solution of **49** (0.090 g, 0.22 mmol) in 3.0 mL of dry CH_2Cl_2 was cooled to −30 °C, then DIBAL-H (1 M in toluene, 0.26 mL, 0.26 mmol) was added dropwise. The reaction was stirred at −30 °C for 1 h. Since **49** is always present in the mixture, DIBAL-H (1 M in toluene, 0.26 mL, 0.26 mmol) was added dropwise and the solution was stirred at −15 °C for 1 h. Upon completion of the reaction, 2.7 mL of 10% NaOH solution were added. The mixture was allowed to reach rt and it was stirred for 15 min, then it was extracted with CH_2Cl_2. The organic layer was washed with brine, dried over Na_2SO_4, and concentrated under vacuum. Finally, the residue was purified by flash chromatography, using CH_2Cl_2/CH_3COCH_3 80:20 as eluent, obtaining **55** (0.015 g, yield 21.5%) as a pale-yellow oil. TLC: ethyl acetate 100. ^{1}H NMR (400 MHz, $CDCl_3$) δ: 7.88 (d, J = 16.0 Hz, 1H, C*H*═CH); 7.49 (d, J = 8.0 Hz, 2H, CH arom.); 7.45 (d, J = 8.0 Hz, 2H, CH arom.); 6.71 (s, 2H, CH arom.); 6.66 (d, J = 16.0 Hz, 1H, CH═C*H*); 3.97 (t, J = 6.4 Hz, 2H, CH_2OH); 3.86 (s, 9H, OCH_3); 3.00 (t, J = 6.4 Hz, 2H, CH_2); 1.90 (bs, 1H, OH) ppm.

*4.1.14. General procedure for the synthesis of the alcohols **56**–**60***

In an ice bath, to a solution of the proper intermediate (**50**–**54**, 1 equiv.) in the adequate amount of dry THF (3–6 mL), $LiAlH_4$ (3 equiv.) was added portion wise. The reaction mixture was kept at rt for 1.5 h, then was quenched with ice, and 10% NaOH solution was added. The obtained suspension was filtered under vacuum and the filtrate was concentrated under reduced pressure, to eliminate THF. The mixture was extracted with CH_2Cl_2, then the organic layer was dried over Na_2SO_4, and the solvent was removed under vacuum. Finally, the residue was purified by flash chromatography using the proper eluting system, obtaining the desired compound as oils.

*4.1.14.1. 2-(4-(5-(3,4,5-Trimethoxyphenyl)-1H-tetrazol-1-yl)phenyl) ethanol (**56**).* From **50** (0.14 g, 0.36 mmol) and $LiAlH_4$ (0.041 g, 1.09 mmol) in 3.0 mL of dry THF, **56** (0.080 g, yield 62.3%) was obtained as a pale-yellow oil. Chromatographic eluent: CH_2Cl_2/CH_3OH 95:5. ^{1}H NMR (400 MHz, $CDCl_3$) δ: 7.37 (d, J = 8.4 Hz, 2H, CH arom.); 7.30 (d, J = 8.4 Hz, 2H, CH arom.); 6.71 (s, 2H, CH arom.); 3.94 (t, J = 6.4 Hz, 2H, CH_2OH); 3.80 (s, 3H, OCH_3); 3.60 (s, 6H, OCH_3); 2.89 (t, J = 6.4 Hz, 2H, CH_2) ppm.

*4.1.14.2. 2-(4-(5-(2,3,4-Trimethoxyphenyl)-1H-tetrazol-1-yl)phenyl) ethanol (**57**).* From **51** (0.24 g, 0.62 mmol) and $LiAlH_4$ (0.071 g, 1.87 mmol) in 6.0 mL of dry THF, **57** (0.11 g, yield 49.8%) was obtained as a pale-yellow oil. Chromatographic eluent: CH_2Cl_2/CH_3OH 95:5. ^{1}H NMR (400 MHz, $CDCl_3$) δ: 7.20 (d, J = 8.8 Hz, 2H, CH arom.); 7.17 (d, J = 8.8 Hz, 2H, CH arom.); 7.11 (d, J = 8.8 Hz, 1H, CH arom.); 6.68 (d, J = 8.8 Hz, 1H, CH arom.); 3.82 (s, 3H, OCH_3); 3.74 (t, J = 6.8 Hz, 2H, CH_2OH); 3.64 (s, 3H, OCH_3); 3.34 (s, 3H, OCH_3); 2.79 (t, J = 6.8 Hz, 2H, CH_2); 2.62 (bs, 1H, OH) ppm.

*4.1.14.3. 2-(4-(5-(2-Methoxyphenyl)-1H-tetrazol-1-yl)phenyl)ethanol (**58**).* From **52** (0.070 g, 0.22 mmol) and $LiAlH_4$ (0.025 g, 0.65 mmol) in 5.0 mL of dry THF, **58** (0.050 g, yield 78.2%) was obtained as a pale-yellow oil. Chromatographic eluent: CH_2Cl_2/CH_3OH 95:5. ^{1}H NMR (400 MHz, $CDCl_3$) δ: 7.52 (d, J = 7.6 Hz, 1H, CH arom.); 7.43 (t, J = 7.6 Hz, 1H, CH arom.); 7.21 (d, J = 8.4 Hz, 2H, CH arom.); 7.15 (d, J = 8.4 Hz, 2H, CH arom.); 7.03 (t, J = 7.6 Hz, 1H, CH arom.); 6.78 (d, J = 7.6 Hz, 1H, CH arom.); 3.79 (t, J = 6.4 Hz, 2H, CH_2OH); 3.25 (s, 3H, OCH_3); 2.83 (t, J = 6.4 Hz, 2H, CH_2); 2.48 (bs, 1H, OH) ppm.

*4.1.14.4. 2-(4-(5-(2-Methoxynaphthalen-1-yl)-1H-tetrazol-1-yl)phenyl) ethanol (**59**).* From **53** (0.070 g, 0.19 mmol) and $LiAlH_4$ (0.021 g, 0.56 mmol) in 4.0 mL of dry THF, **59** (0.050 g, yield 77.3%) was obtained as a pale-yellow oil. Chromatographic eluent: ethyl acetate 100. TLC: cyclohexane/ethyl acetate 50:50. ^{1}H NMR (400 MHz, $CDCl_3$) δ: 7.99 (d, J = 9.2 Hz, 1H, CH arom.); 7.83 (d, J = 8.0 Hz, 1H, CH arom.); 7.51–7.45 (m, 2H, CH arom.); 7.40 (t, J = 8.0 Hz, 1H, CH arom.); 7.20–7.12 (m, 5H, CH arom.); 3.78 (t, J = 6.4 Hz, 2H, CH_2OH); 3.55 (s, 3H, OCH_3); 2.80 (t, J = 6.4 Hz, 2H, CH_2); 1.82 (bs, 1H, OH) ppm.

*4.1.14.5. 2-(4-(5-(2,3-Dimethoxynaphthalen-1-yl)-1H-tetrazol-1-yl) phenyl)ethanol (**60**).* From **54** (0.035 g, 0.086 mmol) and $LiAlH_4$ (0.010 g, 0.26 mmol) in 3.0 mL of dry THF, **60** (0.030 g, yield 94.2%) was obtained as a pure yellow oil. TLC: cyclohexane/ethyl acetate 60:40. ^{1}H NMR (400 MHz, $CDCl_3$) δ: 7.74 (d, J = 8.4 Hz, 1H, CH arom.); 7.41 (t, J = 8.4 Hz, 1H, CH arom.); 7.34–7.27 (m, 2H, CH arom.); 7.24 (d, J = 8.4 Hz, 2H, CH arom.); 7.17 (d, J = 8.4 Hz, 1H, CH arom.); 7.12 (d, J = 8.4 Hz, 2H, CH arom.); 3.96 (s, 3H, OCH_3); 3.74 (t, J = 6.4 Hz, 2H, CH_2OH);

3.65 (s, 3H, OCH_3); 2.76 (t, $J = 6.4$ Hz, 2H, CH_2); 1.83 (bs, 1H, OH) ppm.

*4.1.15. General procedure for the synthesis of the tosyl derivatives **61**–**66***

To a solution of the alcohols **55**–**60** (1 equiv.) and Et_3N (6 equiv.) in dry CH_2Cl_2 (2–7 mL), *p*-toluenesulfonyl chloride (2.5 equiv.) was added at 0 °C. The solution was stirred at rt overnight, then it was treated with water, and the mixture was extracted with CH_2Cl_2. The organic layer was dried over Na_2SO_4, and the solvent was removed under reduced pressure. Finally, the residue was purified by flash chromatography using the proper eluting system, obtaining the desired compounds as oils.

*4.1.15.1. (E)-4-(5-(3,4,5-Trimethoxystyryl)-1H-tetrazol-1-yl)phenethyl 4-methylbenzenesulfonate (**61**).* From **55** (0.055 g, 0.14 mmol) and *p*-toluenesulfonyl chloride (0.069 g, 0.36 mmol) in 3.3 mL of dry CH_2Cl_2, **61** (0.035 g, yield 45.3%) was obtained as a pale-yellow oil. Chromatographic eluent: hexane/ethyl acetate 50:50. TLC: CH_2Cl_2/CH_3OH 95:5. ^{1}H NMR (400 MHz, $CDCl_3$) δ: 7.88 (d, $J = 16.0$ Hz, 1H, C*H*═CH); 7.67 (d, $J = 8.0$ Hz, 2H, CH arom.); 7.42 (d, $J = 8.4$ Hz, 2H, CH arom.); 7.38 (d, $J = 8.4$ Hz, 2H, CH arom.); 7.29 (d, $J = 8.0$ Hz, 2H, CH arom.); 6.70 (s, 2H, CH arom.); 6.65 (d, $J = 16.0$ Hz, 1H, CH═C*H*); 4.29 (t, $J = 6.4$ Hz, 2H, OCH_2); 3.85 (s, 3H, OCH_3); 3.84 (s, 6H, OCH_3); 3.07 (t, $J = 6.4$ Hz, 2H, CH_2); 2.41 (s, 3H, CH_3) ppm.

*4.1.15.2. 4-(5-(3,4,5-Trimethoxyphenyl)-1H-tetrazol-1-yl)phenethyl 4-methylbenzenesulfonate (**62**).* From **56** (0.15 g, 0.42 mmol) and *p*-toluenesulfonyl chloride (0.20 g, 1.05 mmol) in 7.0 mL of dry CH_2Cl_2, **62** (0.080 g, yield 37.2%) was obtained as a pale-yellow oil. Chromatographic eluent: CH_2Cl_2/CH_3OH 99:1. ^{1}H NMR (400 MHz, $CDCl_3$) δ: 7.63 (d, $J = 8.0$ Hz, 2H, CH arom.); 7.32–7.22 (m, 6H, CH arom.); 6.71 (s, 2H, CH arom.); 4.21 (t, $J = 6.0$ Hz, 2H, OCH_2); 3.82 (s, 3H, OCH_3); 3.61 (s, 6H, OCH_3); 3.00 (t, $J = 6.0$ Hz, 2H, CH_2); 2.38 (s, 3H, CH_3) ppm.

*4.1.15.3. 4-(5-(2,3,4-Trimethoxyphenyl)-1H-tetrazol-1-yl)phenethyl 4-methylbenzenesulfonate (**63**).* From **57** (0.11 g, 0.31 mmol) and *p*-toluenesulfonyl chloride (0.15 g, 0.77 mmol) in 6.5 mL of dry CH_2Cl_2, **63** (0.16 g, yield 100.0%) was obtained as a pale-yellow oil. Chromatographic eluent: CH_2Cl_2/CH_3OH 98:2. ^{1}H NMR (400 MHz, $CDCl_3$) δ: 7.56 (d, $J = 8.0$ Hz, 2H, CH arom.); 7.20 (d, $J = 8.0$ Hz, 2H, CH arom.); 7.17–7.09 (m, 5H, CH arom.); 6.69 (d, $J = 8.8$ Hz, 1H, CH arom.); 4.12 (t, $J = 6.4$ Hz, 2H, OCH_2); 3.82 (s, 3H, OCH_3); 3.64 (s, 3H, OCH_3); 3.34 (s, 3H, OCH_3); 2.89 (t, $J = 6.4$ Hz, 2H, CH_2); 2.33 (s, 3H, CH_3) ppm.

*4.1.15.4. 4-(5-(2-Methoxyphenyl)-1H-tetrazol-1-yl)phenethyl 4-methylbenzenesulfonate (**64**).* From **58** (0.050 g, 0.17 mmol) and *p*-toluenesulfonyl chloride (0.050 g, 0.25 mmol) in 3.2 mL of dry CH_2Cl_2, **64** (0.060 g, yield 78.9%) was obtained as a pale-yellow oil. Chromatographic eluent: CH_2Cl_2/CH_3OH 98:2. ^{1}H NMR (400 MHz, $CDCl_3$) δ: 7.60 (d, $J = 8.4$ Hz, 2H, CH arom.); 7.56 (d, $J = 7.6$ Hz, 1H, CH arom.); 7.44 (t, $J = 7.6$ Hz, 1H, CH arom.); 7.24 (d, $J = 8.4$ Hz, 2H, CH arom.); 7.15 (d, $J = 8.4$ Hz, 2H, CH arom.); 7.12 (d, $J = 8.4$ Hz, 2H, CH arom.); 7.05 (t, $J = 7.6$ Hz, 1H, CH arom.); 6.79 (d, $J = 7.6$ Hz, 1H, CH arom.); 4.17 (t, $J = 6.4$ Hz, 2H, OCH_2); 3.24 (s, 3H, OCH_3); 2.92 (t, $J = 6.4$ Hz, 2H, CH_2); 2.37 (s, 3H, CH_3) ppm.

*4.1.15.5. 4-(5-(2-Methoxynaphthalen-1-yl)-1H-tetrazol-1-yl)phenethyl 4-methylbenzenesulfonate (**65**).* From **59** (0.063 g, 0.18 mmol) and *p*-toluenesulfonyl chloride (0.087 g, 0.45 mmol) in 4.0 mL of dry CH_2Cl_2, **65** (0.070 g, yield 77.8%) was obtained as a pale-yellow oil. Chromatographic eluent: hexane/ethyl acetate 50:50. ^{1}H NMR (400 MHz, $CDCl_3$) δ: 7.99 (d, $J = 9.2$ Hz, 1H, CH arom.); 7.83 (d, $J = 8.0$ Hz, 1H, CH arom.); 7.60 (d, $J = 8.4$ Hz, 2H, CH arom.); 7.54 (d, $J = 8.0$ Hz, 1H, CH arom.); 7.48 (t, $J = 8.0$ Hz, 1H, CH arom.); 7.40 (t, $J = 8.0$ Hz, 1H, CH arom.); 7.23 (d, $J = 8.4$ Hz, 2H, CH arom.); 7.17 (d, $J = 9.2$ Hz, 1H, CH arom.); 7.13 (d, $J = 8.4$ Hz, 2H, CH arom.); 7.03 (d, $J = 8.4$ Hz, 2H, CH arom.); 4.14 (t, $J = 6.4$ Hz, 2H, OCH_2); 3.51 (s, 3H, OCH_3); 2.88 (t, $J = 6.4$ Hz, 2H, CH_2); 2.38 (s, 3H, CH_3) ppm.

*4.1.15.6. 4-(5-(2,3-Dimethoxynaphthalen-1-yl)-1H-tetrazol-1-yl)phenethyl 4-methylbenzenesulfonate (**66**).* From **60** (0.031 g, 0.081 mmol) and *p*-toluenesulfonyl chloride (0.039 g, 0.20 mmol) in 2.0 mL of dry CH_2Cl_2, **66** (0.032 g, yield 74.0%) was obtained as a yellow oil. Chromatographic eluent: hexane/ethyl acetate 50:50. ^{1}H NMR (400 MHz, $CDCl_3$) δ: 7.76 (d, $J = 8.4$ Hz, 1H, CH arom.); 7.59 (d, $J = 8.0$ Hz, 2H, CH arom.); 7.43 (t, $J = 8.4$ Hz, 1H, CH arom.); 7.37–7.30 (m, 2H, CH arom.); 7.24–7.15 (m, 5H, CH arom.); 7.01 (d, $J = 8.0$ Hz, 2H, CH arom.); 4.12 (t, $J = 6.4$ Hz, 2H, OCH_2); 3.97 (s, 3H, OCH_3); 3.66 (s, 3H, OCH_3); 2.86 (t, $J = 6.4$ Hz, 2H, CH_2); 2.39 (s, 3H, CH_3) ppm.

*4.1.16. 1-(4-(2-Bromoethyl)phenyl)ethenone (**67**)*

Following the procedure described in Ref. [39], in an ice bath, to a suspension of $AlCl_3$ (1.73 g, 13.00 mmol) in 5.0 mL of CH_2Cl_2, acetyl chloride (2.30 mL, 32.30 mmol) and (2-bromoethyl)benzene (1.46 mL, 10.80 mmol) were added in this order. The reaction was stirred at rt overnight, then quenched with ice and 1.0 mL of cold water. The mixture was stirred 15 min and extracted with CH_2Cl_2. The organic layer was washed twice with water, a 10% NaOH solution and brine, dried over Na_2SO_4, and concentrated under reduced pressure. The residue was purified by flash chromatography using hexane/ethyl acetate 80:20 as eluent, obtaining **67** (0.52 g, yield: 21.2%) as a yellow oil. ^{1}H NMR (400 MHz, $CDCl_3$) δ: 7.92 (d, $J = 8.0$ Hz, 2H, CH arom.); 7.31 (d, $J = 8.0$ Hz, 2H, CH arom.); 3.59 (t, $J = 8.0$ Hz, 2H, CH_2Br); 3.22 (t, $J = 8.0$ Hz, 2H, CH_2); 2.59 (s, 3H, CH_3) ppm.

*4.1.17. 4-(2-Bromoethyl)benzoic acid (**68**)*

Following the procedure described in Ref. [64], NaOH (1.97 g, 49.30 mmol) was dissolved in 8.0 mL of water, then Br_2 (1.04 mL, 20.20 mmol) and at 0 °C a solution of **67** (0.43 g, 1.89 mmol) in 2.0 mL of dioxane were added dropwise: the mixture was stirred at rt for 1.5 h. Upon completion of the reaction (monitored by TLC), the solution was acidified with concentrated HCl: **68** (0.40 g, yield: 92.5%) precipitated as a pure white solid, that was filtered and dried under vacuum. TLC: $CH_2Cl_2/CH_3OH/CH_3COOH$ 90:10:1. Mp: 200–202 °C. ^{1}H NMR (400 MHz, $CDCl_3$) δ: 8.07 (d, $J = 8.0$ Hz, 2H, CH arom.); 7.33 (d, $J = 8.0$ Hz, 2H, CH arom.); 3.60 (t, $J = 7.6$ Hz, 2H, CH_2Br); 3.25 (t, $J = 7.6$ Hz, 2H, CH_2) ppm.

*4.1.18. Methyl 4-(2-bromoethyl)benzoate (**69**)*

To a solution of **68** (0.42 g, 1.83 mmol) in 8.0 mL of dry methanol, $SOCl_2$ (0.20 mL, 2.75 mmol) was added, and the mixture was refluxed for 3 h. Upon completion of the reaction, the solution was concentrated under reduced pressure, then the residue was treated twice with cyclohexane, and the solvent was removed under vacuum. Finally, **69** (0.44 g, yield: 100.0%) was obtained as a brown oil. TLC: CH_2Cl_2/CH_3OH 90:10. ^{1}H NMR (400 MHz, $CDCl_3$) δ: 7.99 (d, $J = 8.0$ Hz, 2H, CH arom.); 7.28 (d, $J = 8.0$ Hz, 2H, CH arom.); 3.91 (s, 3H, OCH_3); 3.58 (t, $J = 7.6$ Hz, 2H, CH_2Br); 3.22 (t, $J = 7.6$ Hz, 2H, CH_2) ppm.

*4.1.19. Methyl 4-(2-(6,7-dimethoxy-3,4-dihydroisoquinolin-2(1H)-yl)ethyl)benzoate (**70**)*

A solution of **69** (0.21 g, 0.86 mmol), 6,7-dimethoxy-1,2,3,4-tetrahydroisoquinoline (0.18 g, 0.95 mmol) and K_2CO_3 (0.094 g, 0.95 mmol) in 4.0 mL of dry CH_3CN was refluxed for 18 h; then, the solvent was removed under reduced pressure. The mixture was treated with CH_2Cl_2: the organic layer was washed twice with water and a saturated solution of $NaHCO_3$, dried over Na_2SO_4 and concentrated under vacuum. The residue was purified by flash chromatography using $CH_2Cl_2/CH_3OH/NH_4OH$ 98:2:0.2 as eluent, obtaining **70** (0.12 g, yield: 68.7%) as a yellow oil. ^{1}H NMR (400 MHz, $CDCl_3$) δ: 7.97 (d, $J = 8.0$ Hz, 2H, CH arom.); 7.31 (d, $J = 8.0$ Hz, 2H, CH arom.); 6.60 (s, 1H, CH arom.); 6.53

(s, 1H, CH arom.); 3.90 (s, 3H, OCH_3); 3.84 (s, 3H, OCH_3); 3.83 (s, 3H, OCH_3); 3.65 (s, 2H, NCH_2Ar); 3.00–2.94 (m, 2H, CH_2); 2.88–2.74 (m, 6H, CH_2) ppm.

4.1.20. 4-(2-(6,7-Dimethoxy-3,4-dihydroisoquinolin-2(1H)-yl)ethyl) benzohydrazide (71)

To a solution of **70** (0.41 g, 1.15 mmol) in 3.0 mL of ethanol, hydrazine hydrate (0.56 mL, 11.50 mmol) was added, and the reaction was refluxed for 24 h. Upon completion of the reaction (monitored by TLC), the solvent was removed under reduced pressure, obtaining **71** (0.41 g, yield: 100.0%) as a yellow oil. TLC: $CH_2Cl_2/CH_3OH/NH_4OH$ 96:4:0.4. ^{1}H NMR (400 MHz, $CDCl_3$) δ: 7.67 (d, $J = 8.0$ Hz, 2H, CH arom.); 7.36 (bs, 1H, NH); 7.31 (d, $J = 8.0$ Hz, 2H, CH arom.); 6.60 (s, 1H, CH arom.); 6.52 (s, 1H, CH arom.); 4.10 (bs, 2H, NH_2); 3.84 (s, 3H, OCH_3); 3.83 (s, 3H, OCH_3); 3.66 (s, 2H, NCH_2Ar); 3.00–2.92 (m, 2H, CH_2); 2.88–2.70 (m, 6H, CH_2) ppm.

4.2. Biology

4.2.1. Materials

Cell culture reagents were purchased from Celbio s.r.l. (Milano, Italy). CulturePlate 96/wells plates were purchased from PerkinElmer Life Science (Waltham, MA) and Falcon (BD Biosciences, Bedford, MA). Calcein-AM, bisBenzimide Hoechst 33342 trihydrochloride were obtained from Sigma-Aldrich (Milan, Italy).

4.2.2. Cell lines and cultures

MDCK-MDR1, MDCK-MRP1 and MDCK-BCRP cells are from Prof. P. Borst, NKI-AVL Institute, Amsterdam, The Netherlands. Caco-2 cells were a gift of Dr. Aldo Cavallini and Dr. Caterina Messa from the Laboratory of Biochemistry, National Institute for Digestive Diseases, "S. de Bellis", Bari (Italy). HT29 cells were purchased from ATCC (Manassas, VA, accession number HTB-38). The doxorubicin-resistant subline, HT29/DX cells, was generated by stepwise selection in medium with increasing concentrations of doxorubicin and were grown in the culture medium containing 100 nM doxorubicin to maintain the chemoresistant phenotype [47].

MDCK and Caco-2 cells were grown in DMEM high glucose, HT29 and HT29/DX in RPMI-1640, all supplemented with 10% fetal bovine serum, 2 mM glutamine, 100 U/mL penicillin, 100 μg/mL streptomycin, in a humidified incubator at 37 °C with a 5% CO_2 atmosphere.

4.2.3. Calcein-AM experiment

Experiments were performed as described by Contino et al. with minor modifications [65]. MDCK-MDR1 and MDCK-MRP1 cell lines (30 000 cells per well), seeded in a 96-well black CulturePlate with 100 μl of medium, were allowed to grow overnight in a humidified atmosphere of 5% CO_2 at 37 °C. 100 μL of test compounds (final concentrations between 0.01 nM and 100 μM; for derivatives with a nanomolar EC_{50} value, we reached 10^{-13} M concentration), solubilized in culture medium, were added to the monolayers. After an incubation time of 30 min in a humidified atmosphere of 5% CO_2 at 37 °C, 100 μL of Calcein-AM in phosphate buffered saline (PBS) was added to obtain a final concentration of 2.5 μM; the plate was then incubated for 30 min. Each well was washed 3 times with 100 μL ice cold PBS and read with Victor3 (PerkinElmer) after adding 100 μL of buffered saline. Excitation and emission wavelengths of 485 nm and 535 nm were used. In these experimental conditions, cell Calcein accumulation in the absence and in the presence of the tested compounds was evaluated and compared to the basal level of fluorescence obtained from untreated cells. The increase in fluorescence from the baseline level was measured in the treated wells. EC_{50} values were determined by fitting the rate of fluorescence increase versus log[dose].

4.2.4. Hoechst 33342 experiment

These experiments were conducted as described by Contino et al. with minor modifications [65]. 30 000 cells in 100 μL of medium per well of the MDCK-BCRP cell line were seeded in a black CulturePlate 96/well and grown to confluence overnight in a humidified atmosphere of 5% CO_2 at 37 °C. 100 μL of test compounds solubilized in culture medium were added to the monolayers, obtaining a final concentration between 0.1 and 100 μM. The plate was then incubated for 30 min in a humidified atmosphere of 5% CO_2 at 37 °C and 100 μL of Hoechst 33342 at the final concentration of 8 μM in PBS were added. The plate was incubated for 30 min in a humidified atmosphere of 5% CO_2 at 37 °C. The supernatants were drained, and the cells were fixed for 20 min under protection from light using 100 μL per well of a 4% PFA solution. The plate was washed 3 times with ice-cold PBS and 100uL of cold saline buffer was added to each well. Fluorescence was read by Victor3 (PerkinElmer) at excitation and emission wavelengths of 340/35 nm and 485/20 nm, respectively. Under these experimental conditions, the baseline fluorescence level of Hoechst 33342 was estimated using untreated cells and compared with the fluorescence emissions of cells treated with the tested compounds. EC_{50} values were determined by plotting the percent increase in fluorescence versus log [dose].

4.2.5. ATPlite assay

The assay has been performed using the luminescence ATP detection assay system ATPlite (PerkinElmer, cat.6016941) based on the production of light caused by the reaction of ATP with added luciferase and D-luciferin. The emitted light is proportional to the ATP concentration. Briefly, MDCK-MDR1 cells, in 100 μL of complete medium at a density of 2×10^4 cells/well, were seeded in a 96-well plate and incubated overnight in a humidified atmosphere of 5% CO_2 at 37 °C. The removal of the medium was then carried out and the addition of 100 μL of complete medium in the absence or in the presence of different concentrations of the compounds to be tested was accomplished. Then follows an incubation of the plate for 2 h in a humidified atmosphere with 5% CO_2 at 37 °C. 50 μl of mammalian cell lysis solution were added to all wells and the plate was shaken for 5 min using an orbital shaker. 50 μL of substrate solution was added to all wells and the plate shacked for 5 min in an orbital shaker. The plate was kept in the dark for 10 min and then the luminescence was measured [65]. Under these experimental conditions, the standard ATP cell level (100%ATP) correspond to the emission by the untreated cells and compared with the emissions of cells treated with the tested compounds.

4.2.6. Caco-2 cell monolayer preparation

Caco-2 cells (20 000 cells/well) were seeded on a Millicell® Transwell Assay System (Millipore), where the cell monolayer was grown in a filter (apical side) which was inserted in a receiving plate (basolateral side). The culture medium was replaced every 48 h and the cells were maintained for 21 days in culture. The transepithelial electrical resistance (TEER) of the monolayers was measured daily, using an epithelial voltmeter (Millicell®-ERS). In general, TEER values above 1000 Ω for a 21-day culture are considered optimal [65].

4.2.7. Drug-transport experiment

After 21 days of Caco-2 cell growth, the plate was washed twice using Hank's Balanced Salt Solution (HBSS) buffer (Invitrogen). The plate was then incubated at 37 °C for 30 min. The HBSS buffer was removed and the compounds to be tested in solution at a concentration of 100 μM were added, only fresh HBSS was added to the receiving plate. The plates were incubated at 37 °C for 120 min. After this time, the samples were removed from the apical (filter plate) and basolateral (recipient plate) side. The residual concentration of the compounds in both plates was measured spectroscopically to calculate the apparent permeability (P_{app}), in units of nm/second, using the following equation:

$$P_{app} = \left(\frac{V_A}{Area \times time}\right) \times \left(\frac{[drug]_{acceptor}}{[drug]_{initial}}\right)$$

VA = the volume (in mL) in the acceptor well;

Area = the surface area of the membrane (0.11 cm^2 of the well);

time = the total transport time in seconds (7200 s);

$[drug]_{acceptor}$ = the concentration of the drug measured by U.V. spectroscopy;

$[drug]_{initial}$ = the initial drug concentration (100 μM) in the apical or basolateral wells.

4.2.8. Co-administration assay in MDCK, MDCK-MDR1, MDCK-MRP1, MDCK-BCRP, HT29 and HT29/DX cells

The co-administration assay with doxorubicin was performed in MDCK, MDCK-MDR1, MDCK-MRP1, MDCK-BCRP, HT29 and HT29/DX cells at 48 h as reported with minor modifications [34]. 10 000 cells/-well were seeded into 96-well plates. After 24 h, the compounds at 1 μM and 10 μM concentrations were added with 5 μM doxorubicin. After 48 h, MTT (0.5 mg/mL) was added to each well and incubated 3–4 h at 37 °C. The supernatant was removed, while the formazan crystals were solubilized with 100 μL of DMSO/EtOH (1:1). The absorbance values at 570 and 630 nm were read using a Victor3 microplate reader (PerkinElmer Life Sciences).

4.2.9. Lactate dehydrogenase (LDH) release

The release of LDH, taken as an index of doxorubicin cytotoxicity [46], was measured on 50 μl of extracellular culture medium of 500 000 cells incubated 24 h with 5 μM doxorubicin, with or without the compounds at 1 μM and 10 μM concentrations. The remaining part of cells was detached and sonicated in 200 μL of triethanolamine phosphate (TRAP) buffer, pH 8.0; the activity of intracellular LDH was measured on 5 μl cell lysates. The reaction was started by adding 20 mM pyruvic acid and 5 mM NADH. The rate of NADH oxidation was measured spectrophotometrically for 6 min, using a Synergy HTX 96-well plate reader (Bio-Tek Instruments, Winooski, VT). The kinetics was linear during the whole assay. Results were expressed as percentage of extracellular LDH/total (extracellular + intracellular) LDH.

4.2.10. Intracellular doxorubicin accumulation in MDCK-MDR1 and HT29/DX cells

Intracellular doxorubicin was measured in 10 000 cells, seeded into 96-well plates and incubated for 24 h with 5 μM doxorubicin, with or without 1 μM and 10 μM of each compound. The intracellular drug content was measured fluorimetrically as detailed previously [66], using a Synergy HTX 96-well plate reader. The results were expressed as nmol doxorubicin/mg cell proteins, based on the titration curve previously prepared.

4.2.11. Statistical analysis

All data in the tables and figures are provided as means ± SEM (Table 1) or SD. The results were analyzed by a Student's t-test and ANOVA test, using Graph-Pad Prism (Graph-Pad software, San Diego, CA, USA).

4.3. Molecular modeling studies

Initial structure of murine P-gp (4XWK [52]) and of BCRP (8BHT [58]) were retrieved from Protein Data Bank (www.rcsb.org [67]). Inner missing regions were modeled using Modeller [68] as implemented in UCSF Chimera 1.11.2 [69]. The structure was then minimized with Amber force field ff14SB [70]. Molecular docking was carried out with Gold software v.2020.2.0 [71] using default settings. PyMOL was used for analysis and picture rendering (The PyMOL Molecular Graphics System, Version 1.8 Schrödinger, LLC.).

Declaration of competing interest

The authors declare that they have no known competing financial interests or personal relationships that could have appeared to influence the work reported in this paper.

Data availability

Data will be made available on request.

Acknowledgments

The authors thank Dr. Cristina Bellucci for her excellent technical assistance. This work was supported by grants from the University of Florence (Fondo Ricerca Ateneo RICATEN21 and RICATEN22) and from the University of Turin (Fondo Ricerca Locale) for S.G.

Appendix A. Supplementary data

Supplementary data to this article can be found online at https://doi.org/10.1016/j.ejmech.2023.115716.

Abbreviations

P-gp, P-glycoprotein; MRP1, multidrug-resistance-associated protein-1; BCRP, breast cancer resistance protein; DOX, Doxorubicin; EDC, 1-ethyl-3-(3′-dimethylaminopropyl)-carbodiimmide; PDB, Protein Data Bank; MDCK, Madin-Darby Canine Kidney; P_{app}, apparent permeability; BA, basolateral to apical; AB, apical to basolateral; Calcein-AM, calcein acetoxy methyl ester; MTT, 3-(4,5-dimethylthiazolyl-2)-2,5-diphenyl tetrazolium bromide; LDH, lactate dehydrogenase.

References

[1] C. Holohan, S. Van Schaeybroeck, D.B. Longley, P.G. Johnston, Cancer drug resistance: an evolving paradigm, Nat. Rev. Cancer 13 (2013) 714–726.
[2] R. El-Awady, E. Saleh, A. Hashim, N. Soliman, A. Dallah, A. Elrasheed, G. Elakraa, The role of eukaryotic and prokaryotic ABC transporter family in failure of chemotherapy, Front. Pharmacol. 7 (2017) 535.
[3] T.W. Loo, D.M. Clarke, Mutational analysis of ABC proteins, Arch. Biochem. Biophys. 476 (2008) 51–64.
[4] S. Dei, L. Braconi, M.N. Romanelli, E. Teodori, Recent advances in the search of BCRP- and dual P-gp/BCRP-based multidrug resistance modulators, Cancer Drug Resist 2 (2019) 710–743.
[5] R.W. Robey, K.M. Pluchino, M.D. Hall, A.T. Fojo, S.E. Bates, M.M. Gottesman, Revisiting the role of ABC transporters in multidrug-resistant cancer, Nat. Rev. Cancer 18 (2018) 452–464.
[6] Y.H. Choi, A.-M. Yu, ABC transporters in multidrug resistance and pharmacokinetics, and strategies for drug development, Curr. Pharmaceut. Des. 20 (2014) 793–807.
[7] K.D. Bunting, ABC transporters as phenotypic markers and functional regulators of stem cells, Stem Cell. 20 (2002) 11–20.
[8] A.E. Stacy, P.J. Jansson, D.R. Richardson, Molecular pharmacology of ABCG2 and its role in chemoresistance, Mol. Pharmacol. 84 (2013) 655–669.
[9] C. Riganti, M. Contino, S. Guglielmo, M.G. Perrone, I.C. Salaroglio, V. Milosevic, R. Giampietro, F. Leonetti, B. Rolando, L. Lazzarato, N.A. Colabufo, R. Fruttero, Design, biological evaluation, and molecular modeling of tetrahydroisoquinoline derivatives: discovery of A potent P-glycoprotein ligand overcoming multidrug resistance in cancer stem cells, J. Med. Chem. 62 (2019) 974–986.
[10] W. Li, H. Zhang, Y.G. Assaraf, K. Zhao, X. Xu, J. Xie, D.H. Yang, Z.S. Chen, Overcoming ABC transporter-mediated multidrug resistance: molecular mechanisms and novel therapeutic drug strategies, Drug Resist. Updates 27 (2016) 14–29.
[11] R.J. Kathawala, P. Gupta, C.R. Ashby, Z.S. Chen, The modulation of ABC transporter-mediated multidrug resistance in cancer: a review of the past decade, Drug Resist. Updates 18 (2015) 1–17.
[12] H. Zhang, H. Xu, C.R. Ashby, Y.G. Assaraf, Z.S. Chen, H.M. Liu, Chemical molecular-based approach to overcome multidrug resistance in cancer by targeting P-glycoprotein (P-gp), Med. Res. Rev. 41 (2021) 525–555.
[13] R.L. Juliano, V. Ling, A surface glycoprotein modulating drug permeability in Chinese hamster ovary cell mutants, BBA - Biomembr. 455 (1976) 152–162.
[14] K. Yang, J. Wu, X. Li, Recent advances in research on P-glycoprotein inhibitors, Biosci. Trends. 2 (2008) 137–146.
[15] A. Palmeira, E. Sousa, M.H. Vasconcelos, M.M. Pinto, Three decades of P-gp inhibitors: skimming through several generations and scaffolds, Curr. Med. Chem. 19 (2012) 1946–2025.
[16] M.L. Amin, P-glycoprotein inhibition for optimal drug delivery, Drug Target Insights 7 (2013) 27–34.
[17] L.D. Cripe, H. Uno, E.M. Paietta, M.R. Litzow, R.P. Ketterling, J.M. Bennett, J. M. Rowe, H.M. Lazarus, S. Luger, M.S. Tallman, Zosuquidar, a novel modulator of P-glycoprotein, does not improve the outcome of older patients with newly

diagnosed acute myeloid leukemia: a randomized, placebo-controlled trial of the Eastern Cooperative Oncology Group 3999, Blood 116 (2010) 4077–4085.
[18] R.J. Kelly, D. Draper, C.C. Chen, R.W. Robey, W.D. Figg, R.L. Piekarz, X. Chen, E. R. Gardner, F.M. Balis, A.M. Venkatesan, S.M. Steinberg, T. Fojo, S.E. Bates, A pharmacodynamic study of docetaxel in combination with the P-glycoprotein antagonist tariquidar (XR9576) in patients with lung, ovarian, and cervical cancer, Clin. Cancer Res. 17 (2011) 569–580.
[19] S. Mollazadeh, A. Sahebkar, F. Hadizadeh, J. Behravan, S. Arabzadeh, Structural and functional aspects of P-glycoprotein and its inhibitors, Life Sci. 214 (2018) 118–123.
[20] D. Waghray, Q. Zhang, Inhibit or evade multidrug resistance P-glycoprotein in cancer treatment, J. Med. Chem. 61 (2018) 5108–5121.
[21] Z. Yang, Y. Cai, S. Mao, Q. Wu, M. Zhu, X. Cao, B. Wei, J.M. Tian, X. Bao, X. Ye, J. Chen, S. Wang, Y. Yu, H. Zhang, X. Sun, Z.N. Cui, Y.S. Li, H. Wang, Discovery of 2,5-disubstituted furan derivatives featuring a benzamide motif for overcoming P-glycoprotein mediated multidrug resistance in MCF-7/ADR cell, Eur. J. Med. Chem. 257 (2023), 115462.
[22] E. Teodori, L. Braconi, S. Bua, A. Lapucci, G. Bartolucci, D. Manetti, M. N. Romanelli, S. Dei, C.T. Supuran, M. Coronnello, Dual P-glycoprotein and CA xii inhibitors : a new strategy to reverse the P-gp mediated multidrug resistance (MDR) in cancer cells, Molecules 25 (2020) 1–26.
[23] L. Braconi, E. Teodori, C. Riganti, M. Coronnello, A. Nocentini, G. Bartolucci, M. Pallecchi, M. Contino, D. Manetti, M.N. Romanelli, C.T. Supuran, S. Dei, New dual P-glycoprotein (P-gp) and human carbonic anhydrase XII (hCA XII) inhibitors as multidrug resistance (MDR) reversers in cancer cells, J. Med. Chem. 65 (2022) 14655–14672.
[24] S. Chatterjee, A.A. Deshpande, H. Shen, Recent advances in the in vitro and in vivo methods to assess impact of P-glycoprotein and breast cancer resistance protein transporters in central nervous system drug disposition, Biopharm Drug Dispos. (2023) 1–19.
[25] M. Myer, G. Joone, C. M, et al., The chemosensitizing potential of GF120918 is independent of the magnitude of P-glycoprotein-mediated resistance to conventional chemotherapeutic agents in a small cell lung cancer line, Oncol. Rep. 6 (1999) 217–218.
[26] E. Fox, S.E. Bates, Tariquidar (XR9576): a P-glycoprotein drug efflux pump inhibitor, Expert Rev. Anticancer Ther. 7 (2007) 447–459.
[27] H. Thomas, H.M. Coley, Overcoming multidrug resistance in cancer: an update on the clinical strategy of inhibiting P-glycoprotein, Cancer Control 10 (2003) 159–165.
[28] H.M. Coley, Overcoming multidrug resistance in cancer: clinical studies of P-glycoprotein inhibitors, Methods Mol. Biol. 596 (2010) 341–358.
[29] M. Kühnle, M. Egger, C. Müller, A. Mahringer, G. Bernhardt, G. Fricker, B. König, A. Buschauer, Potent and selective inhibitors of breast cancer resistance protein (ABCG2) derived from the p-glycoprotein (ABCB1) modulator tariquidar, J. Med. Chem. 52 (2009) 1190–1197.
[30] P. Kakarla, M. Inupakutika, A.R. Devireddy, S.K. Gunda, T.M. Willmon, K. C. Ranjana, U. Shrestha, I. Ranaweera, A.J. Hernandez, S. Barr, M.F. Verela, 3D-QSAR and contour map analysis of tariquidar analogues as multidrug resistance protein-1 (MRP1) inhibitors, Int. J. Pharma Sci. Res. 7 (2016) 554–572.
[31] Y.L. Sun, J.J. Chen, P. Kumar, K. Chen, K. Sodani, A. Patel, Y.L. Chen, S.D. Chen, W. Q. Jiang, Z.S. Chen, Reversal of MRP7 (ABCC10)-Mediated multidrug resistance by tariquidar, PLoS One 8 (2013), e55576.
[32] E. Teodori, L. Braconi, D. Manetti, M.N. Romanelli, S. Dei, The tetrahydroisoquinoline scaffold in ABC transporter inhibitors that act as multidrug resistance (MDR) reversers, Curr. Top. Med. Chem. 22 (2022) 2535–2569.
[33] E. Teodori, S. Dei, G. Bartolucci, G. Perrone, M.G. Perrone, D. Manetti, M. N. Romanelli, M. Contino, N.A. Colabufo, G. Perrone, Structure–activity relationship studies on 6,7-Dimethoxy-2-phenethyl-1,2,3,4-tetrahydroisoquinoline derivatives as multidrug resistance reversers, ChemMedChem 12 (2017) 1369–1379.
[34] L. Braconi, G. Bartolucci, M. Contino, N. Chiaramonte, R. Giampietro, D. Manetti, M.G. Perrone, M.N. Romanelli, N.A. Colabufo, C. Riganti, S. Dei, E. Teodori, 6,7-Dimethoxy-2-phenethyl-1,2,3,4-tetrahydroisoquinoline amides and corresponding ester isosteres as multidrug resistance reversers, J. Enzym. Inhib. Med. Chem. 35 (2020) 974–992.
[35] J.C. Kim, K.S. Kim, D.S. Kim, S.G. Jin, D.W. Kim, Y. Il Kim, J.H. Park, J.O. Kim, C. S. Yong, Y.S. Youn, J.S. Woo, H.G. Choi, Effect of HM30181 mesylate salt-loaded microcapsules on the oral absorption of paclitaxel as a novel P-glycoprotein inhibitor, Int. J. Pharm. 506 (2016) 93–101.
[36] S.C. Köhler, S. Vahdati, M.S. Scholz, M. Wiese, Structure activity relationships, multidrug resistance reversal and selectivity of heteroarylphenyl ABCG2 inhibitors, Eur. J. Med. Chem. 146 (2018) 483–500.
[37] F. Orlandi, M. Coronnello, C. Bellucci, S. Dei, L. Guandalini, D. Manetti, C. Martelli, M.N. Romanelli, S. Scapecchi, M. Salerno, H. Menif, I. Bello, E. Mini, E. Teodori, New structure-activity relationship studies in a series of N,N-bis(cyclohexanol) amine aryl esters as potent reversers of P-glycoprotein-mediated multidrug resistance (MDR), Bioorg. Med. Chem. 21 (2013) 456–465.
[38] S.C. Köhler, M. Wiese, HM30181 derivatives as novel potent and selective inhibitors of the breast cancer resistance protein (BCRP/ABCG2), J. Med. Chem. 58 (2015) 3910–3921.
[39] M. Morone, V. Razzano, S. Postle, G. Norcini, Water Soluble 3-ketocoumarins, WO2019116177A1, 2018.
[40] P. Stabile, A. Lamonica, A. Ribecai, D. Castoldi, G. Guercio, O. Curcuruto, Mild and convenient one-pot synthesis of 1,3,4-oxadiazoles, Tetrahedron Lett. 51 (2010) 4801–4805.
[41] J.W. Polli, S.A. Wring, J.E. Humphreys, L. Huang, J.B. Morgan, L.O. Webster, C. S. Serabjit-Singh, Rational use of in vitro P-glycoprotein assays in drug discovery, J. Pharmacol. Exp. Therapeut. 299 (2001) 620–628.
[42] C. Inglese, M.G. Perrone, F. Berardi, R. Perrone, N.A. Colabufo, Modulation and absorption of xenobiotics: the synergistic role of CYP450 and P-gp activities in cancer and neurodegenerative disorders, Curr. Drug Metabol. 12 (2011) 702–712.
[43] N.A. Colabufo, M. Contino, M. Cantore, E. Capparelli, M.G. Perrone, G. Cassano, G. Gasparre, M. Leopoldo, F. Berardi, R. Perrone, Naphthalenyl derivatives for hitting P-gp/MRP1/BCRP transporters, Bioorg. Med. Chem. 21 (2013) 1324–1332.
[44] L. Kangas, M. Grönroos, A. Nieminen, Bioluminescence of cellular ATP: a new method for evaluating cytotoxic agents in vitro, Med. Biol. 62 (1984) 338–343.
[45] B. Feng, J.B. Mills, R.E. Davidson, R.J. Mireles, J.S. Janiszewski, M.D. Troutman, S. M. De Morais, In vitro P-glycoprotein assays to predict the in vivo interactions of P-glycoprotein with drugs in the central nervous system, Drug Metab. Dispos. 36 (2008) 268–275.
[46] C. Riganti, E. Gazzano, G.R. Gulino, M. Volante, D. Ghigo, J. Kopecka, Two repeated low doses of doxorubicin are more effective than a single high dose against tumors overexpressing P-glycoprotein, Cancer Lett. 360 (2015) 219–226.
[47] C. Riganti, J. Kopecka, E. Panada, S. Barak, M. Rubinstein, The role of C/EBP-β LIP in multidrug resistance, J. Natl. Cancer Inst. 107 (2015) 1–14.
[48] Flare™, V5, Cresset®, litlington, cambridgeshire, UK. http://www.cresset-group.com/flare/, 2023.
[49] T. Cheeseright, M. Mackey, S. Rose, A. Vinter, Molecular field extreme as descriptors of biological activity: definition and validation, J. Chem. Inf. Model. 46 (2006) 665–676.
[50] M.R. Bauer, M.D. Mackey, Electrostatic complementarity as a fast and effective tool to optimize binding and selectivity of protein-ligand complexes, J. Med. Chem. 62 (2019) 3036–3050.
[51] M. Kuhn, S. Firth-Clark, P. Tosco, A.S.J.S. Mey, M. MacKey, J. Michel, Assessment of binding affinity via alchemical free-energy calculations, J. Chem. Inf. Model. 60 (2020) 3120–3130.
[52] S.C.T. Nicklisch, S.D. Rees, A.P. McGrath, T. Gökirmak, L.T. Bonito, L.M. Vermeer, C. Cregger, G. Loewen, S. Sandin, G. Chang, A. Hamdoun, Global marine pollutants inhibit P-glycoprotein: environmental levels, inhibitory effects, and cocrystal structure, Sci. Adv. 2 (2016).
[53] L. Braconi, E. Teodori, M. Contino, C. Riganti, G. Bartolucci, D. Manetti, M. N. Romanelli, M.G. Perrone, N.A. Colabufo, S. Guglielmo, S. Dei, Overcoming multidrug resistance (MDR): design, biological evaluation and molecular modelling studies of 2,4-substituted quinazoline derivatives, ChemMedChem 17 (2022), e202200027.
[54] F. Pedregosa, G. Varoquaux, A. Gramfort, V. Michel, B. Thirion, O. Grisel, M. Blondel, P. Prettenhofer, R. Weiss, V. Dubourg, J. Vanderplas, A. Passos, D. Cournapeau, M. Brucher, M. Perrot, É. Duchesnay, Scikit-learn: machine learning in Python, J. Mach. Learn. Res. 12 (2011) 2825–2830.
[55] S. Jo, T. Kim, V.G. Iyer, W. Im, CHARMM-GUI: a web-based graphical user interface for charmm, J. Comput. Chem. 29 (2008) 1859–1865.
[56] J. Lee, D.S. Patel, J. Ståhle, S.J. Park, N.R. Kern, S. Kim, J. Lee, X. Cheng, M. A. Valvano, O. Holst, Y.A. Knirel, Y. Qi, S. Jo, J.B. Klauda, G. Widmalm, W. Im, CHARMM-GUI membrane builder for complex biological membrane simulations with glycolipids and lipoglycans, J. Chem. Theor. Comput. 15 (2019) 775–786.
[57] P. Bauer, B. Hess, E. Lindahl, GROMACS 2022.3 Source Code, 2022, https://doi.org/10.5281/zenodo.7037338.
[58] A. Rasouli, Q. Yu, S. Dehghani-Ghahnaviyeh, P.C. Wen, J. Kowal, K.P. Locher, E. Tajkhorshid, Differential dynamics and direct interaction of bound ligands with lipids in multidrug transporter ABCG2, Proc. Natl. Acad. Sci. U. S. A 120 (2023), e2213437120.
[59] R. Callaghan, R.C. Ford, I.D. Kerr, The translocation mechanism of P-glycoprotein, FEBS Lett. 580 (2006) 1056–1063.
[60] A.G. Marshall, C.L. Hendrickson, High-resolution mass spectrometers, Annu. Rev. Anal. Chem. 1 (2008) 579–599.
[61] N.A. Gujarati, L. Zeng, P. Gupta, Z.S. Chen, V.L. Korlipara, Design, synthesis and biological evaluation of benzamide and phenyltetrazole derivatives with amide and urea linkers as BCRP inhibitors, Bioorg. Med. Chem. Lett 27 (2017) 4698–4704.
[62] J. Li, L. Ackermann, Cobalt-catalyzed C-H arylations with weakly-coordinating amides and tetrazoles: expedient route to angiotensin-ii-receptor blockers, Chem. Eur J. 21 (2015) 5718–5722.
[63] G.S. Jedhe, D. Paul, R.G. Gonnade, M.K. Santra, E. Hamel, T.L. Nguyen, G. J. Sanjayan, Correlation of hydrogen-bonding propensity and anticancer profile of tetrazole-tethered combretastatin analogues, Bioorg. Med. Chem. Lett 23 (2013) 4680–4684.
[64] L. Boukli, M. Touaibia, N. Meddad-Belhabich, A. Djimdé, C.H. Park, J.J. Kim, J. H. Yoon, A. Lamouri, F. Heymans, Design of new potent and selective secretory phospholipase A2 inhibitors. Part 5: synthesis and biological activity of 1-alkyl-4-[4,5-dihydro-1,2,4-[4H]-oxadiazol-5-one-3-ylmethylbenz-4′-yl(oyl)] piperazines, Bioorg. Med. Chem. 16 (2008) 1242–1253.
[65] M. Contino, S. Guglielmo, C. Riganti, G. Antonello, M.G. Perrone, R. Giampietro, B. Rolando, R. Fruttero, N.A. Colabufo, One molecule two goals: a selective P-glycoprotein modulator increases drug transport across gastro-intestinal barrier and recovers doxorubicin toxicity in multidrug resistant cancer cells, Eur. J. Med. Chem. 208 (2020), 112843.
[66] J. Kopecka, M. Godel, S. Dei, R. Giampietro, D.C. Belisario, M. Akman, M. Contino, E. Teodori, C. Riganti, Insights into P-glycoprotein inhibitors: new inducers of immunogenic cell death, Cells 9 (2020) 1–17.
[67] H.M. Berman, J. Westbrook, et al., The protein Data Bank, Nucleic Acids Res. 28 (2000) 235–242.

[68] A. Šali, T.L. Blundell, Comparative protein modelling by satisfaction of spatial restraints, J. Mol. Biol. 234 (1993) 779–815.
[69] E.F. Pettersen, T.D. Goddard, C.C. Huang, G.S. Couch, D.M. Greenblatt, E.C. Meng, T.E. Ferrin, UCSF Chimera - a visualization system for exploratory research and analysis, J. Comput. Chem. 25 (2004) 1605–1612.
[70] J.A. Maier, C. Martinez, K. Kasavajhala, L. Wickstrom, K.E. Hauser, C. Simmerling, ff14SB: improving the accuracy of protein side chain and backbone parameters from ff99SB, J. Chem. Theor. Comput. 11 (2015) 3696–3713.
[71] G. Jones, P. Willett, R.C. Glen, A.R. Leach, R. Taylor, Development and validation of a genetic algorithm for flexible docking, J. Mol. Biol. 267 (1997) 727–748.